AD 295 096

63-2-3

AIR FORCE INSTITUTE OF TECHNOLOGY

AIR UNIVERSITY
UNITED STATES AIR FORCE

SCHOOL OF ENGINEERING

WRIGHT-PATTERSON AIR FORCE BASE, OHIO

AF-WP-O-MAY 62 3,500

THESIS

Presented to the Faculty of the School of Engineering

The Institute of Technology

Air University

in Partial Fulfillment of the

Requirements for the

Master of Science Degree

in Electrical Engineering

INVESTIGATION AND ANALOG SIMULATION OF THE TYPE TWO AND TYPE THREE PHASE-LOCK LOOP

By

Edgar F. Thomas
Captain USAF

GE/EE/62-20

Graduate Electronics

December 1962

Preface

This report is the result of my endeavors to investigate the ability of the Phase-Lock Loop to operate in a Type Two and Type Three Configuration. The primary method of analysis is the Analog Computer Simulation. Servo Analysis is also utilized and the two compared. Step, Ramp, and Parabolic inputs are used separately, in a random process.

All the bibliography listed on Pages 61 and 62 is not referred to directly in this report; however, the complete recording of all available literature on the Phase-Lock Loop will serve as a valuable aid to any advanced study in this field.

I wish to acknowledge my gratitude to the following individuals:

Captain John MacCallum, Thesis Advisor, for his guidance, suggestions, encouragement and patience.

Lt. Gustave Wendland, Sponsor, for his valuable assistance in so many ways throughout this ordeal.

Captain Charles Richards, Jr. for his assistance in the digital computer program and Analog Computer Course.

Mr. William Neal, Analog Computation Division, for his aid in programming, and the dogwork of preparing the Analog Computer patch boards.

My son, Keith Joseph, for his great contribution of many long hours of peace and quiet and for giving up his daily playtime with "Daddy" during the months required for completion of this report.

And last, but not least, to my wife, Elaine Mary, for the hours she spent doing the proofreading, lettering, drawings and preliminary typing of this report.

This report would have been impossible if it were not for the patience, encouragement and understanding of my family.

Edgar F. Thomas
Captain, USAF

Contents

List of Figures and Tables

Figure

Table

Definition of Abbreviations

Abbreviation	Definition
rps	Radians per second
cps	Cycles per second
kcps	Thousand cycles per second
VCO	Voltage Controlled Oscillator
PLL	Phase-Lock Loop
DC	Direct Current
AC	Alternating Current
FM	Frequency modulation
PM	Phase modulation
sec	Seconds
cm	Centimeters
ma	Milliamperes
v	Volts

Definition of Symbols

Symbol	Definition
$\Delta\omega$	Change in frequency, step, radians/sec
$\Delta\omega/t$	Change in frequency (ramp) radians/sec
$\Delta\omega/t^2$	Change in frequency (parabolic) radians/sec
ω_o	Basic oscillator frequency radians/sec
e_c	Control signal voltage to VCO, volts
Δf	Change in frequency, cps
K_1	Gain constant of phase detector, volts/radian
K_2	Gain constant of notch filter
F(s)	Loop filter transfer function
K_3	Gain constant of low pass filter
K_4	Gain of constant of VCO, radians per sec, per volt
e_m	Modulation Product Signal, volts
A	Amplitude of output signal from input oscillator
B	Amplitude of output from Voltage Controlled Oscillator
ω_1	Frequency of Input Oscillator, rps
ω_2	Frequency of Voltage Controlled Oscillator, rps
θ	Phase angle of Input Oscillator radians
ϕ	Phase angle of VCO radians
θ_n	Phase error, radians
G	Forward loop adjustable gain
G_T	Total forward loop gain
e_n	Phase Error Detector Voltage, volts
$\approx$	Approximately equal

Symbol	Definition
$\equiv$	Defined as
$\neq$	Not equal to
G(s)	Forward transfer function
H(s)	Feedback Transfer function
M_p	Peak overshoot
t_p	Time to peak overshoot
t_s	Settling time
E_N	Peak to peak voltage, volts
K_o'	Step static error coefficient
K_1'	Ramp static error coefficient
K_2'	Parabolic static error coefficient

Abstract

This report is the result of an investigation and simulation of a Type Two and Type Three Phase-Lock Loop. Standard Root Locus Analysis and Analog Computer Simulation were both accomplished, and the results compared. Step, Ramp, and Parabolic inputs were tested separately and in a random sequence to obtain the response of the Phase-Lock Loop.

This report demonstrates that it is possible to operate the Phase-Lock Loop in Type Two and Type Three configuration with large variations in the basic frequency. Recommendations for further study and physical realization are made.

INVESTIGATION AND ANALOG SIMULATION OF THE TYPE TWO AND TYPE THREE PHASE-LOCK LOOP

I. Introduction

The advent of the Space Age has introduced the Phase-Lock Loop (PLL), also known as Automatic-Phase-Control, into the foreground of communications. The ability of the PLL to receive a weak FM signal from outer space, increase the power level, and attenuate the noise, has been widely used in Space Telemetry. The major advantage of the PLL is that the loop separates the gain of the system from phase stability. This is helpful, because additional amplifiers may be added to the loop without being concerned about the phase stability of the individual amplifier. The PLL also tends to isolate the output amplitude from the input amplitude, which reduces the power requirements to a relatively low level. Low power leads to transistorized circuitry which explains the wide use for space communications.

One important use in the field of video transmitters is the Automatic Three Dimensional Electronics Scanned Array (Ref 14). PLL is also used in advanced FM/PM telemetry systems, such as the Phase Coherent Detection System (Ref 19).

Basically, the PLL is used to synchronize an oscillator with a low power reference signal. The main component of a PLL is shown in Figure 1.

The electronic loop consists of a Phase Detector, a Voltage

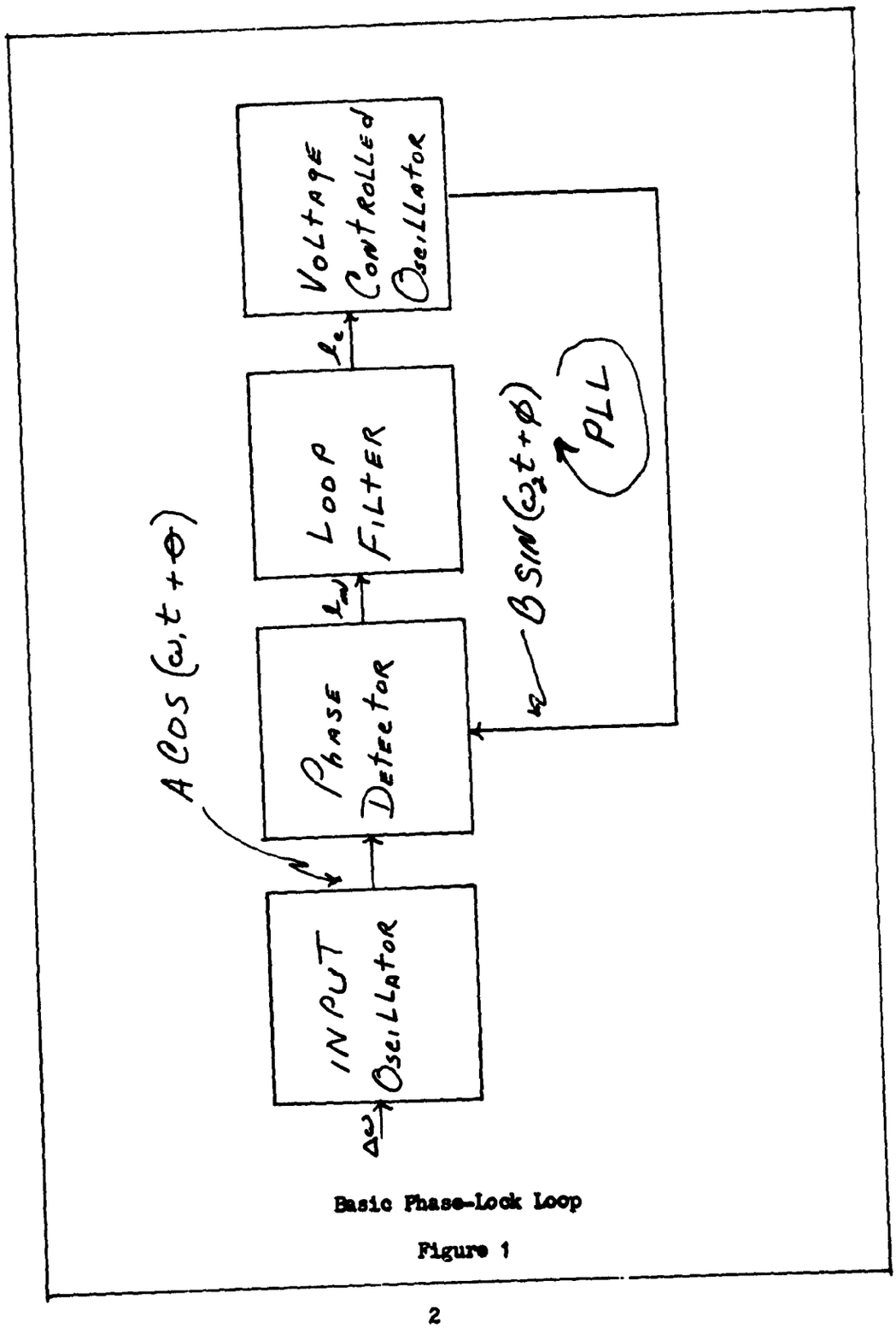

Basic Phase-Lock Loop

Figure 1

Controlled Oscillator (VCO) and a Loop or Low Pass Filter (Ref 7). The operation of the system is best understood by assuming that the frequency (ω_1) of input oscillator is equal to the frequency (ω_2) of the VCO. The D.C. output of the phase detector is proportional to the phase difference between the input oscillator and VCO. If the frequency of the input oscillator tends to change, the phase difference will change first and present a correction voltage to the VCO to maintain the VCO at the same frequency. The Loop Filter removes the harmonics that are generated in the Phase Detector. This system is unique in that the frequency remains unchanged, a characteristic which would be impossible in an Automatic Frequency Control System (Ref 12).

Previous Work

Lt. Wendland (GGC-62) investigated the feasibilities of using the Type One PLL as a feedback amplifier for use with a Nuclear Magnetic Gyroscope. His preliminary investigation demonstrated that the PLL will perform satisfactorily, provided the inputs are step change in frequency, and a finite constant phase error can be tolerated. Lt. Wendland's preliminary investigation also concluded that the phase of any amplifier added to the circuit was negligible (Ref 19).

To optimize the PLL, it is necessary to have zero phase and frequency error under random inputs. In order to accomplish this, the system type must be increased. This investigation will attempt to increase the type of the system used by Lt. Wendland and to reduce the phase error when operated under step, ramp, parabolic, and random inputs.

Analysis Procedure

The analysis procedure used in this investigation was designed to demonstrate clearly the function of the PLL when operated under Type Two and Type Three conditions.

Method of Analysis. The major method of analysis selected for this investigation was physical simulation on the Analog Computer. The computer results were compared, when possible, with normal feedback control system Root Locus techniques. The Analog simulation was used for three reasons.

(1) The PLL is concerned with two basic quantities, frequency and phase. The frequency is, by definition, the time rate of change of the phase. $\left(f = \frac{d\theta_n}{dt}\right)$ Because of this interrelation, the two cannot be completely separated in any system. The Analog simulation retains these two in their prospective within the system.

(2) The phase detector is basically a non linear device. Because of the presence of a non linear device in PLL, the dynamic analysis becomes extremely difficult. These non linearities are all taken into account by Analog simulation, which simplifies the problem of dynamic analysis.

(3) Analog Computer simulation provides a permanent set of graphs which can be used for study and evaluation.

Plan of Investigation. The basic Analog simulation components used by Lt. Wendland were redesigned and improved to produce a Type Two and a Type Three system. The loop was then connected and analyzed to determine its dynamic response characteristics.

The investigation continued with the theoretical analysis of the PLL. The loop's Root Locus were plotted by means of the IBM 1620 Digital Computer. The program was derived from a thesis written by Lt. H.M. Paskin with improvements made by Captain C. W. Richards, Jr. The program is given in Appendix B. The results will then be compared.

The concluding chapter will contain conclusions and recommendations for further study and experiment.

II. Analog Computer Simulation for the Phase-Lock Loop

The individual components of the PLL are designed and simulated separately, and then formed into a loop as shown in Figure 2.

The basic frequency of 5 rps was chosen because of the design of the input OSC and VCO and the frequency range of the ocmputer. In actual operation, the frequency of the PLL is 10 to 20 kcps. This means that 10 seconds on the simulation is equivalent to approximately 10 milliseconds in the actual system.

Input Oscillator Simulation

The Input Oscillator requires a variation in frequency tantamount to ω = 5 rps without changing the amplitude of the output. As can be seen in Figure 2 both the COS ω_i t and SIN ω_it must be generated by the Input Oscillator. The basic sin cos generator in Figure 3 must be modified slightly to meet the above requirements. The ω in Figure 3 could not be changed smoothly and evenly. In Figure 4, the potentiometers ω/G are replaced by servo potentiometers. The potentiometers must be equally loaded or they will change the amplitude when large step, ramp, or parabolic changes in frequency are made. When $\Delta\omega$ = 0, the potentiometers are set at .5. This makes the center frequency of the oscillator 5 rps. With the proper value of $\Delta\omega$, the ω_i of the oscillator will vary over a range of zero to ten rps.

Phase Detector Simulation

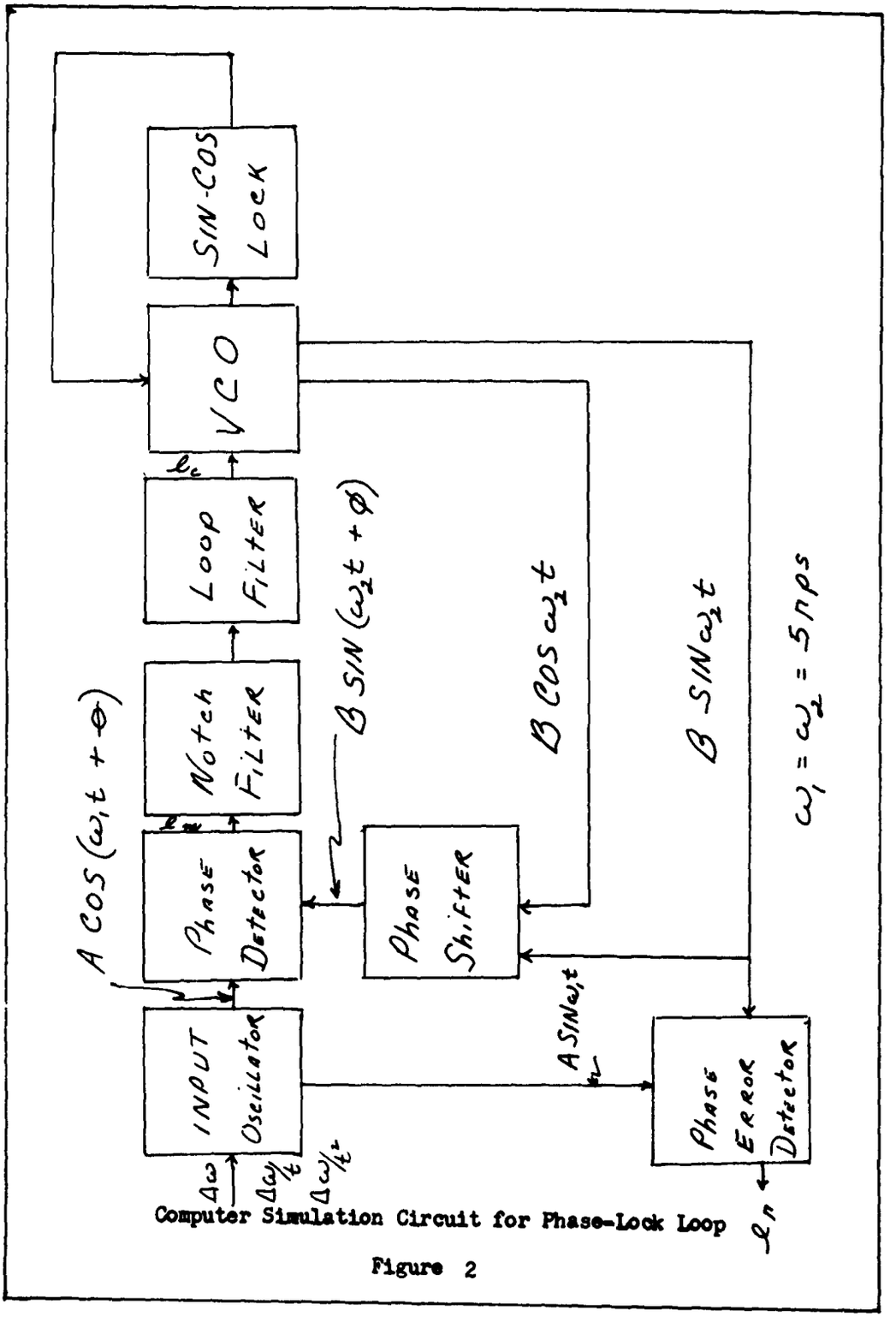

Computer Simulation Circuit for Phase-Lock Loop

Figure 2

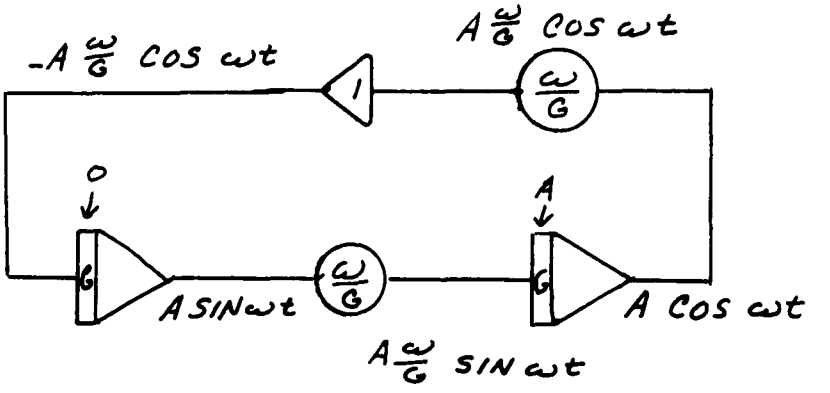

Sin Cos Generator

Analog Computer Diagram (Ref 5)

Figure 3

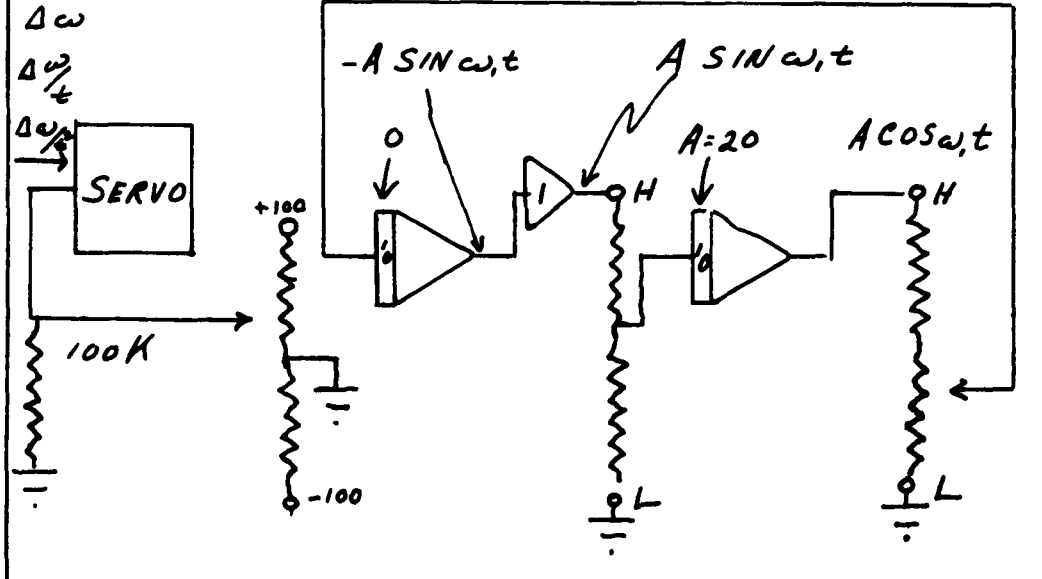

Input Oscillator Computer Simulation Circuit

Figure 4

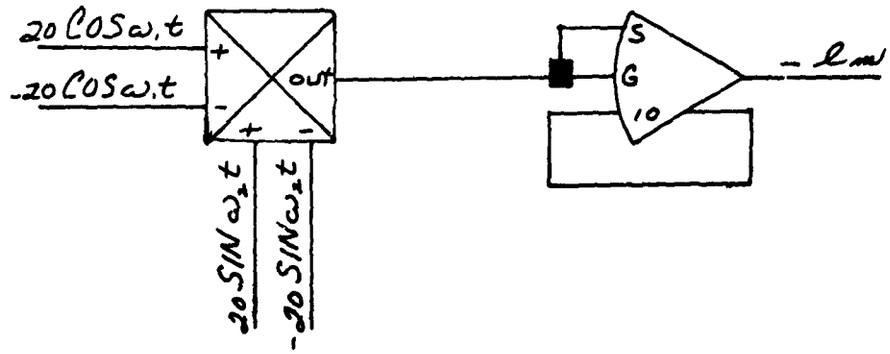

$$-\ell_m = \frac{-A\cos(\omega_1 t + \theta)\, B \sin(\omega_2 t + \phi)}{100}$$

$A = 20 = B \qquad \omega_1 = \omega_2$

SINCE $\cos\beta \sin\alpha = \frac{1}{2}\sin(\alpha+\beta) + \frac{1}{2}\sin(\alpha-\beta)$

$$\ell_m = \frac{400}{(100)(2)}\left[\sin(2\omega t + \phi + \theta) + \sin(\phi - \theta)\right]$$

$$\theta_n \equiv \phi - \theta$$

$$\ell_m = 2\sin(2\omega t + \phi + \theta) + 2\sin\theta_n$$

$$\therefore K_1 = 2$$

Phase Detector Computer Simulation Circuit

Figure 5

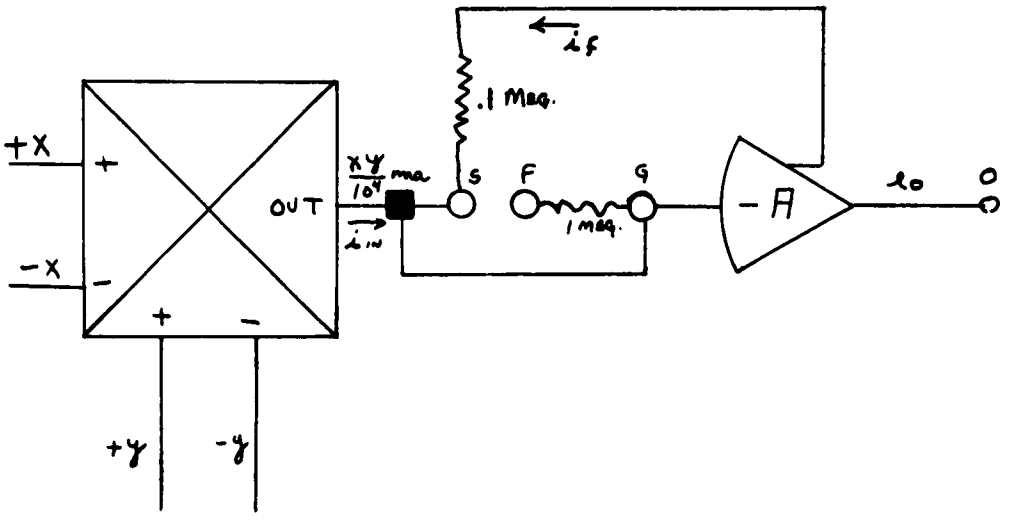

$$i_f + i_{IN} = 0$$

$$\frac{xy}{10^4} + \frac{e_o}{10^2} = 0$$

$$\frac{e_o}{10^2} = -\frac{xy}{10^4}$$

$$e_o = -\frac{xy}{10^2}$$

$$e_o = -\frac{xy}{100}$$

Quarter Square Type Multiplier

Figure 6

The phase detector is the most critical part of the PLL. For this reason an electronic multiplier is used to simulate the phase detector. The simulation is shown in Figure 5. The most accurate type multiplier available on the Electronic Association Incorporated Computer, which was utilized in this investigation, is the Quarter-Square Type. Diodes are used to generate the square waves for a quarter or square multiplier where

$$x\,y = \tfrac{1}{4}\left[(x+y)^2 - (x-y)^2\right]. \tag{1}$$

The multiplier requires both signs of the input variables. The connection made to S and G effectively remove the normal feedback resistor (Ref 6). The proper scale factor and sign at the output amplifier is best determined by solving the current equation at the amplifier summing junction, as illustrated in Figure 6.

Notch Filter Simulation

The notch filter used is the one designed by Lt. Wendland (Ref 19). The filter consists of two paths. One path has a unity gain and the other contains a high phase filter set enabling the notch to attenuate the second harmonic ($2\omega t$). The high pass filter assumes the form of

$$H(s) = \frac{4\,s^4}{(s+10)^4} \text{ or } \frac{4\,(10^{-4})\,(j\omega)^4}{\left(1+\frac{j\omega}{10}\right)^4} = H(j\omega) \tag{2}$$

From the log magnitude and angle plot in Figure 7, one can see that if $\omega < 10$ rps, the signal will be attenuated, and when $\omega > 10$ rps

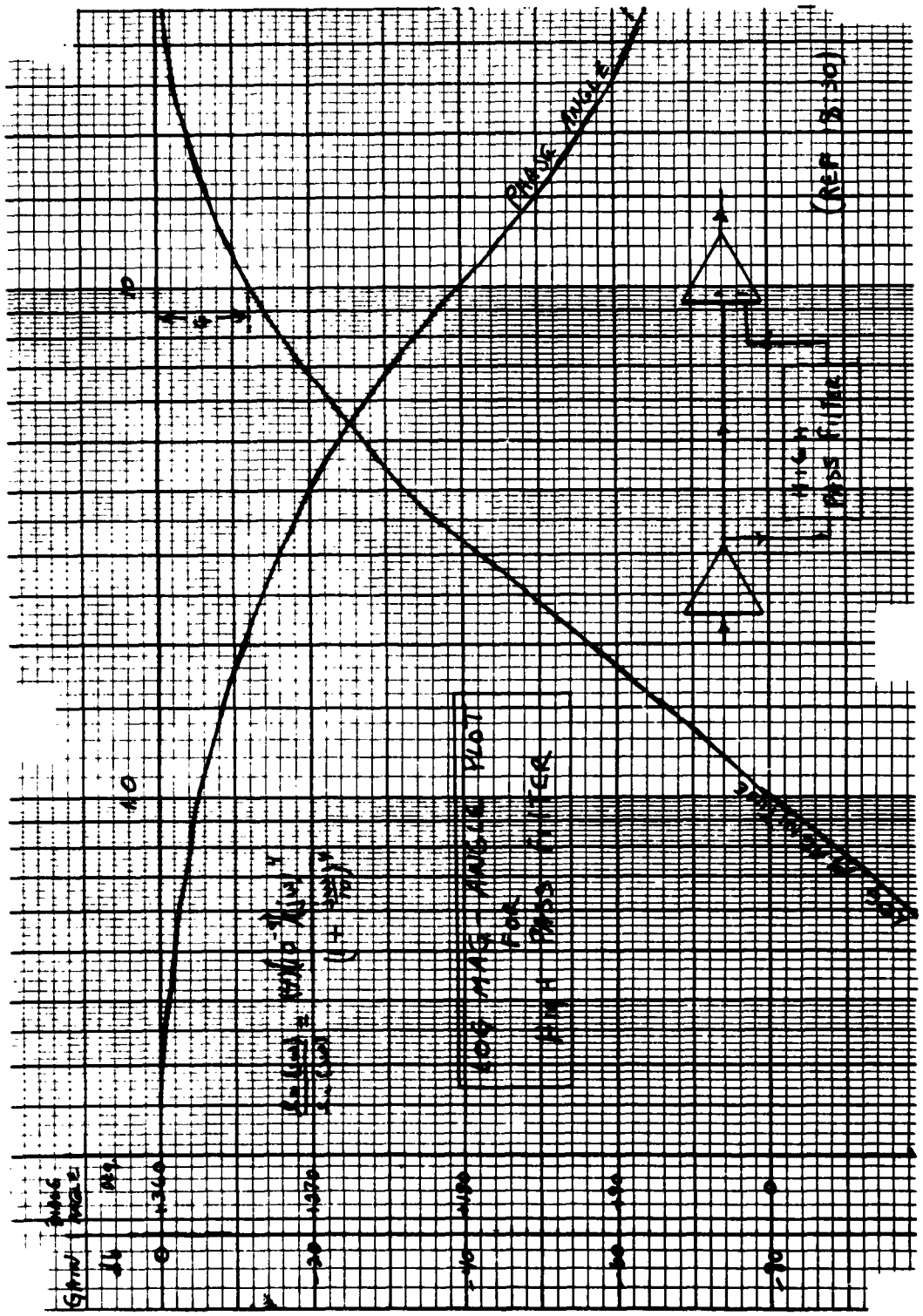

Figure 7

1. $\frac{e_o}{e_i} = \frac{S}{S+10} = \left(1 - \frac{10}{S+10}\right)$

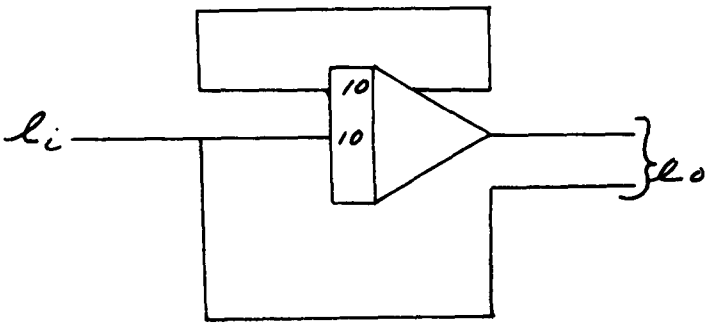

2. $\frac{e_o}{e_i} = \frac{S}{S+10} = \frac{1}{1+\frac{10}{S}}$

$e_o = e_i - \frac{10}{S} e_o$

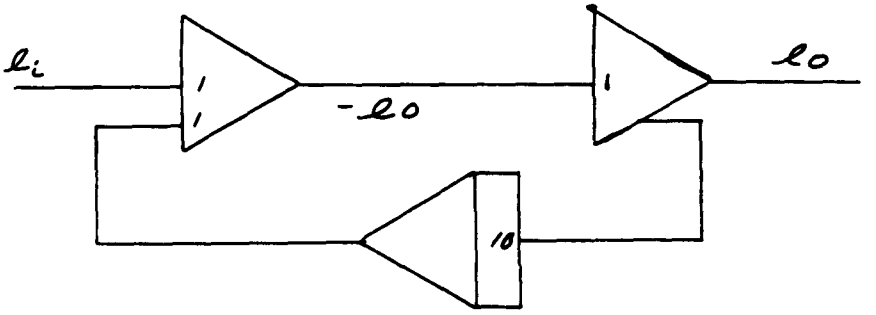

High Pass Filter Factor Simulation

Figure 8

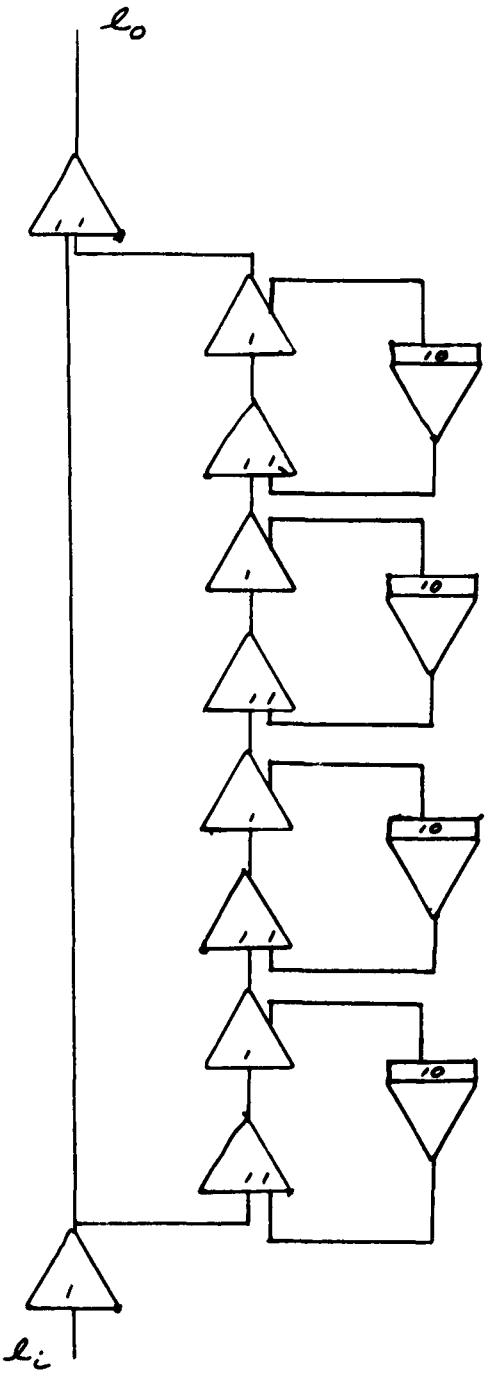

Notch Filter Simulation Circuit (Ref 19)

Figure 9

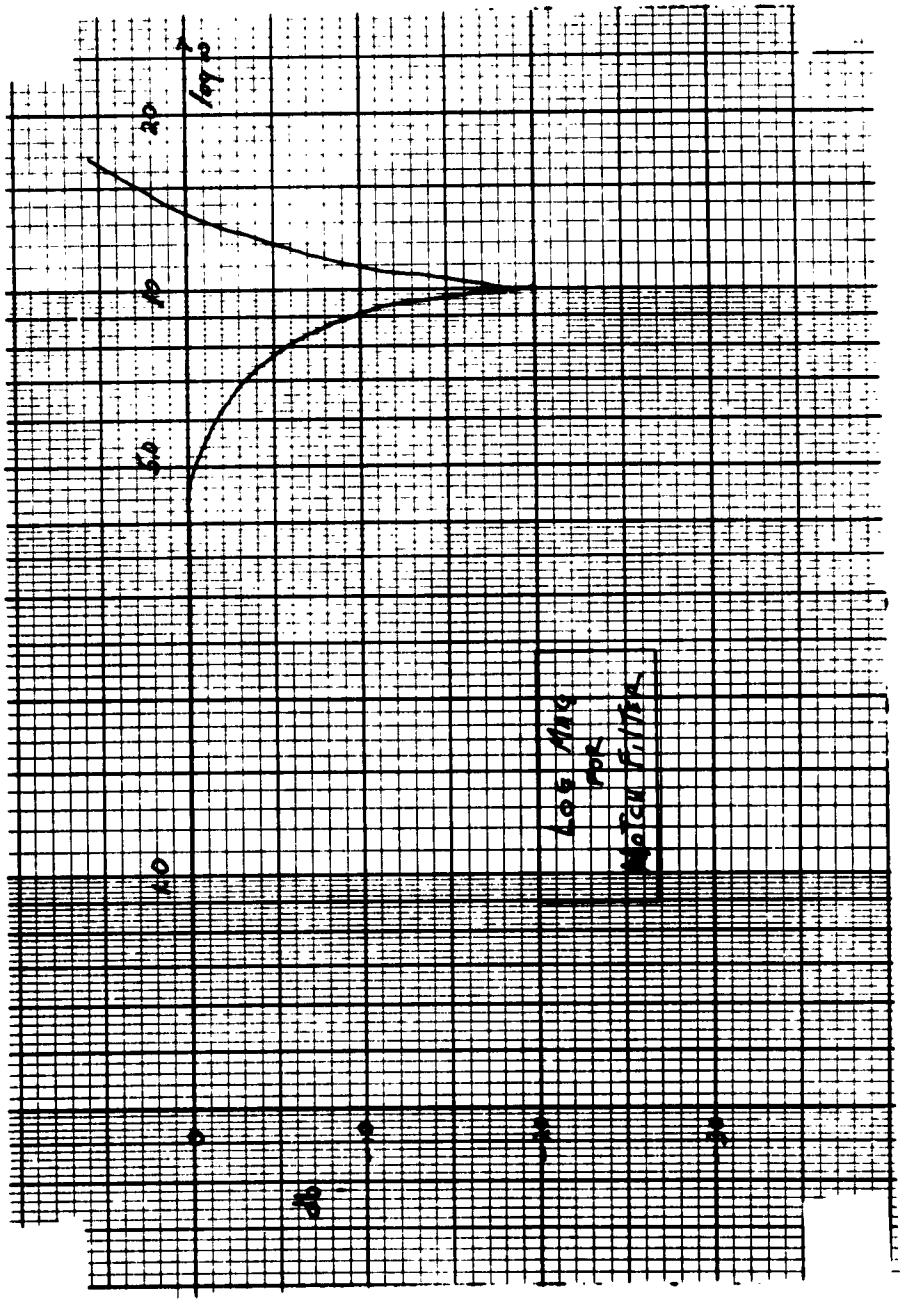

Figure 10

the signal will pass at gain 1. When ω = 10 rps, the signal will have a gain of one, but will be 180 out of phase. Effectively, the high pass filter is replaced by an amplifier, and the output is zero.

Cascading four $s/(s + 10)$ circuits together will give the simulation of the high pass filter. Two methods of simulation are possible, as shown in Figure 8. The second one was used because of the high forward gain in number 1. The complete computer simulation for the Notch Filter is in Figure 9.

Theoretically, this Notch Filter will only suppress the second harmonic at ω = 10 rps as can be seen in the experimental Log Magnitude Plot in Figure 10. The Notch Filter performed satisfactorily for the range of ω used in this investigation.

Loop Filter Simulation

Most Loop or Low Pass filters are represented by factored transfer functions. The only restriction on the transfer function is that the order of numerator be equal to or less than the denominator. The factors of the transfer function are first simulated and then cascaded to form the low pass filter. The factors fall into three general forms, the simulation of which is shown in Figure 11. The simulation of the low pass filters used in this investigation is found in Appendix Figure A-2.

Voltage Controlled Oscillator Simulation

The VCO, as its name implies, states that it must tolerate being controlled by a voltage. In addition, both the cos and sin must be

1. $\frac{e_o}{e_c} = \frac{1}{S}$

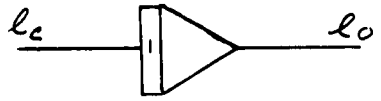

2. $\frac{e_o}{e_i} = \frac{S+a}{S+b} = 1 - \frac{b-a}{S+b}$

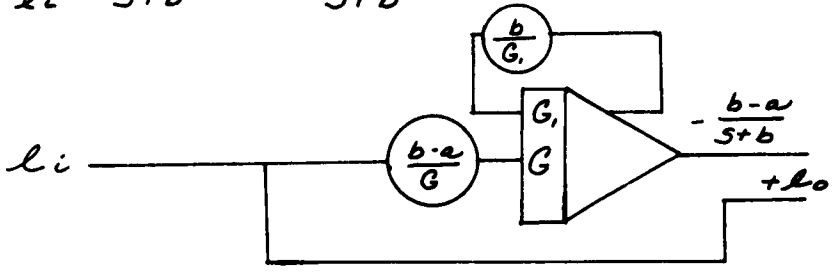

3. $\frac{e_o}{e_i} = \frac{S^2+aS+b}{S^2+cS+d} = \frac{1+\frac{a}{S}+\frac{b}{S^2}}{1+\frac{c}{S}+\frac{d}{S^2}}$

$e_o = +e_i - \frac{c}{S}e_o + \frac{a}{S}e_i - \frac{d}{S^2}e_o + \frac{b}{S^2}e_i$

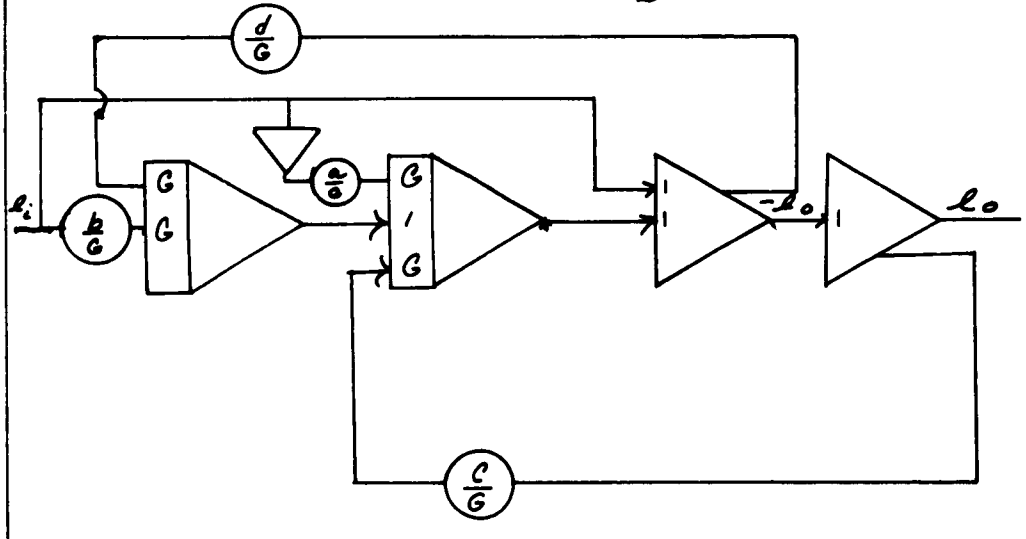

Loop Filter Factor Simulation Circuits

Figure 11

generated to provide the feedback and phase error detector inputs, and the amplitude of the output must be independent of any change in frequency. These requirements are the same as the Input Oscillator. The VCO is basically the same as the Input Oscillator. If A is replaced by B and ω by ω_2 , the simulation is shown in Figure 4.

Phase Shifter Simulation

In order to start the Input Oscillator and the VCO at relatively equal phase and to prevent the stability point from shifting, a phase shifter was placed in the feedback loop. The feedback is B SIN $(\omega_2 t + \phi)$ with the shifting circuit controlling ϕ .

The basis for the circuit is the trigonometric identity

$$\text{SIN } (a + b) = \text{SIN } a \ \text{ COS } b + \text{COS } a \ \text{ SIN } b \qquad (3)$$

let

$$a = \omega_2 t$$
$$b = \phi$$

it becomes

$$\text{SIN } (\omega_2 t + \phi) = \text{SIN } \omega_2 t \ \text{ COS } \phi + \text{COS } \omega_2 t \ \text{ SIN } \phi \qquad (4)$$

Figure 12 demonstrates the basic computer diagram while Figure 13 shows the circuit as it appears in the loop (Ref 19).

Voltage Controlled Oscillator Locking Simulation

Due to the inherent instability of the Analog Computer, the integrator drifts, and the power loss in the feedback capacitors, the amplitude of VCO tends to change when large or rapid variations in $\Delta \omega$ are attempted. In order to completely analyze the phase of the PLL,

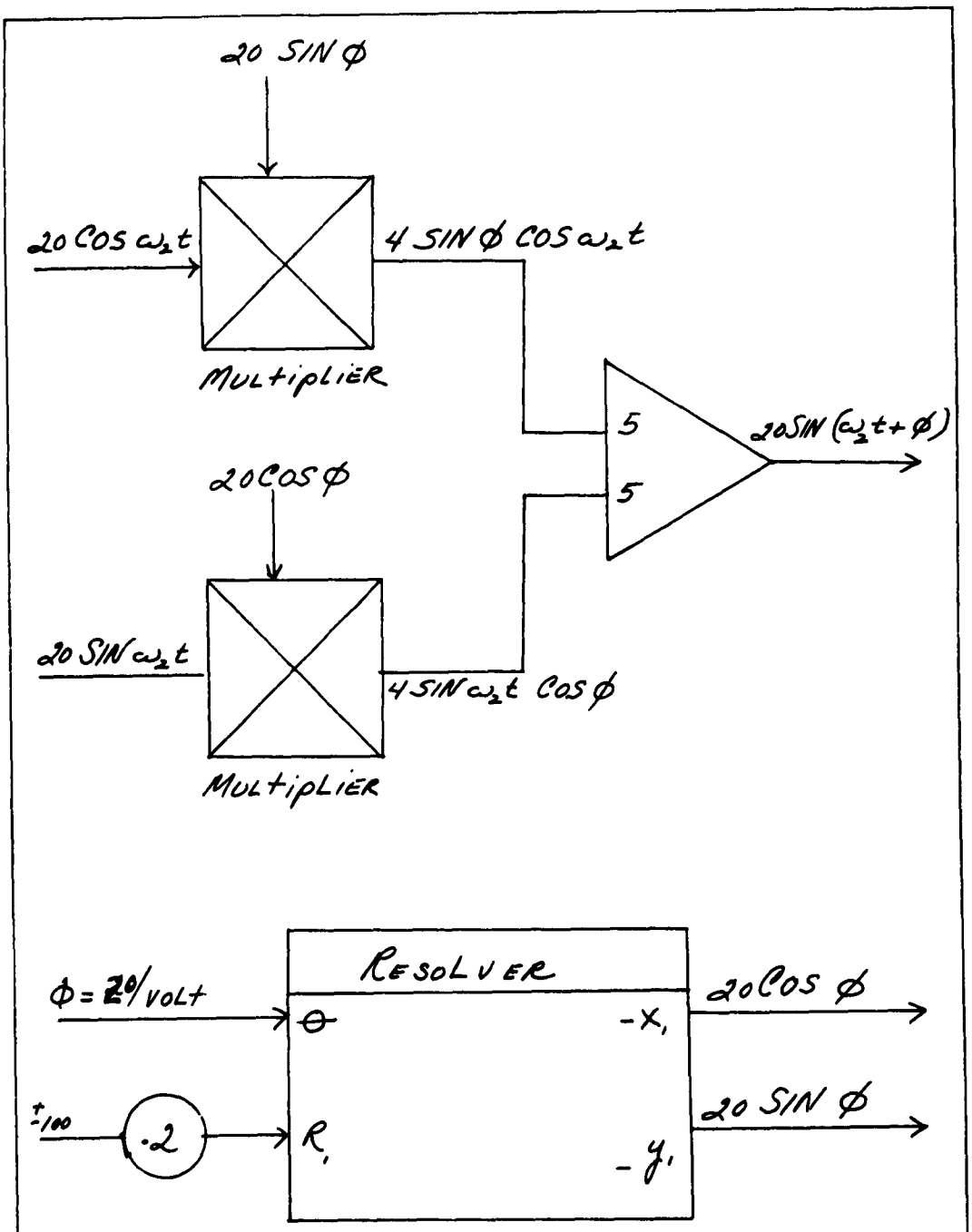

Basic Computer Simulation of the Phase Shifter

Figure 12

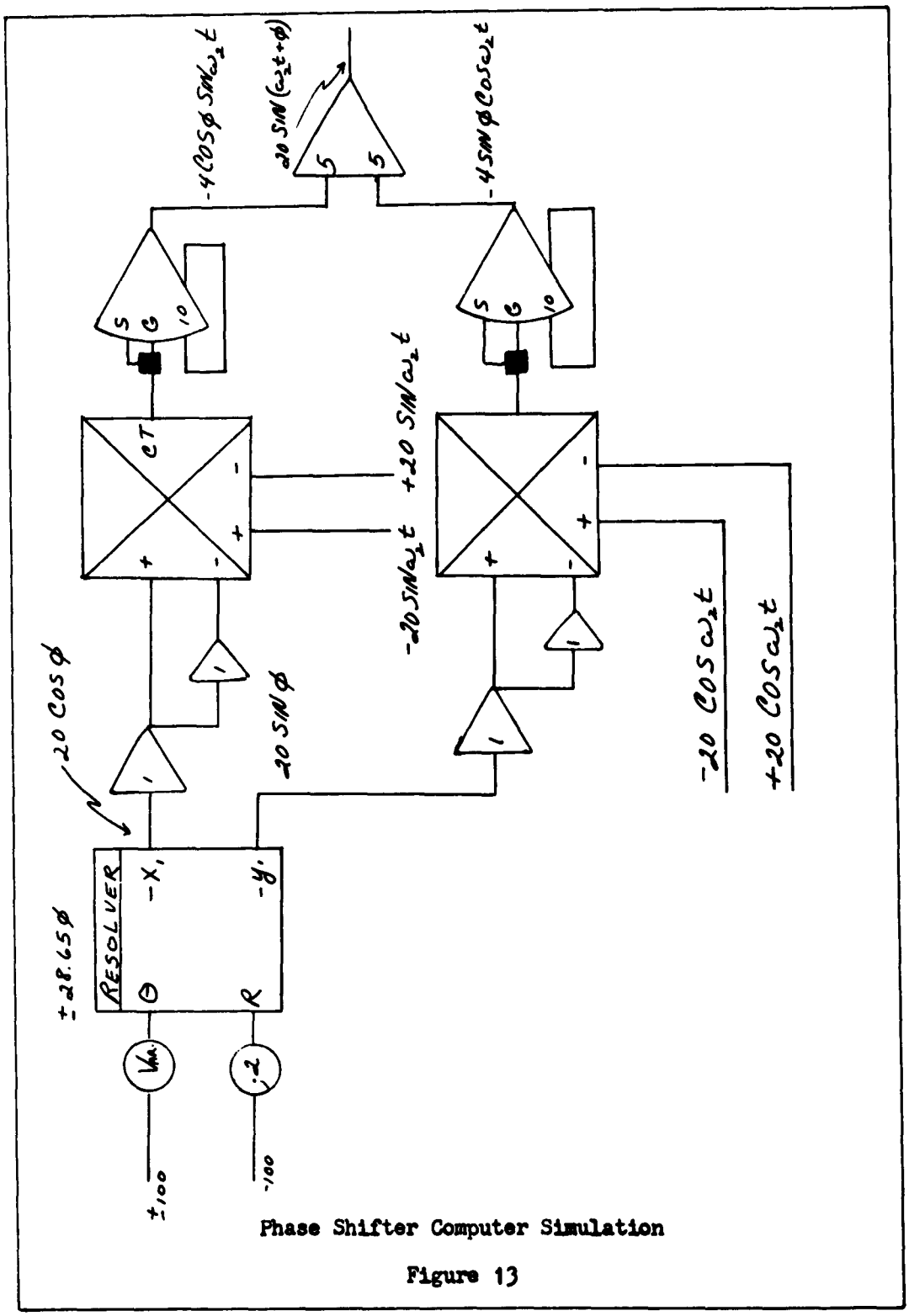

Phase Shifter Computer Simulation

Figure 13

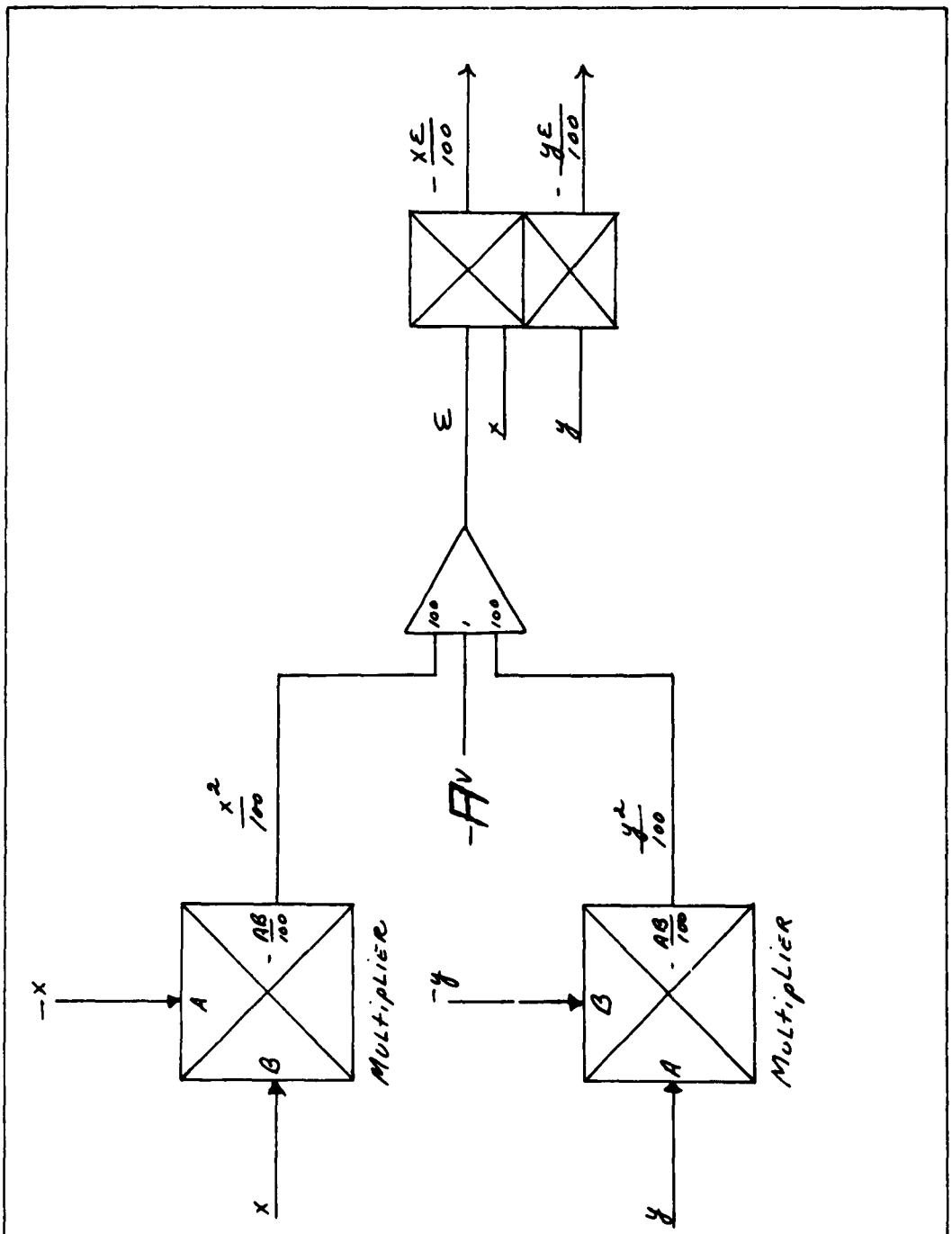

Basic Computer Circuit for Sin Cos Lock

Figure 14

the amplitude of the VCO is locked to the correct value.

In any oscillator, the

$$A \cos^2 \alpha + A \sin^2 \alpha = A (\cos^2 \alpha + \sin^2 \alpha) = A = \text{constant} \quad (5)$$

Whenever the amplitude of A changes or drifts to A'

$$A' \cos^2 \alpha + A' \sin^2 \alpha \neq A \quad (6)$$

Let

$$x = A \sin^2 \alpha$$
$$y = A \cos^2 \alpha$$
$$\alpha = \omega t$$

then

$$A' - (x + y) \equiv \mathcal{E} \quad (7)$$

where $\mathcal{E}$ is equal to the error of A.

By use of multipliers and summers, $\left[A' - (x + y)\right]$ can be generated, and if fed into each integrator of the oscillator as a negative or positive damping proportional to $\mathcal{E}$, will maintain A at the correct level. Figure 14 illustrates the basic computer simulation needed (Ref 11). If x (or y) increases, $\mathcal{E}$ becomes negative, and $-\mathcal{E}\, x/100$ becomes positive. When $-\mathcal{E}\, x/100$ is fed to the input of an integrator, the output decreases.

The simulation used in the PLL, as shown in Appendix Figure A-1, can be obtained

if

$$x = 20 \sin \omega_2 t$$
$$y = 20 \cos \omega_2 t$$

The multipliers used are of the Time Division Type. These are used because of the unavailability of the Quarter Square Type.

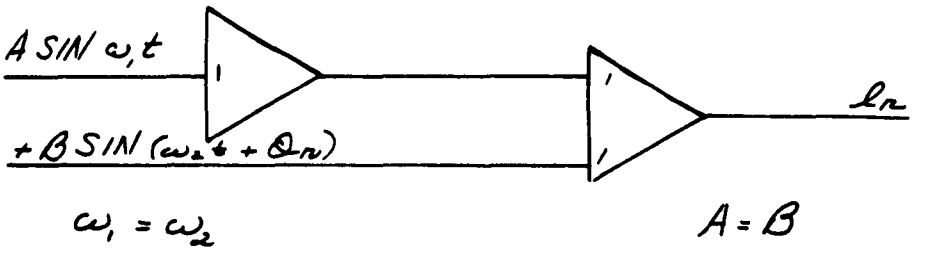

Phase Error Detector Simulation (Ref 17)

Figure 15

$$\ell_n = A \sin \omega_1 t - B \sin (\omega_2 t + \theta_n)$$

if $A = B$ $\quad \omega_1 = \omega_2$

$$\ell_n = A \sin \left(\omega_1 t - \frac{\theta_n}{2} + \frac{\theta_n}{2}\right) - A \sin \left(\omega_1 t + \frac{\theta_n}{2} + \frac{\theta_n}{2}\right)$$

since $\quad -\sin \alpha = \sin(-\alpha)$

then $\ell_n = A\left[\sin \left(\omega_1 t - \frac{\theta_n}{2} + \frac{\theta_n}{2}\right) + \sin \left(-\omega_1 t - \frac{\theta_n}{2} - \frac{\theta_n}{2}\right)\right.$

since $2 \cos \beta \sin \alpha = \sin(\alpha + \beta) + \sin(\alpha - \beta)$

if $\alpha = -\frac{\theta_n}{2}$ $\qquad \beta = \omega_1 t + \frac{\theta_n}{2}$

then $\ell_n = 2A \cos \left(\omega_1 t + \frac{\theta_n}{2}\right) \sin \left(-\frac{\theta_n}{2}\right)$

$$\ell_n = -2A \sin \frac{\theta_n}{2} \left[\cos \left(\omega_1 t + \frac{\theta_n}{2}\right)\right]$$

$$|\ell_n|_{max} = 2A \sin \frac{\theta_n}{2}$$

for small angles $\quad \sin \frac{\theta_n}{2} \doteq \frac{\theta_n}{2}$

$$|\ell_n| = 2A \left(\frac{\theta_n}{2}\right) = A \theta_n$$

Phase Error Detector Analysis

Figure 16

Phase Error Detector Simulation

The Analog Simulation requires that the phase difference between Input Oscillator and VCO be plotted as an output signal. If the negative of A SIN $\omega_1 t$ and + B COS ($\omega_2 t + \theta_n$) are totaled, assuming that A = B and $\omega_1 = \omega_2$, then the output is proportional to the phase angle. Figure 16 demonstrates the theory from which this simulation is derived. Figure 15 illustrates the actual simulation (Ref 19). If the amplitudes of the oscillator vary, the phase error voltage detected will not depend on the phase error alone. With the locking circuit on the VCO, the reading of the phase error detector more closely approximates the phase error.

The next step of the investigation consists of integrating the PLL components and obtaining the dynamic responses.

III. Dynamic Analysis of the Simulated Phase-Lock Loop

The simulation of the Phase-Lock Loop, as shown in Appendix A, was analyzed to determine the characteristics with different filters which make the loop Type Two and Type Three. The system was examined with five filters.

The inputs to the system assumed three forms, step, ramp, and, in Type Three, parabolic. In the Type Two system, the step was set at 1 volt and the ramp at 1 volt/second. In the Type Three system, the step was 1 volt, ramp was .13 volts/second and parabolic was .13 volts/second^2. In terms of frequency

Input	Type Two	Type Three
step	.05 radians/second	.05 radians/second
ramp	.05 radians/second^2	.0065 radians/second^2
parabolic	----------	.0065 radians/second^3

The system was tested by inserting the filter desired and then applying the various input. The system gain was varied to determine the limits of G for stability, and to obtain the best operating point.

Two, Type Two filters of the forms

$$F(s) = \frac{(s + a)(s + b)}{s(s + c)} \qquad \text{where } c > a \text{ and } b \tag{8}$$

and

$$F(s) = \frac{s^2 + a s + b}{s(s + c)} \qquad \text{where } s^2 + a s + b \text{ has complex roots} \tag{9}$$

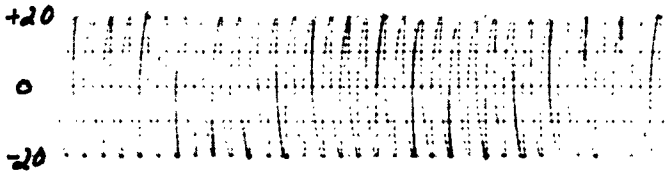

$A \sin \omega_1 t$

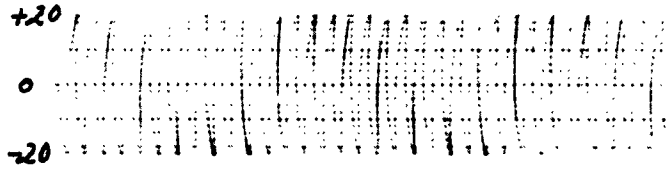

$B \sin \omega_2 t$

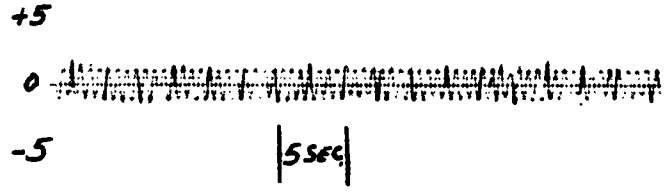

e_w

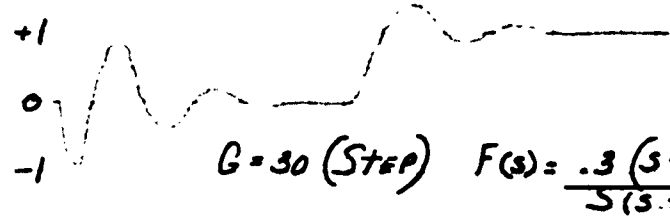

e_o

Step Response for Type Two System

e_n

Figure 17

were attempted, but due to computer instability, oscillations of 8000 cycles/second were generated in the loop and prevented the analysis of the PLL (Ref 5:6 100-105).

The filter used for Type Two (G = 30) is

$$F(s) = \frac{.3\ (s + .1)}{s\ (s + .5)} \qquad \text{(Figures 17 and 18)} \qquad (10)$$

The filter used for Type Two (G = 70) is

$$F(s) = \frac{.3\ (s + .6)\ (s + .1)}{s\ (s + 1)\ \ (s + .5)} \qquad \text{(Figures 19 and 20)} \qquad (11)$$

The filter used for Type Three (G = 150) is

$$F(s) = \frac{.3\ (s + .1)\ (s^2 + 5s + 2.5)}{s^2\ (s^2 + 8s + 20)} \qquad \text{(Figures 21,22 \& 23)} \qquad (12)$$

The above figures are typical results for the gain shown. The figures consist of five separate graphs which correspond to the recorder channels in Appendix A. All scales are marked in volts and the time scale is 5 seconds/cm.

The first curve, A SIN $\omega_1 t$ is the sine output from the input oscillator in the simulation circuit. The frequency is five radians/second up to the point where the input is applied. When the input is applied, the frequency becomes $\omega_1 + \Delta\omega$ where $\Delta\omega$ is a step, ramp, or parabolic inputs.

The second curve, B SIN $\omega_2 t$ is the sine output of the VCO. The frequency is ω_2, and after initial locking oscillation, will be

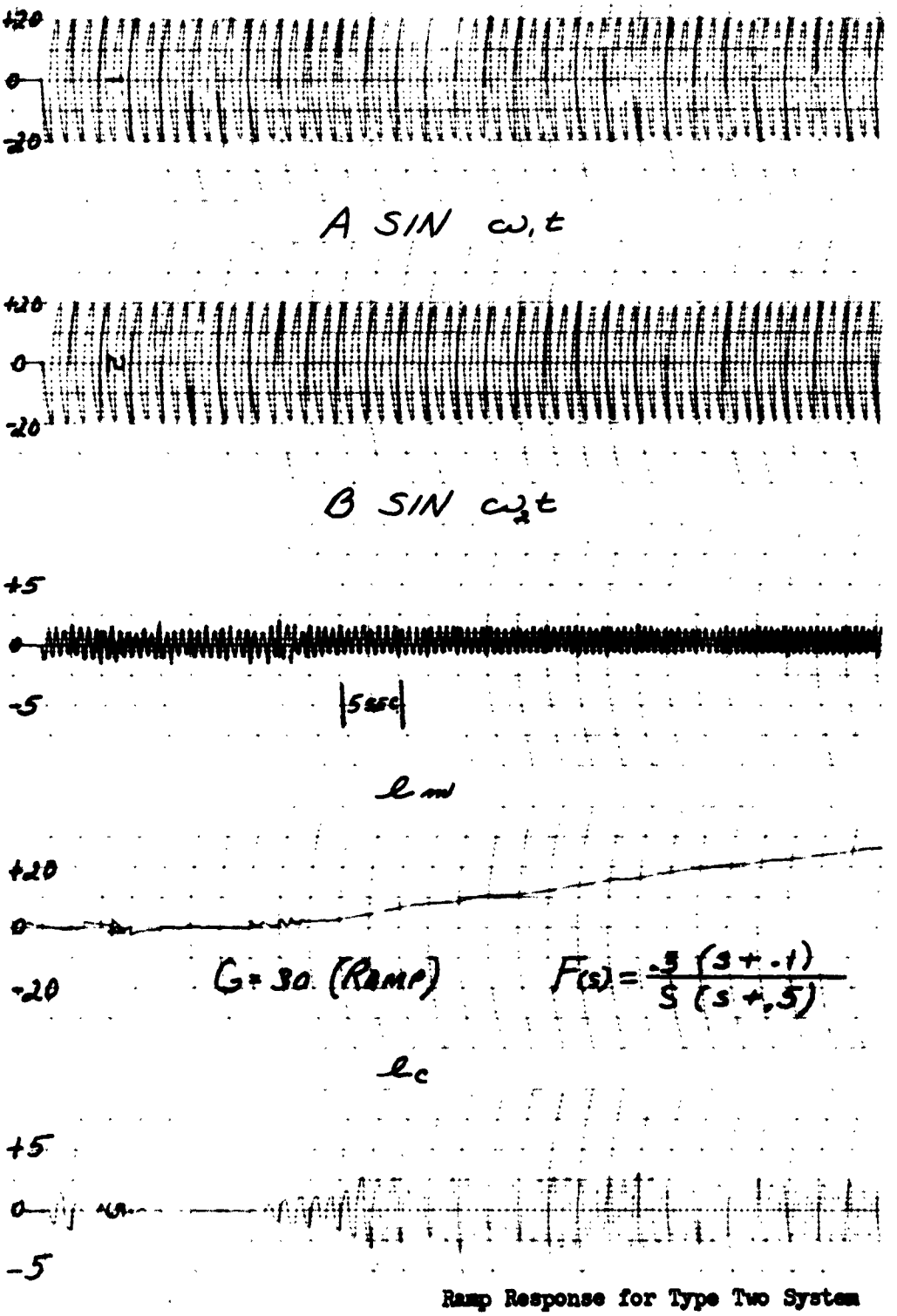

Ramp Response for Type Two System

Figure 18

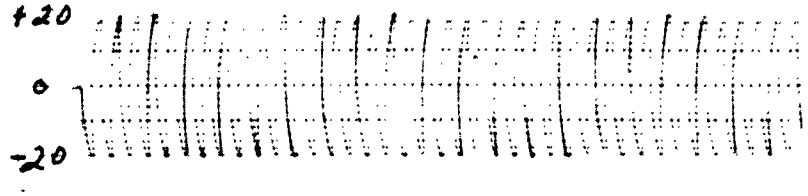

$A \sin \omega_1 t$

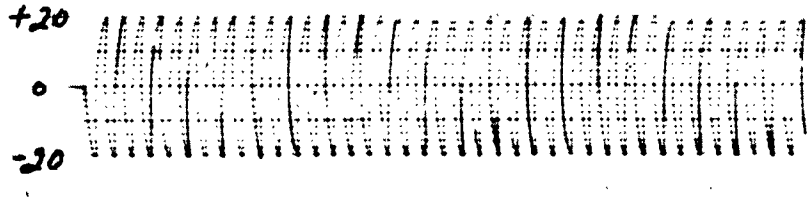

$B \sin \omega_2 t$

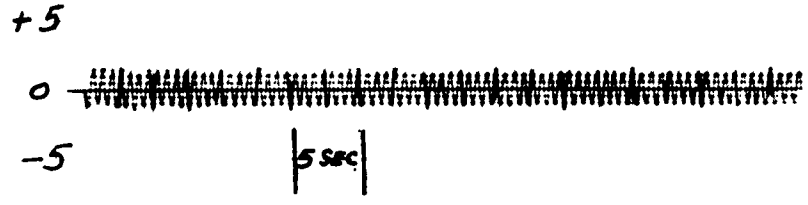

e_m

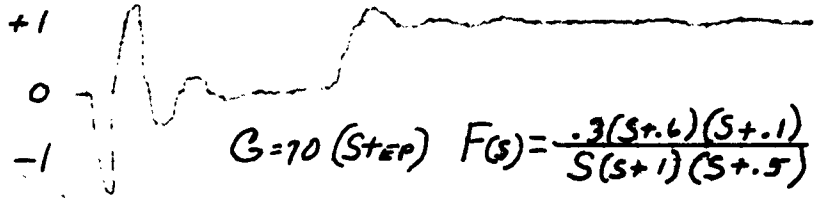

e_c

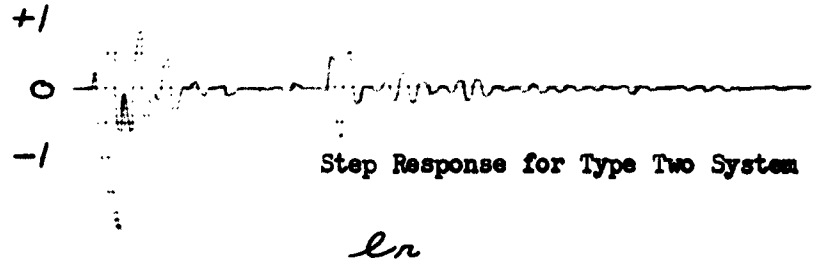

Step Response for Type Two System

e_r

Figure 19

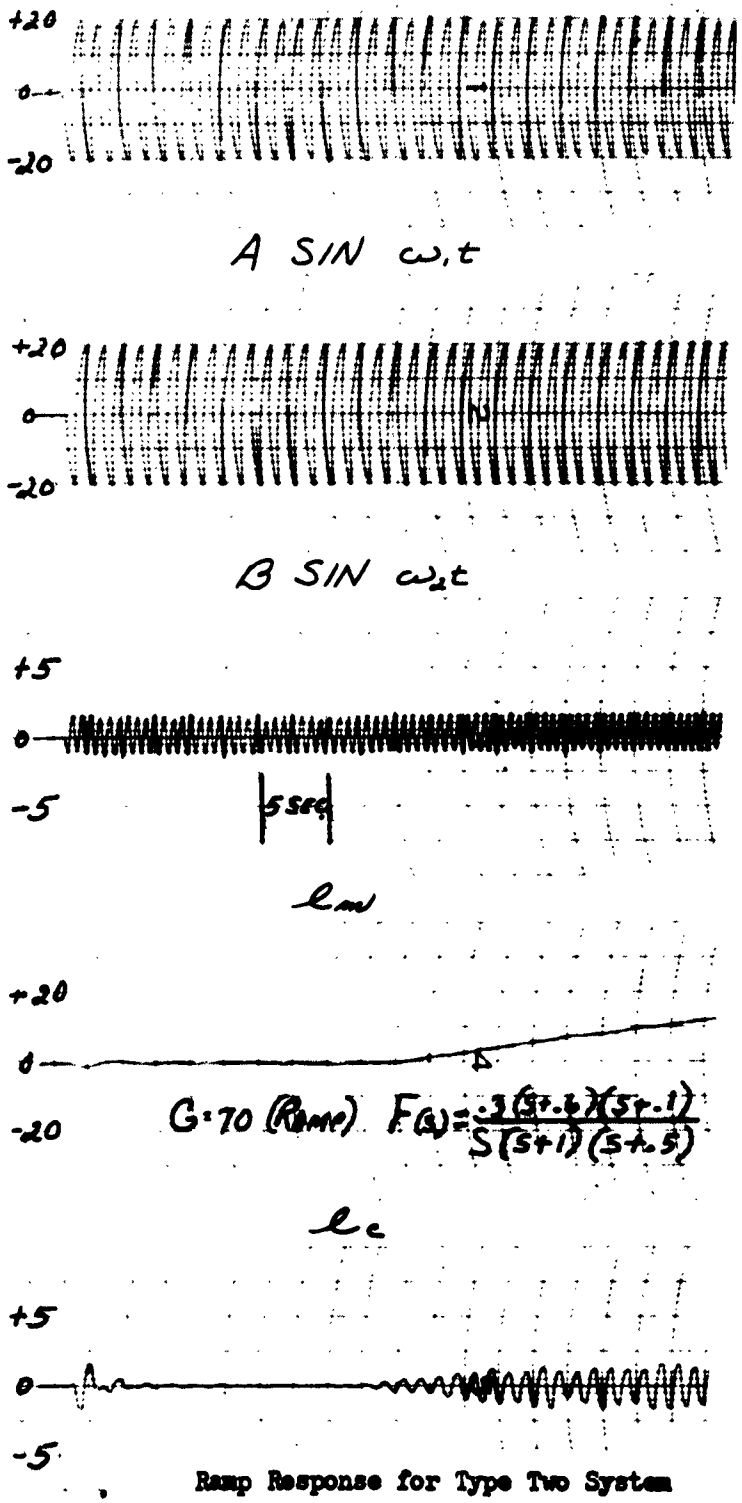

Ramp Response for Type Two System

Figure 20

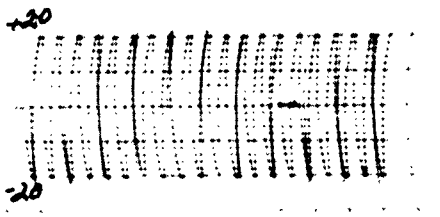

A SIN $\omega_1 t$

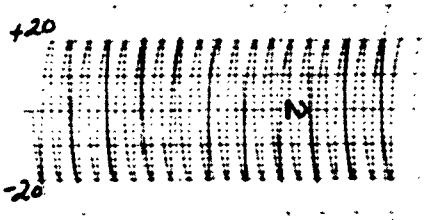

B SIN $\omega_2 t$

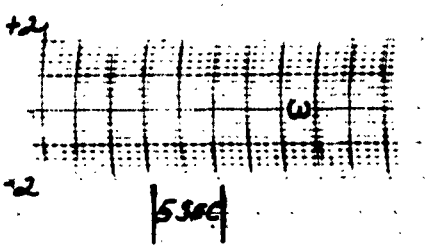

e_{in}

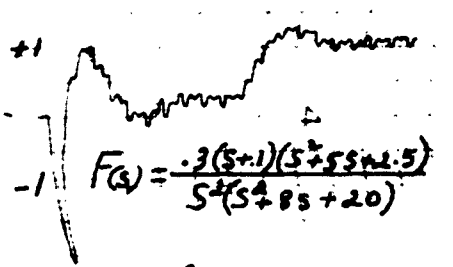

e_c

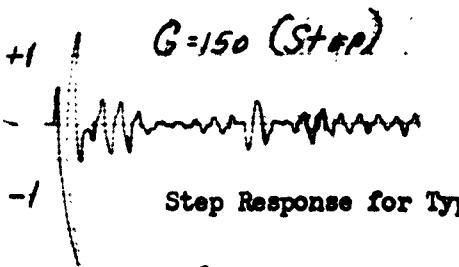

e_n

Figure 21 Step Response for Type Three System

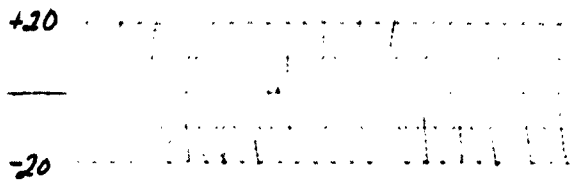

$A \sin \omega_1 t$

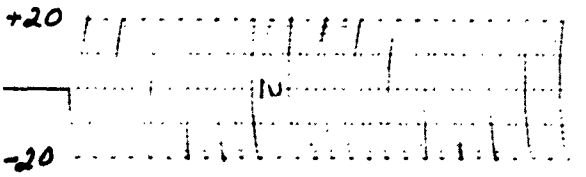

$B \sin \omega_2 t$

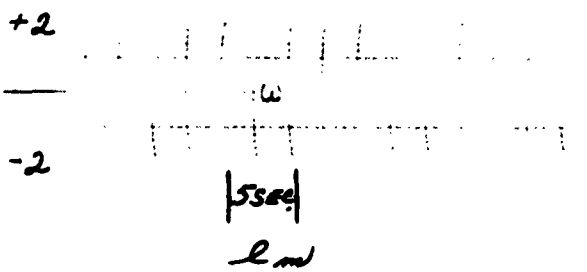

e_m

$$F(s) = \frac{.3(s+.1)(s^2+5s+2.5)}{s^2(s^2+8s+20)}$$

e_c

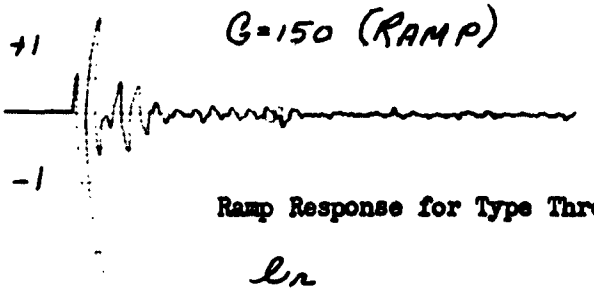

Ramp Response for Type Three System

e_r

Figure 22

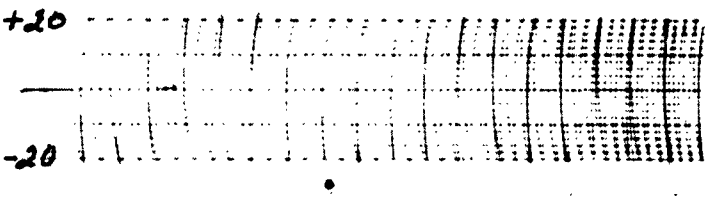

$A \sin \omega_1 t$

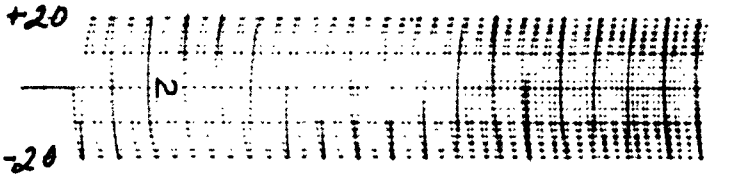

$B \sin \omega_2 t$

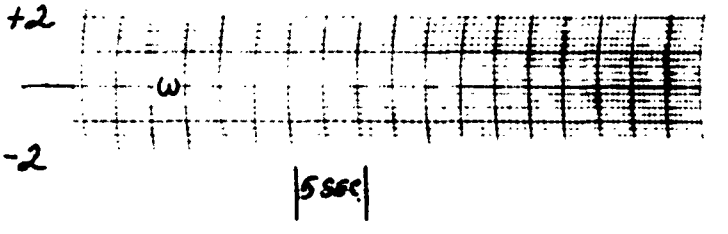

ℓ_m

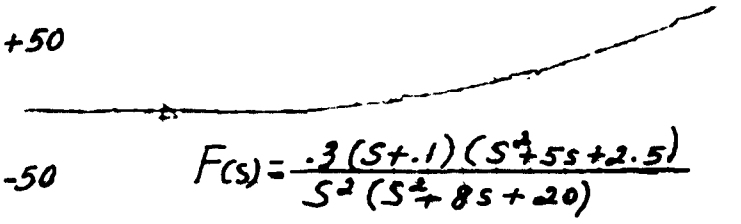

$$F(s) = \frac{.3(s+.1)(s^2+5s+2.5)}{s^2(s^2+8s+20)}$$

ℓ_c

$G = 150$ (Parabolic)

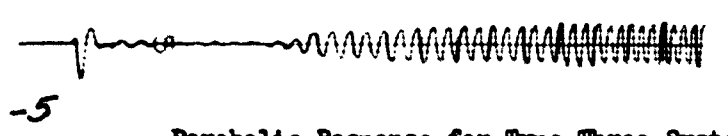

Parabolic Response for Type Three System

ℓ_r

Figure 23

TABLE ONE

COMPARISON OF SYSTEM RESPONSE

INPUT	TYPE	FIGURE	F(S)	RESPONSE	GAIN	Θ_R STEADY STATE RADIANS
STEP	TWO	17	$\frac{S+.1}{S(S+.5)}$	FAIR $t_s \approx 15$ sec	30	0
RAMP	TWO	18	$\frac{S+.1}{S(S+.5)}$	POOR $t_s \approx 22$ sec	30	.100
STEP	TWO	19	$\frac{(S+.1)(S+.6)}{S(S+.5)(S+1)}$	GOOD $t_s \approx 12$ sec	70	0
RAMP	TWO	20	$\frac{(S+.1)(S+.6)}{S(S+.5)(S+1)}$	FAIR $t_s \approx 15$ sec	70	.0625
STEP	THREE	21	$\frac{(S+.1)(S^2+5S+2.5)}{S^2(S^2+8S+20)}$	EXCELLENT $t_s \approx 7$ sec	150	.0075
RAMP	THREE	22	$\frac{(S+.1)(S^2+5S+2.5)}{S^2(S^2+8S+20)}$	EXCELLENT $t_s \approx 7$ sec	150	0
PARABOLIC	THREE	23	$\frac{(S+.1)(S^2+5S+2.5)}{S^2(S^2+8S+20)}$	GOOD $t_s \approx 11$ sec	150	.075

equal to ω_1. In theory ω_2 will follow ω_1 with no error.

The third curve, modulation product (ℓ_m) is the output of the phase detector. This signal is the product of A COS $\omega_1 t$ and B SIN $\omega_2 t$ and contains harmonics plus a DC level, which is equal to the phase error as can be seen in Figure 5.

The fourth curve (ℓ_c) is the control voltage that is applied to the voltage controlled oscillator after filters of the system remove the harmonics. This curve represents the response to the input. In steady state the curve will assume the form of the input.

The fifth curve (ℓ_n) is the phase error voltage and is obtained from the phase error detector. The amplitude of this voltage is a direct measure of the difference in phase between the input oscillator and the VCO.

The important characteristics of the system are:

1. The type of filter used
2. The gain of the system used
3. The type of input used
4. The type of overall system

After selecting or setting the above, the characteristics of the system's performance are:

1. The steady state phase error of the system
2. The general characteristics of transient response

Table One gives the comparison of the three systems under step, ramp, and parabolic inputs. These curves and tables illustrate the reason for the choosing of the higher degree Type Two filter for remainder of this report.

The complete step, ramp, and parabolic responses are given in Appendix C and Appendix D for the Type Two and Type Three systems respectively.

A limitation of the Analog Computer Simulation is seen in Figure 20 and Appendix Figures C-15, C-17, D-18, and D-21. When a high forward gain is used, the inherent noise of the DC amplifiers used in the Analog Computer produces a considerable amount of noise in the control signal.

Stability Point

When the system is started at t = 0, the loop will oscillate until both frequency and phase of the input oscillator and VCO are exactly alike. One point of interest is that the loop has the ability to lock at one of two points. Lock can be obtained at 0 or π radians phase difference depending on the initial phase of the input oscillator and VCO. Whenever $(\phi - \theta)$ is positive and between 0 and π radians, the loop will lock in at 0. When $(\phi - \theta)$ is negative and between 0 and π radians, it will lock in at π radians phase difference. This can best be seen by looking at the expression for the output of the phase detector

$$e_m = 2 \text{ SIN } (2\omega t + \phi + \theta) + 2 \text{ SIN } (\phi - \theta) \qquad (13)$$

when the $(\phi - \theta)$ is negative the DC level 2 SIN $(\phi - \theta)$ becomes negative since

$$\text{SIN } (-\alpha) = - \text{ SIN } \alpha \qquad (14)$$

This negative voltage will tend to decrease the phase of the VCO until the point where SIN α = SIN $-\alpha$ = 0 which will happen when $\phi - \theta$ = 0 radians.

This means the loop will lock at phase difference of π radians. The phase shifter assured that $(\phi - \theta)$ is always positive and will make the loop lock in at the 0 radians phase difference stability point.

Static Phase Error

From the Phase Error Detector Analysis in Figure 16

$$|\ell_n|_{MAX} = A\,\theta_n \tag{15}$$

if $E_N \equiv$ peak to peak voltage of ℓ_n

then

$$E_N = 2\,A\,\theta_n \tag{16}$$

$$\therefore \theta_n = \frac{E_N}{2\,A} = \frac{E_N}{40} \tag{17}$$

IV. Theoretical Servo Analysis of the Phase-Lock Loop

The servo block diagram of the PLL is given in Figure 24. It is a simple unity feedback system in ω . K_1 represents the gain of the Phase Detector, while the 1/s term shows the integration of the frequency which is equal to phase difference.

If K_1, K_2, K_3, K_4, N(s), F(s) are known, we can plot the Root Locus. The Root Locus is a plot of the roots of the characteristic equation (1 + G H) of the closed-loop system as a function of gain (Ref 2). From the Root Locus, one can obtain the roots of the characteristic equation and the important parameters such as, time to peak overshoot (t_p), settling time (t_s), and peak overshoot (M_p).

M_p is defined as the maximum overshoot of the steady state value. t_p is the time required to reach the maximum overshoot. A small t_p means a quicker response. t_s is the time required for the response to come within two percent of the steady state value. A small t_s indicates the system tends to be more stable.

Phase Detector

In this investigation the multiplier was used for the phase detector. The same results could have been obtained by using the balanced modulator (Ref 19). The output of the phase detector took on the form in Figure 25.

When using standard computer equipment, the term is divided by 100.

If A = B = 20 then $K_1 = 2$

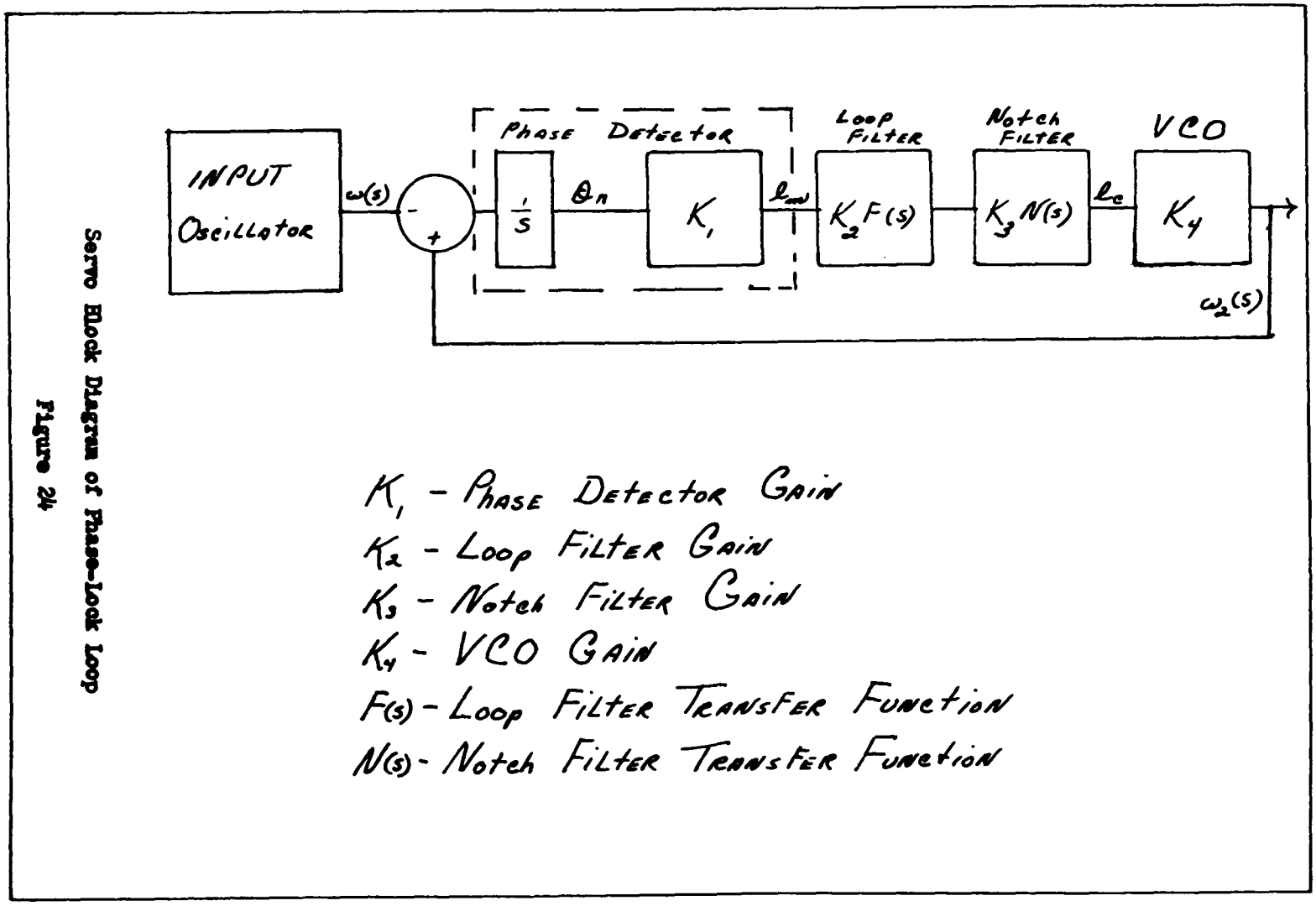

Figure 24

Servo Block Diagram of Phase-Lock Loop

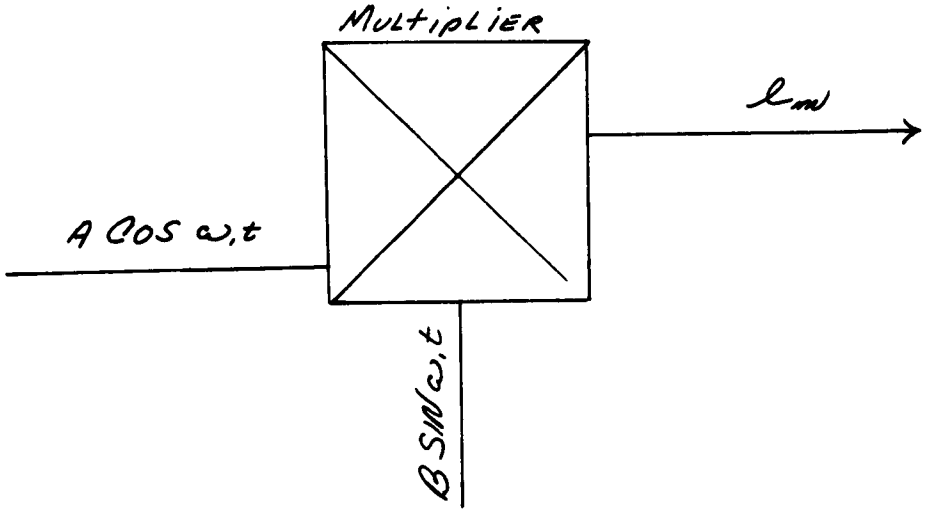

$$e_m = [A\,COS(\omega_1 t + \theta)]\ [B\,SIN(\omega_2 t + \phi)]$$

SINCE $SIN\alpha COS\beta = \frac{1}{2} SIN(\alpha+\beta) + \frac{1}{2} SIN(\alpha-\beta)$

$$e_m = \frac{AB}{2}\left[SIN(\omega_2 t + \phi + \omega_1 t + \theta) + SIN(\omega_2 t + \phi - \omega_1 t - \theta)\right]$$

$\omega_1 = \omega_2$

$$e_m = \frac{AB}{2}\left[SIN(2\omega t + \phi + \theta) + SIN(\phi - \theta)\right]$$

$$e_m = K_1 SIN(2\omega t + \phi + \theta) + K_1 SIN(\phi - \theta)$$

Phase Detector Analysis

Figure 25

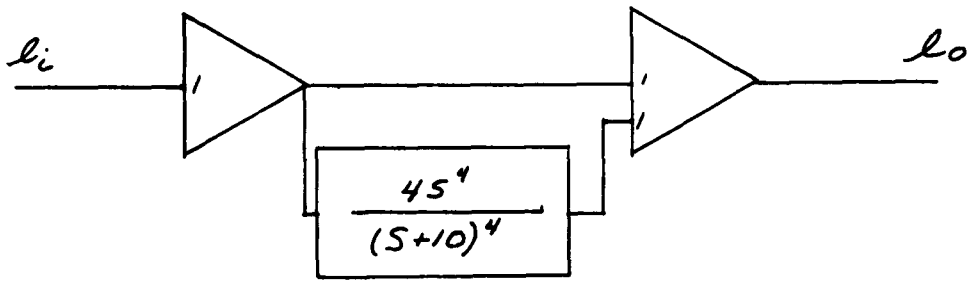

$$\frac{e_o}{e_i} = N(S) = 1 + \frac{4S^2}{(S+10)^4}$$

$$N(S) = \frac{(S+10)^4 + 4S^2}{(S+10)^4}$$

$$N(S) = \frac{5(S^4 + 8S^3 + 120S^2 + 800S + 2000}{(S+10)^4}$$

$$N(S) = \frac{5(S+4+j2)(S+4-j2)(S+j10)(S-j10)}{(S+10)^4}$$

$$\therefore K_3 = 5$$

Notch Filter Transfer Function (Ref 17:34A)

Figure 26

Loop Filter

The gain K_1 of the loop filter transfer function is taken arbitrarily as .3 . The remaining part of the transfer function is dependent on the type system, and the filtering desired. Two systems, one Type Two and one Type Three were finally selected, for analysis. The two filters are

$$F(s) = \frac{.3\ (s + .6)\ (s + .1)}{s\ \ (s + 1)\ (s + .5)} \tag{18}$$

and

$$F(s) = \frac{.3\ (s^2 + 5s + 2.5)\ (s + .1)}{s^2\ (s^2 + 8s + 20)} \tag{19}$$

Notch Filter

The notch filter transfer function is dependent on the high pass filter. The determination of the N(s) is given in Figure 26 (Ref 19).

Voltage Controlled Oscillator

Adjusting the input to the VCO by 100 volts, varies the VCO frequency by 5 radians. Therefore, the VCO sensitivity is .05 rps/volt. Any variable gain must be multiplied by .05. Lt. Wendland determined the dynamic transfer function of the VCO to be

$$VCO\ (s) = \frac{289}{(s + 6 + j16)\ (s + 6 - j16)} \tag{20}$$

$$\therefore\ K_4 = (289)\ (.05)\ G$$

(Ref 19:44)

Using normal Servo techniques, the forward transfer function becomes, for Type Two

$$G(s) = \frac{G_T(s^2 + 100)(s + .6)\ (s + .1)(s + 4 - j2)(s + 4 = j2)}{s^2\ (s + .5)(s + 1)(s + 6 + j16)(s + 6 - j16)(s + 10)} \qquad (21)$$

where $G_T = (5)\ (2)\ (.3)\ (289)\ G$

$H(s) = 1$

The Root Locus plots are given in Figures 27 and 28.

For Type Three

$$G(s) = \frac{G_T\,(s^2 + 100)(s + .1)(s^2 + 5s + 2.5)(s + 4 + j2)(s + 4 - j2)}{s^3\,(s^2 + 8s + 20)(s + 6 - j16)(s + 6 + j16)(s + 10)^4} \qquad (22)$$

where $G_T = (5)\ (2)\ (.3)\ (289)\ G$

$H(s) = 1$

The Root Locus plots are given in Figures 29 and 30.

Figures 31, 32, and 33 illustrate the Root Locus if the poles and zeros of the VCO and notch filter are neglected. It clearly shows that great error is presented if we neglect these poles and zeros when operating with the present filter under Type Three conditions.

When the poles and zeros of the forward transfer function are known, the Root Locus was accurately plotted by the Digital Computer, and the thesis written by Lt. Paskin with improvements by Captain Richards of the Mathematics Department. The program and operating instructions for the IBM 1620 are found in Appendix B.

Theoretical Static Phase Error

If $\Delta\,\omega$ is the steady state error of the system, then the theoretical phase error of the system can be derived.

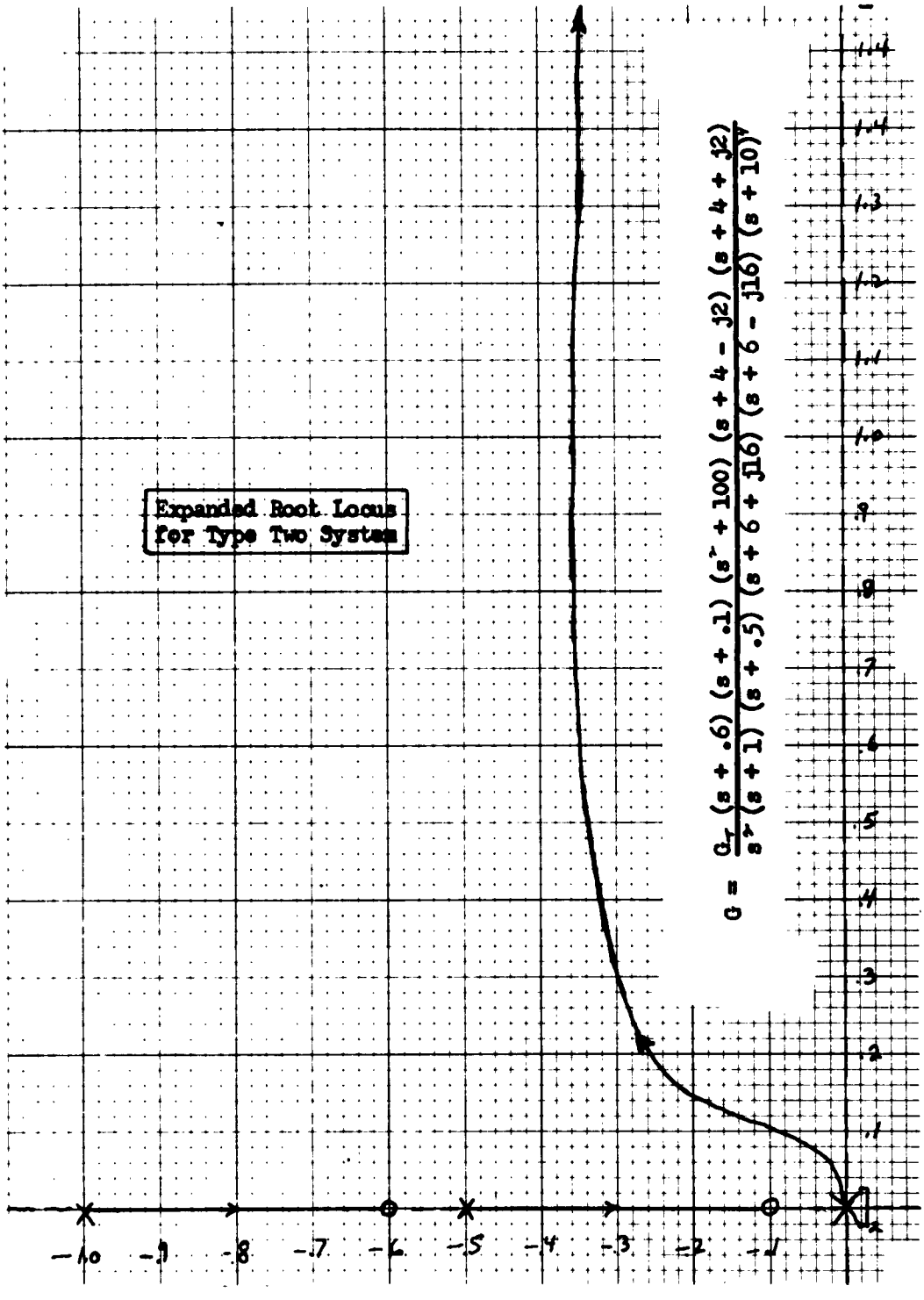
Expanded Root Locus
for Type Two System
$G = \frac{G_T (s + .6)(s + .1)(s^2 + 100)(s + 4 - j2)(s + 4 + j2)}{s^2 (s + 1)(s + .5)(s + 6 + j16)(s + 6 - j16)(s + 10)}$
-10
-9
-8
-7
-6
-5
-4
-3
-2
-1

Figure 27

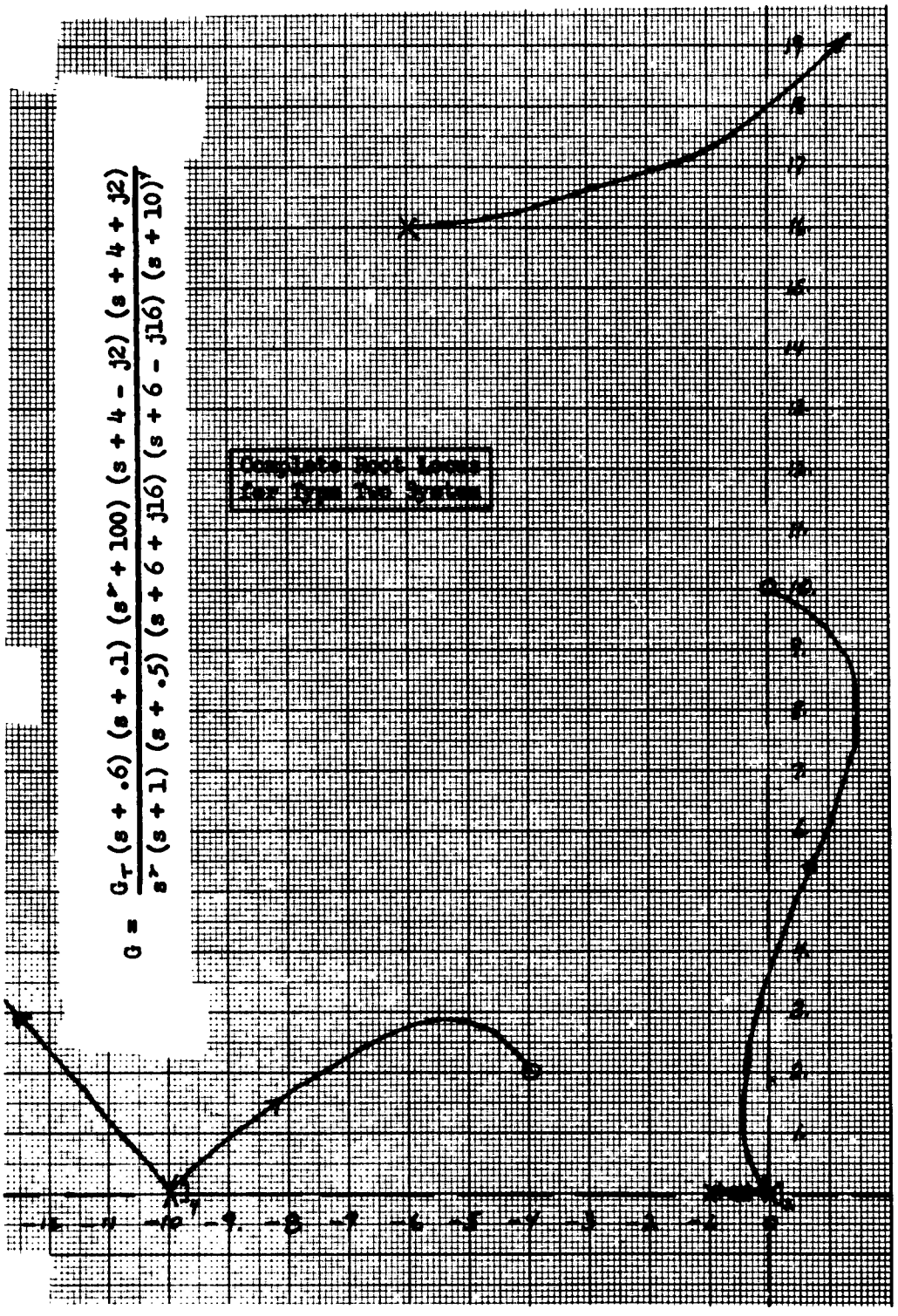
Complete Root Locus
For Type Two System
$G = \frac{G_T (s + .6)(s + .1)(s^2 + 100)(s + 4 - j2)(s + 4 + j2)}{s^2 (s + 1)(s + .5)(s + 6 + j16)(s + 6 - j16)(s + 10)^2}$

Figure 28

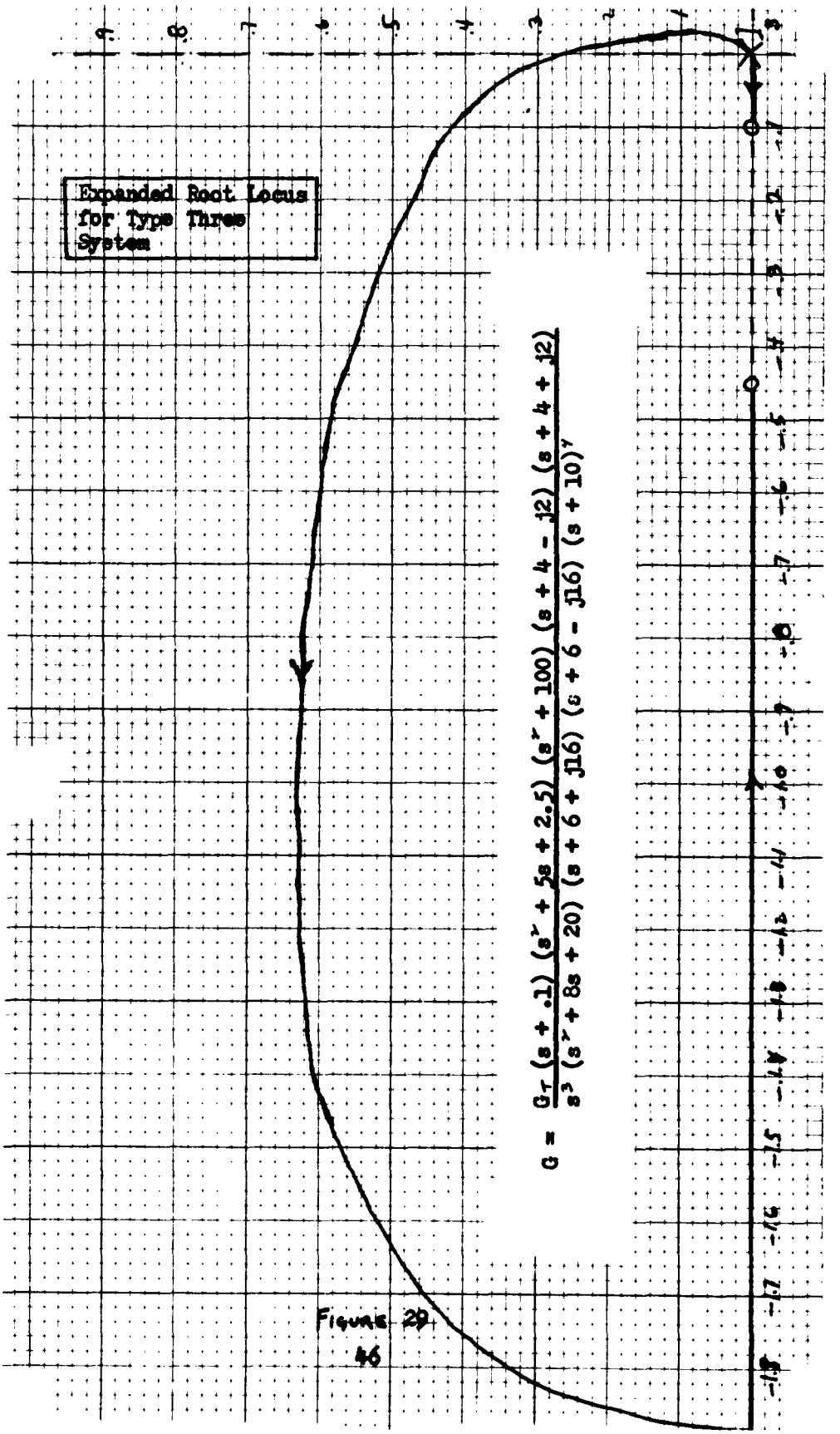
Expanded Root Locus
for Type Three
System
$G = \frac{G_T (s + .1)(s^2 + 5s + 2.5)(s^2 + 100)(s + 4 - j2)(s + 4 + j2)}{s^3 (s^2 + 8s + 20)(s + 6 + j16)(s + 6 - j16)(s + 10)^2}$

Figure 29

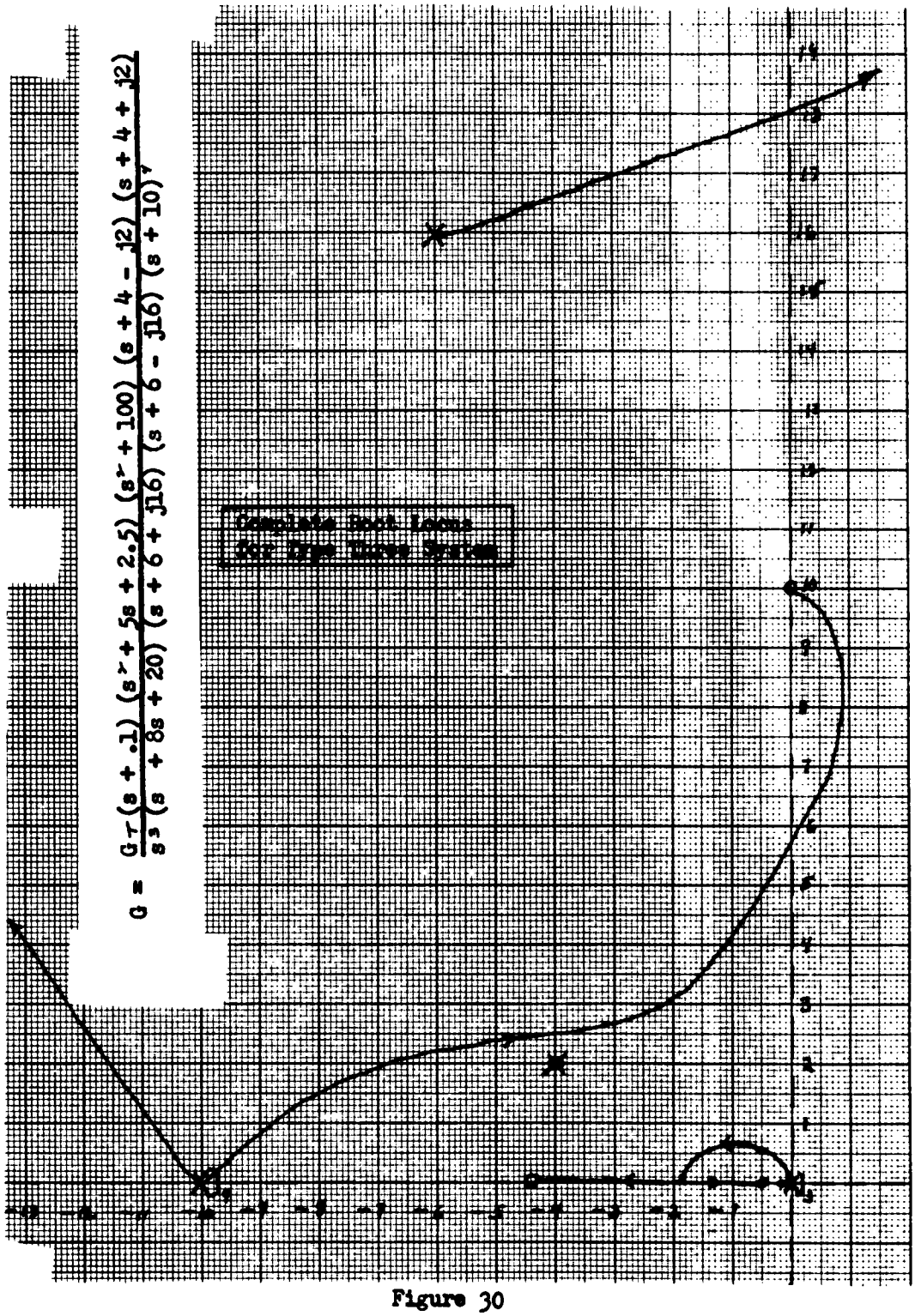
Complete Root Locus
For Type Three System
$G = \frac{G_T(s+.1)(s^2+5s+2.5)(s^2+100)(s+4-j12)(s+4+j12)}{s^3(s+8s+20)(s+6+j16)(s+6-j16)(s+10)^2}$

Figure 30

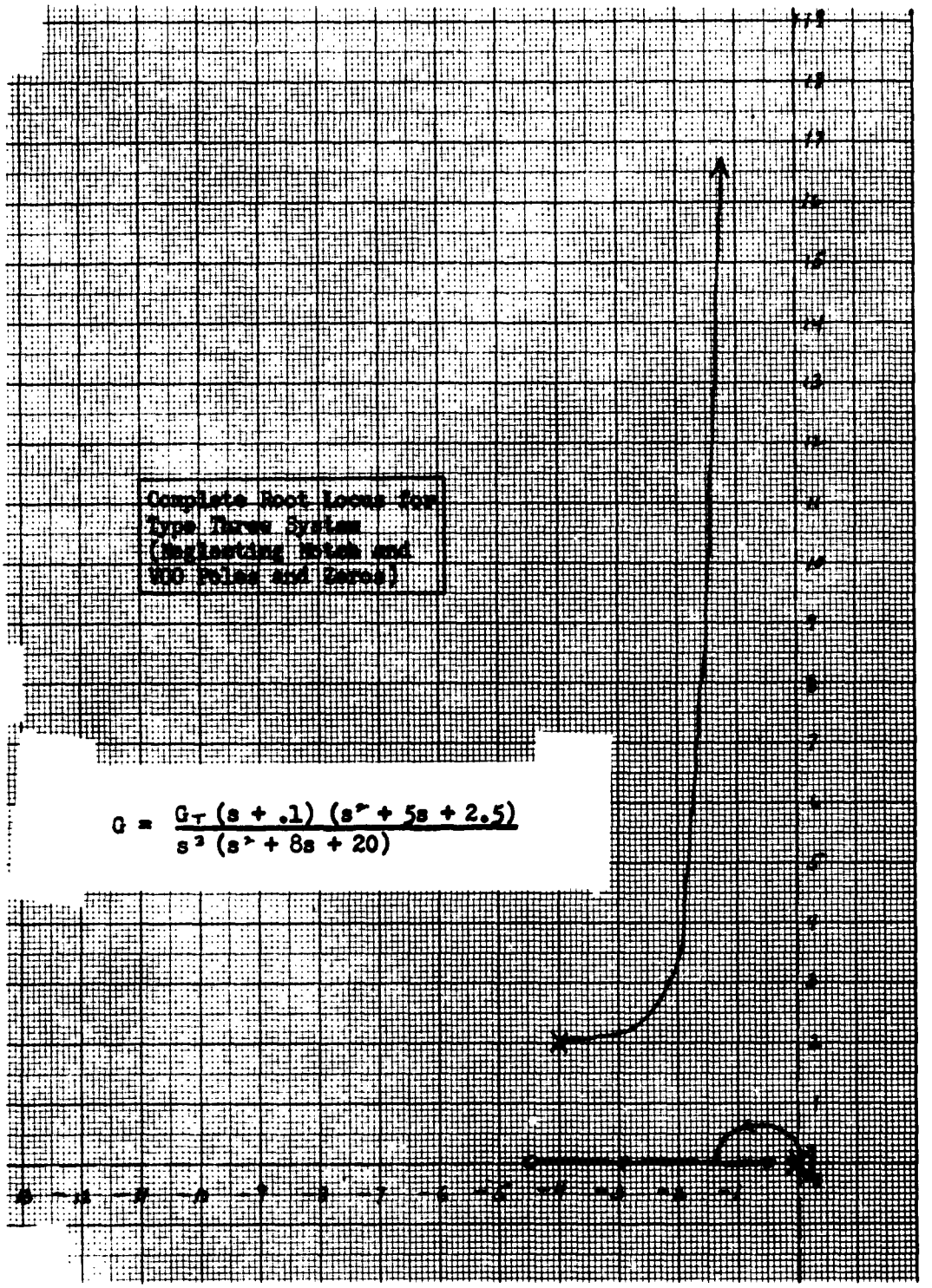
Complete Root Locus for Type Three System (Neglecting Notch and 400 Poles and Zeros)
$G = \frac{G_T (s + .1)(s^2 + 5s + 2.5)}{s^3 (s^2 + 8s + 20)}$

Figure 31

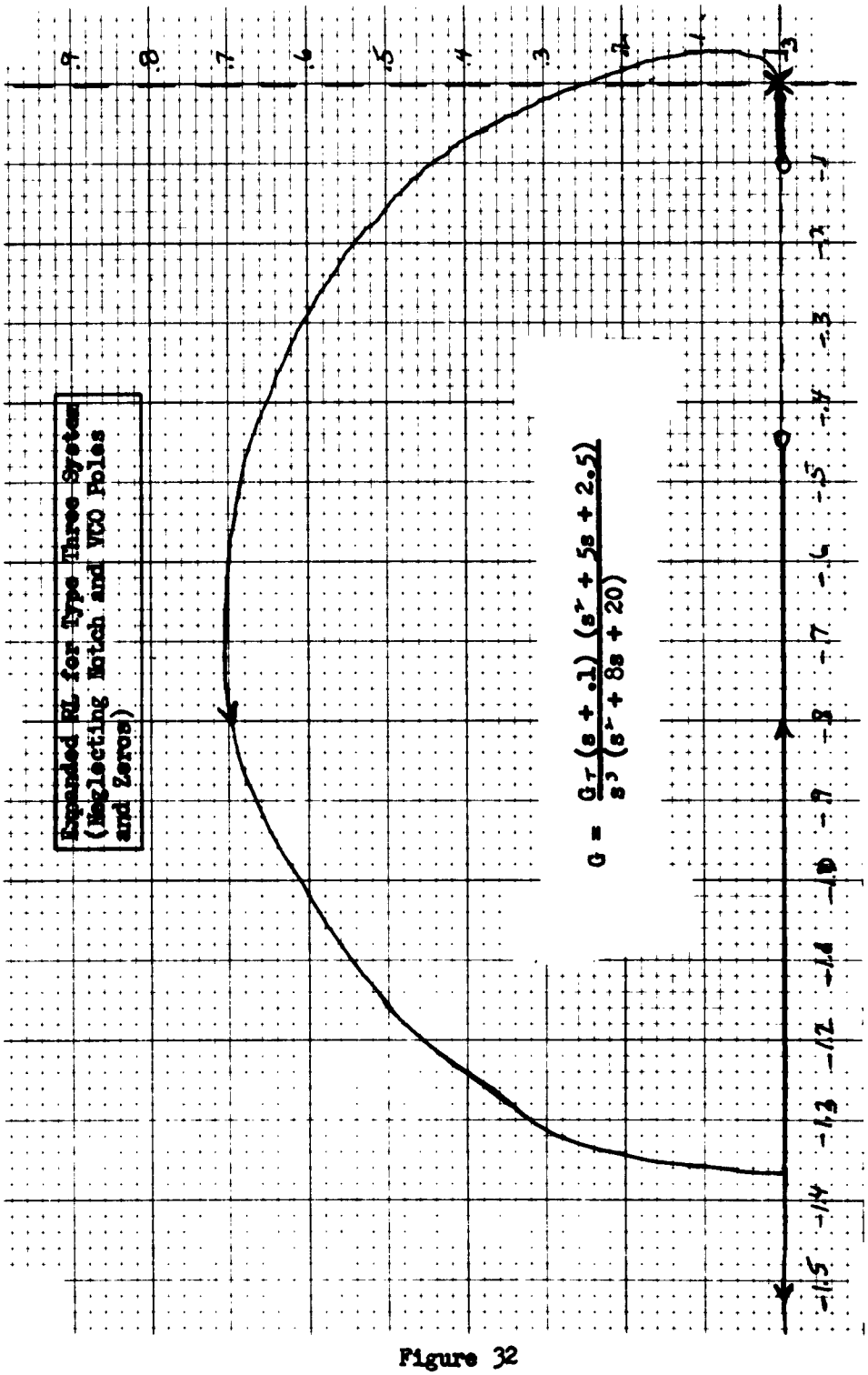
Expanded RL for Type Three System
(Neglecting Notch and VCO Pole
and Zeros)
$G = \frac{G_T(s+.1)(s^2+5s+2.5)}{s^3(s^2+8s+20)}$

Figure 32

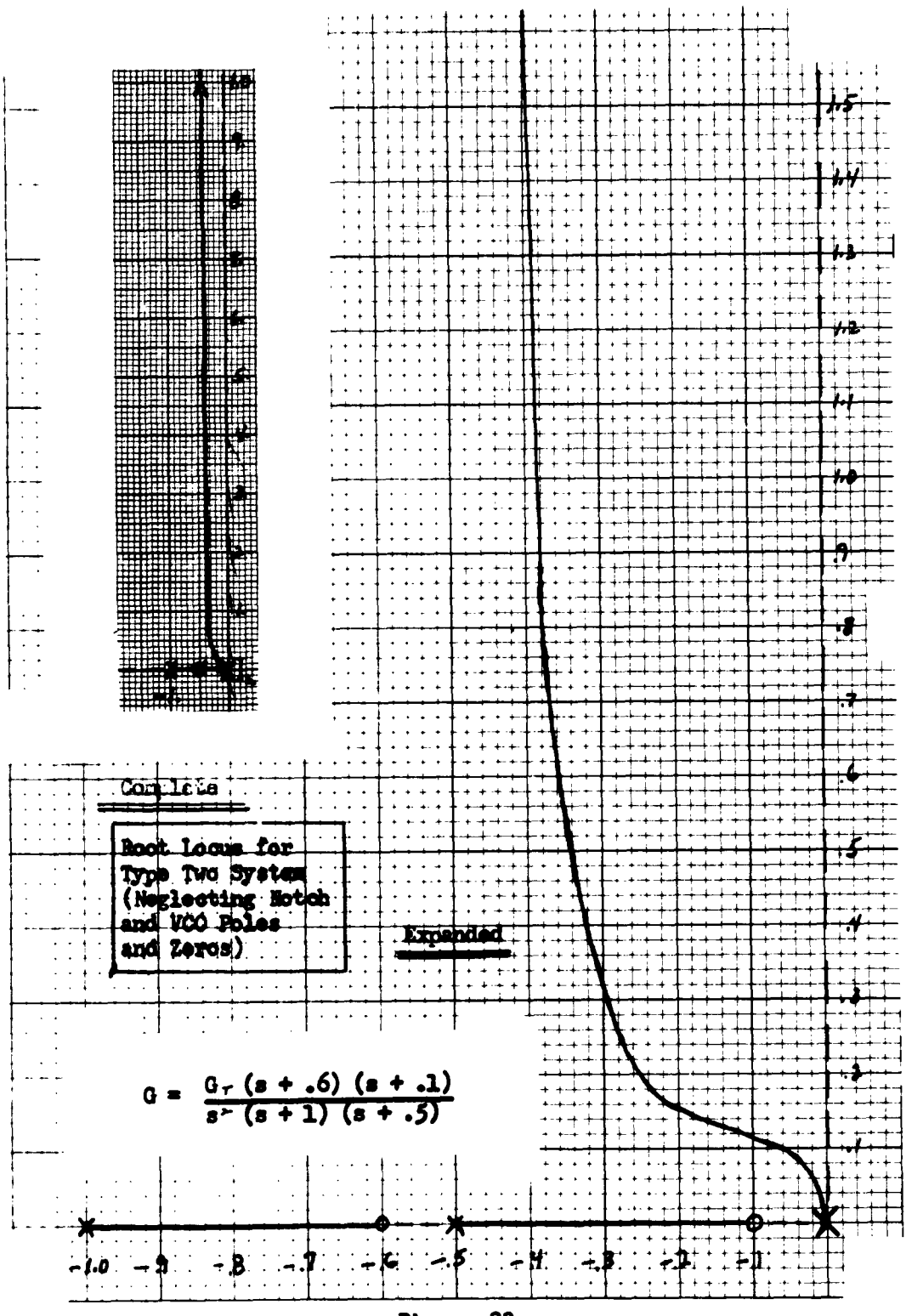
Complete
Root Locus for Type Two System (Neglecting Notch and VCO Poles and Zeros)
Expanded
$G = \frac{G_T (s + .6)(s + .1)}{s^2 (s + 1)(s + .5)}$
-1.0
-.9
-.8
-.7
-.6
-.5
-.4
-.3
-.2
-.1

Figure 33

From Figure 24

$$\ell_m = K_1 \theta_n \tag{23}$$

$$\ell_e = K_2 K_3 F(s) N(s) \tag{24}$$

$$\Delta\omega = K_4 \ell_e = K_1 K_2 K_3 K_4 F(s) N(s) \tag{25}$$

$$\therefore \theta_n = \frac{\Delta\omega}{K_1 K_2 K_3 K_4 N(s) F(s)} \tag{26}$$

For a Type Two system

a. For a step input

$$\Delta\omega = \frac{\omega(t)_{ss}}{K_0'} \tag{27}$$

where K_0' is the step static error coefficient, defined as

$$K_0' \equiv \lim_{S \to 0} G(s) = \infty \tag{28}$$

(Ref 2:123-129)

$$\therefore \Delta\omega = 0$$

and $$\theta_n = 0$$

b. For a ramp input, where K_1' is the ramp static error coefficient

$$K_1' \equiv \lim_{S \to 0} sG(s) = K_1 K_2 K_3 K_4 N(s)\Big|_{S=0} \quad F(s)\Big|_{S=0} \tag{29}$$

$$\Delta\omega = \frac{\Delta\omega(t)\ (ss\ )}{K_1'} = \frac{R_1}{K_1'} \tag{30}$$

where R_1 is the input (Ref 2:123-129)

$$\therefore \theta_n = \frac{\Delta\omega}{K_1 K_2 K_3 K_4 N(s) F(s)} = \frac{R_1}{(K_1 K_2 K_3 K_4 N(s) F(s))^2} \tag{31}$$

In a like manner for Type Three

$$\mathcal{O}_n = 0 \qquad \text{for step and ramp inputs}$$

and

$$\mathcal{O}_n = \frac{R_2}{(K_1 K_2 K_3 K_4 N(s) F(s))_2} \text{ for parabolic inputs.} \quad (32)$$

V. Results, Conclusions, and Recommendations

Results

The theoretical values of M_p, t_p, and t_s, were found using the conventional Root Locus methods from the location of the closed loop poles and zeros. In both cases, there is a real root that must be considered to obtain the accurate values of M_p, t_p, and t_s (Ref 2:11 264-268).

Table Two illustrates the theoretical and experimental values of M_p, t_p, t_s, and $\mathcal{O}_n$. The M_p, t_p, and t_s were determined by the step response of the system. The $\mathcal{O}_n$ was obtained for Type Two from the ramp, and for Type Three from the parabolic. The values compare favorably.

Stray Voltage Error. The amplifiers of the Analog Computer tend to drift during operation. Any drift in the amplifier is integrated in the loop and becomes a parabolic error. This error will vary with different gain or may even change from day to day, or run to run. An example for G = 150 Type Three is given in Figure 35. An error of this type produces a growing phase error in Type Two, while in Type Three it produces a constant phase error. This error can be subtracted from the steady state phase error found in Type Three.

Random Input Response. The final step in the dynamic analysis of the Phase-Lock Loop was the response of the system under random inputs. To better exhibit the quality of response of the Type Two and Type Three system, a Type One system using the filter designed by Lt. Wendland was

Table Two

Comparison of Theoretical and Experimental Values

System Type	Experimental				Theoretical			
	M_p	T_p sec	T_s sec	θ_n Radians	M_p	T_p Sec	T_s sec	θ_n Radians
Two $G = 70$	1.20	2.5	7.5	.0625	1.258	2.33	10.1	.083
Three $G = 150$	1.25	3.5	7.0	.075	1.34	3.8	8.2	.087

$$F(s) = \frac{.3}{(S+.5)}$$

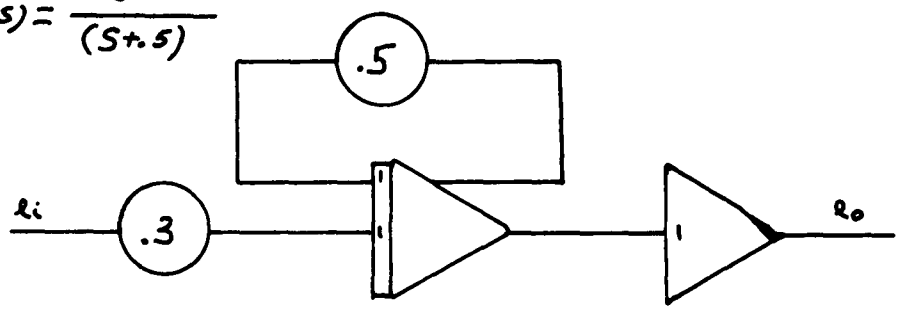

Type One Filter

Figure 34

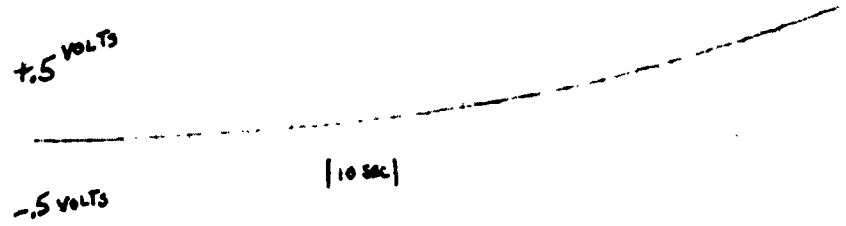

l_a

CONTROL VOLTAGE

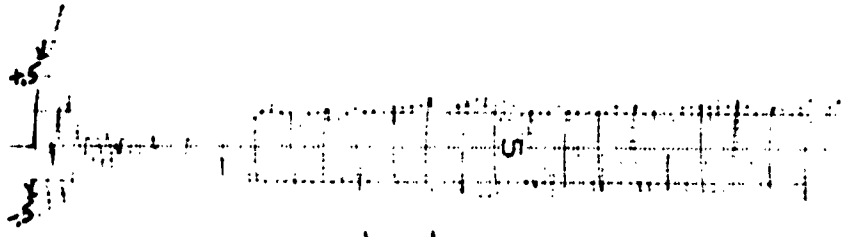

l_b

PHASE ERROR VOLTAGE

Stray Error Voltage

Figure 35

GE/EE/62-20

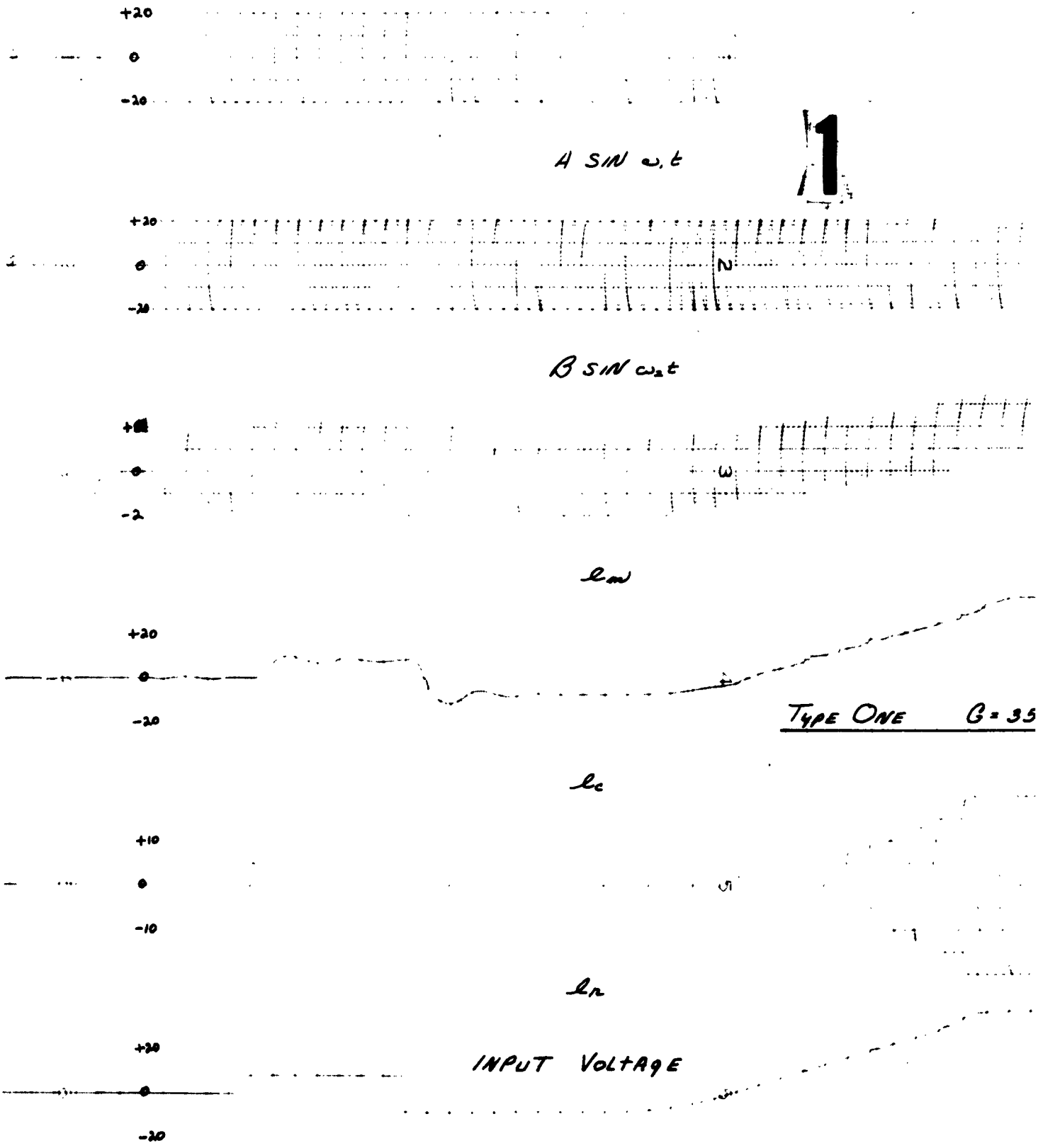
+20
0
-20
A SIN ω₁t
1
+20
0
-20
N
B SIN ω₂t
+2
0
-2
ω
ℓm
+20
0
-20
TYPE ONE G = 35
ℓc
+10
0
-10
ℓn
+20
0
-20
INPUT VOLTAGE

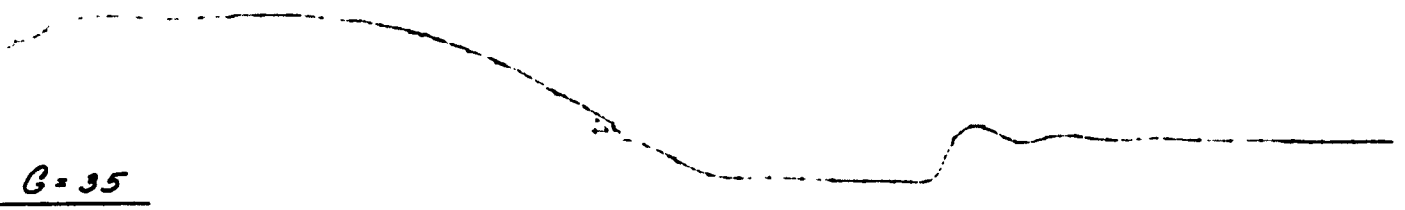

Random Response for Type One System

FIGURE 36

CE/EE/62-20

1

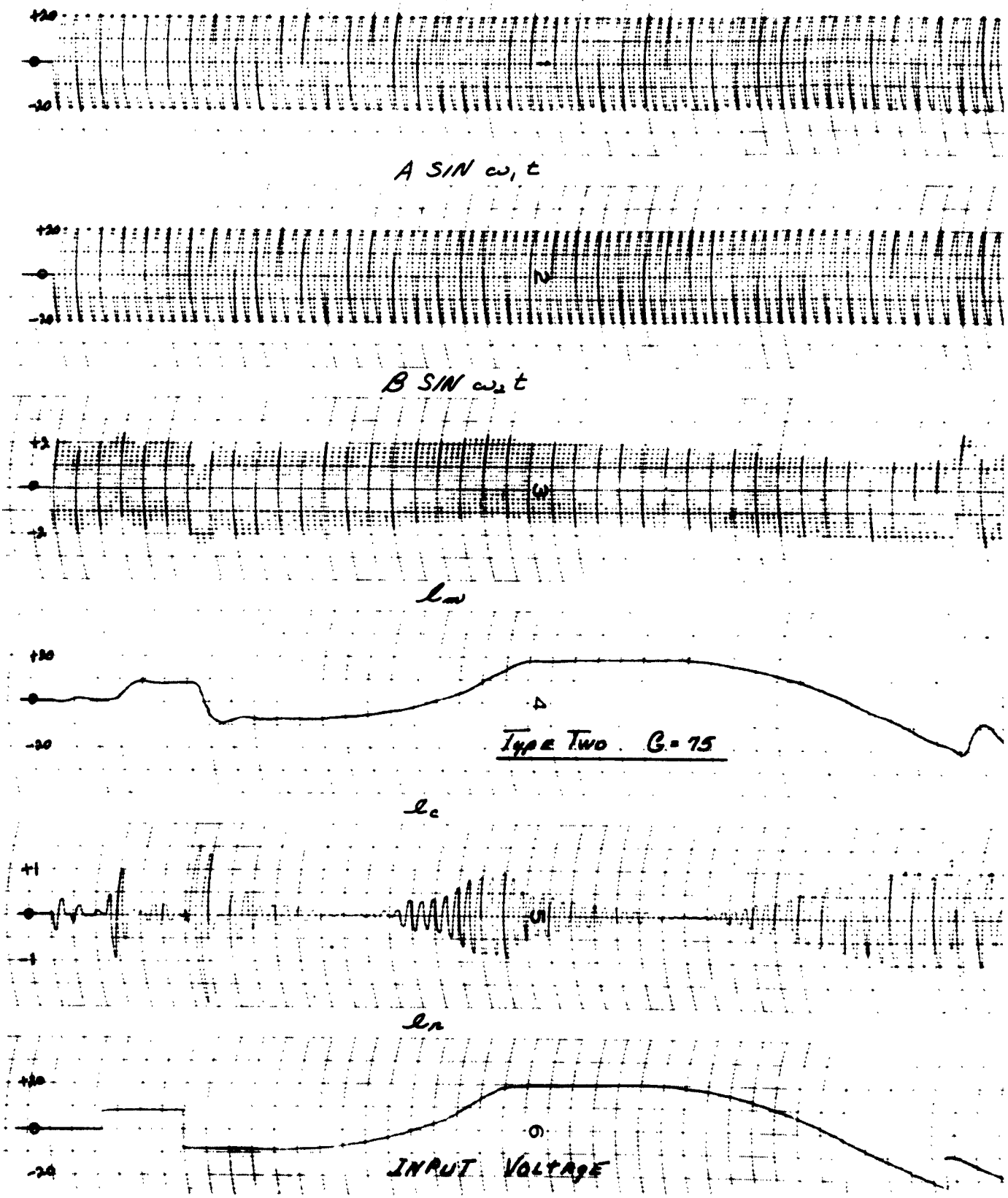
+20
-20
A SIN ω, t
+20
-20
B SIN ω₂ t
+2
-2
I_{ω}
+30
-20
Type Two. G = 75
I_c
+1
-1
I_n
+40
-20
INPUT VOLTAGE

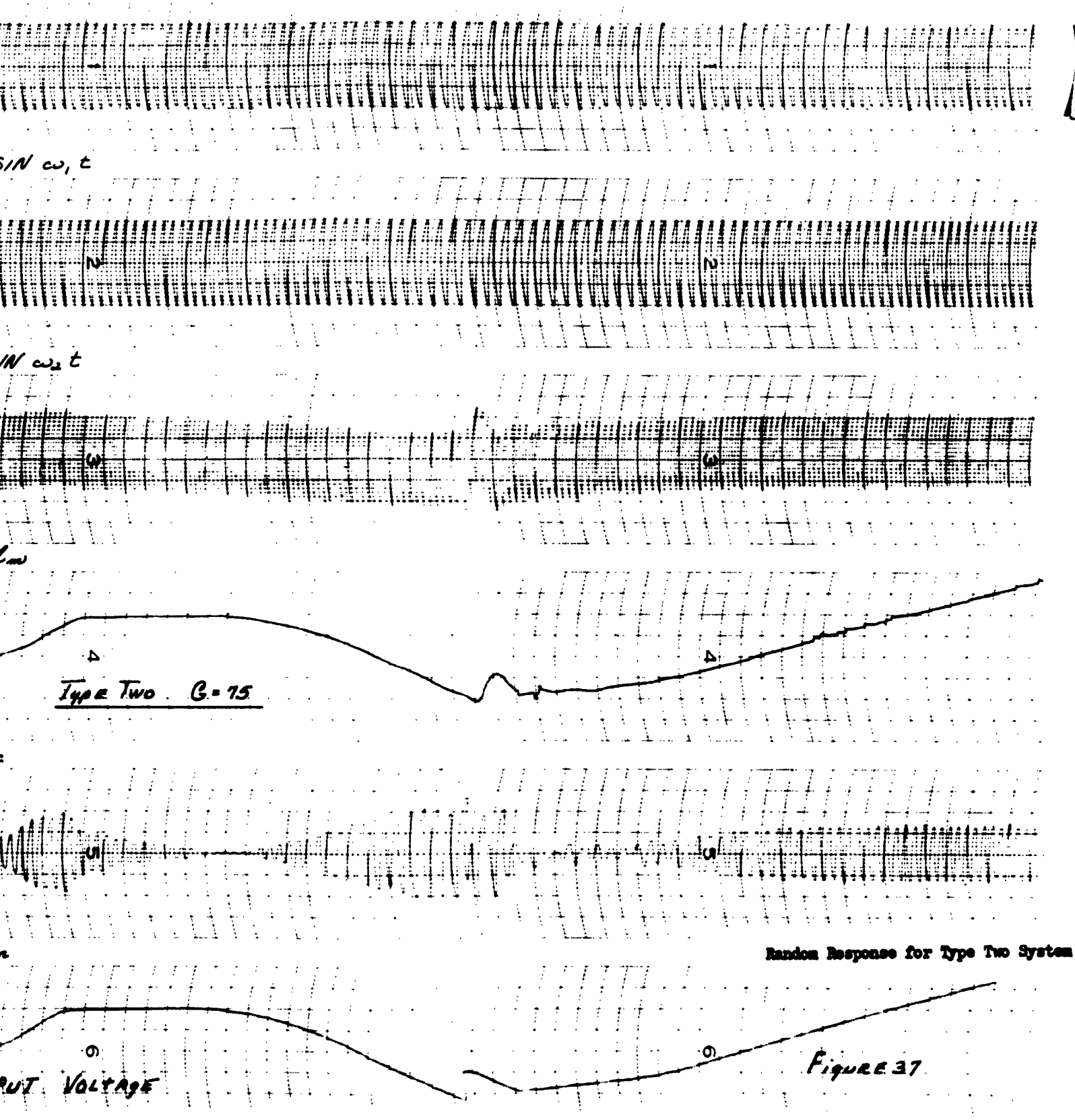

Random Response for Type Two System

Figure 37

GE/EE/62-20

1

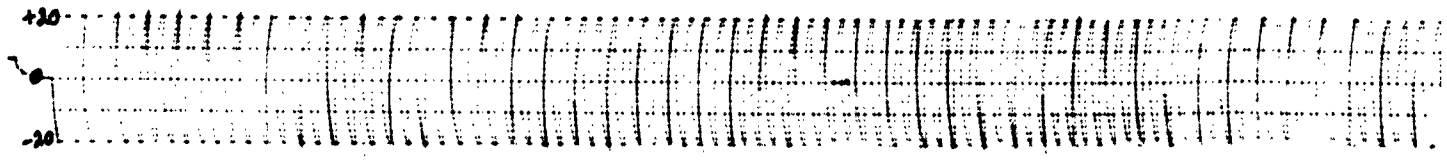

$A \sin \omega_1 t$

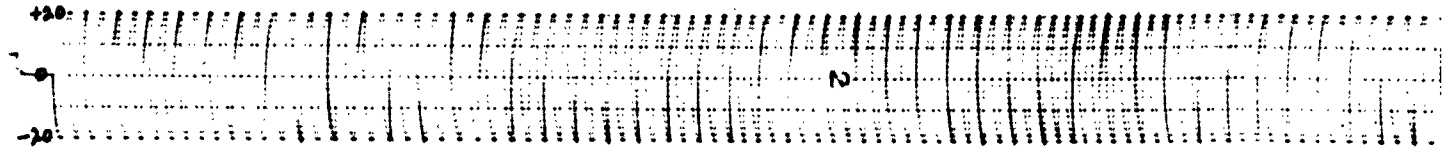

$B \sin \omega_2 t$

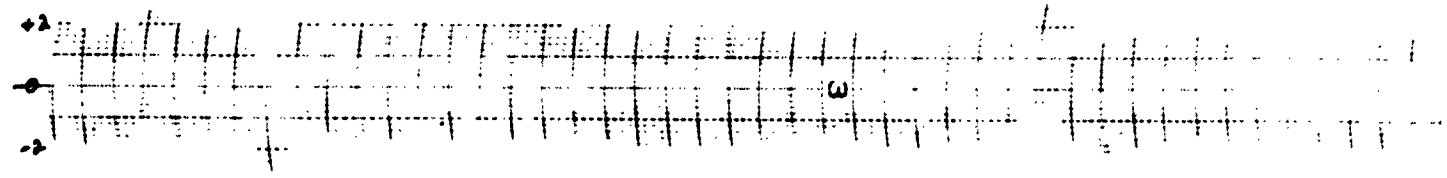

e_{in}

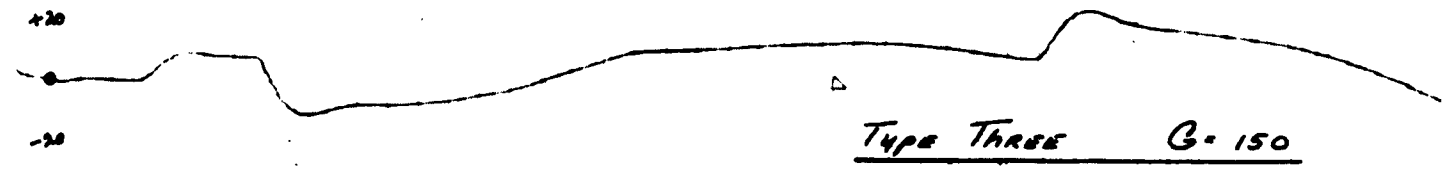

Type Three G = 150

e_o

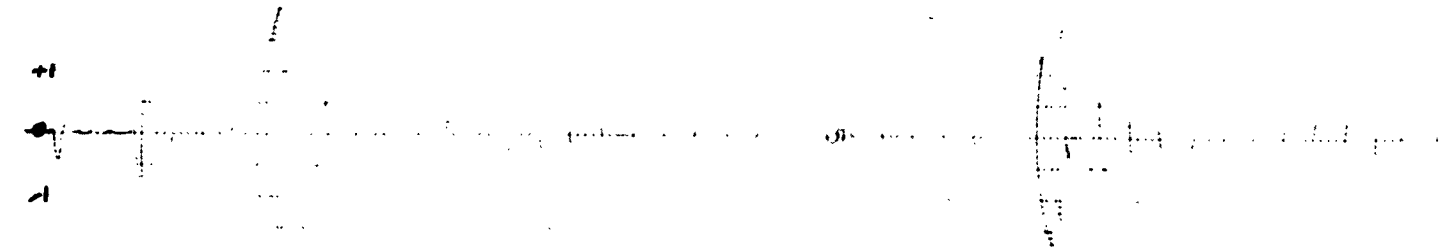

e_{in}

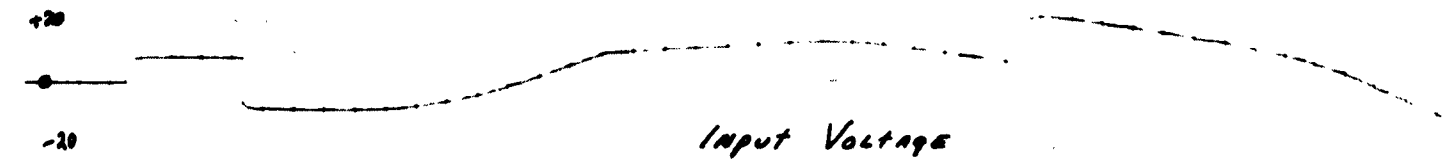

Input Voltage

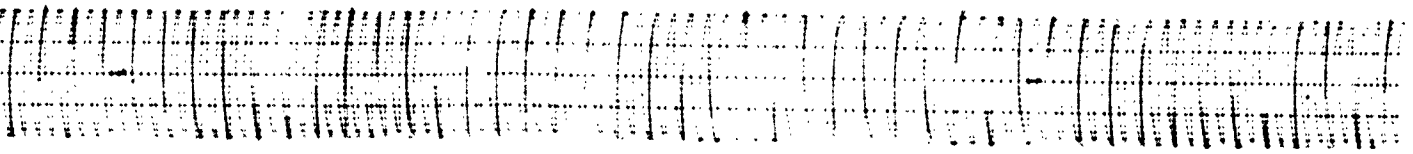

SIN $\omega_1 t$

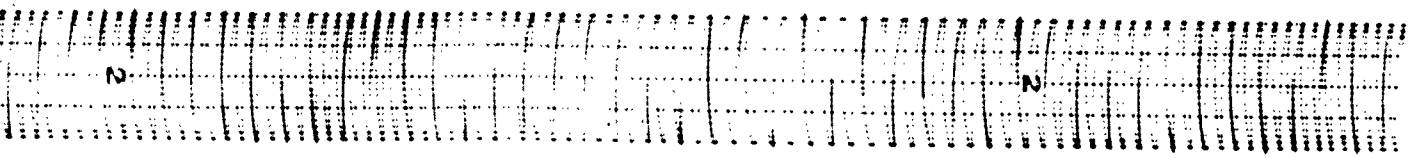

SIN $\omega_2 t$

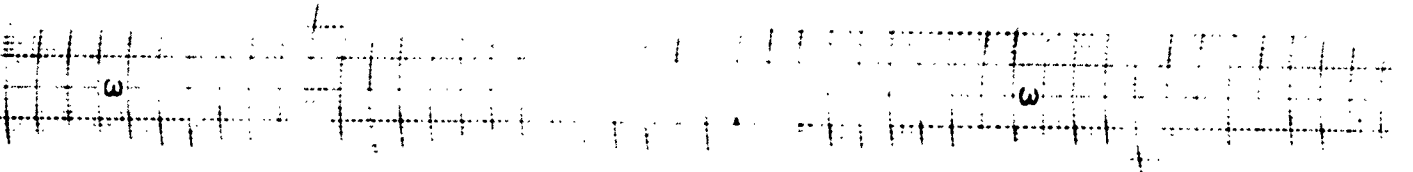

l_m

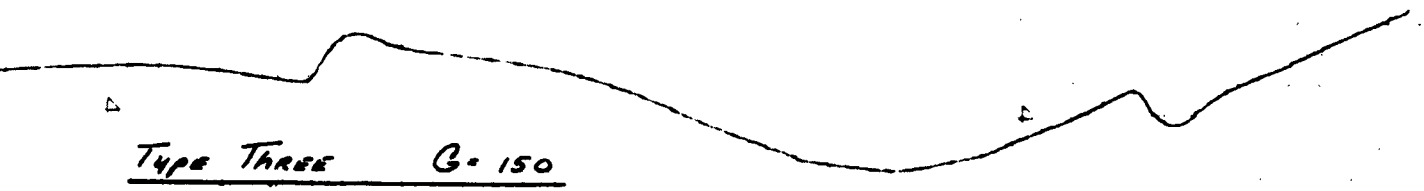

Type Three G = 150

l_o

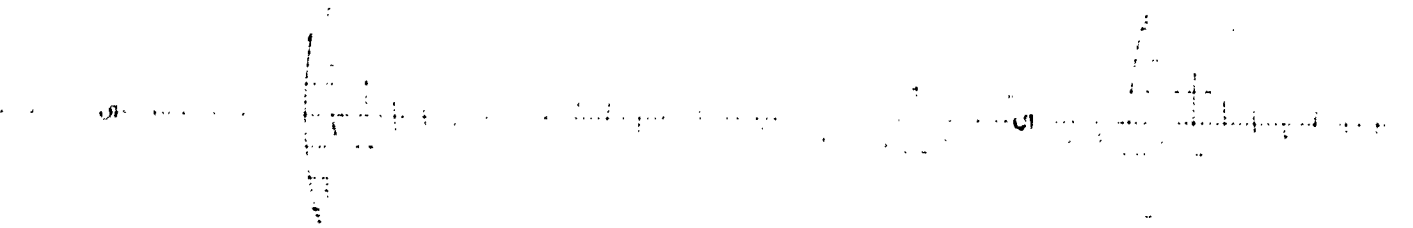

l_n

Random Response for Type Three System

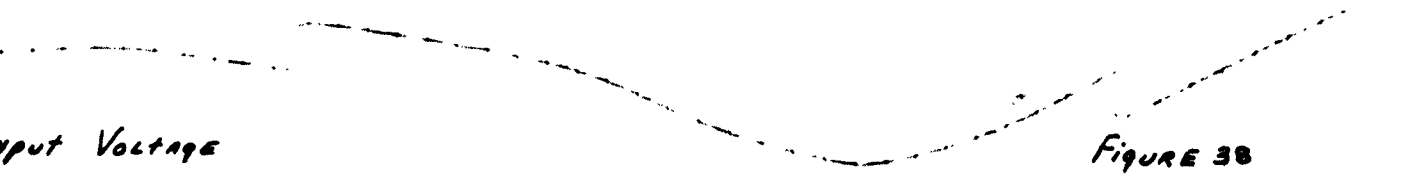

Input Voltage

FIGURE 38

examined (Ref 19). This filter is illustrated in Figure 34. The response of the three systems is shown in Figures 36, 37, and 38.

The Gains of the three systems are

Type One----------35

Type Two----------70

Type Three--------150

The first five curves are identical to the remainder of the runs. The sixth curve is an indication of the input to the Input Oscillator. All scales are in volts/cm and the time scale is 5 seconds/cm. These three curves clearly indicate the tremendous improvements that were accomplished by increasing the type of the general system. Note the amplitude scales on the phase error voltage (ℓ_e) and on the control voltage (ℓ_c). The range of frequency variation was from $\omega \approx 2.7$ rps to $\omega \approx 7.5$ rps.

Conclusions

The results of this investigation clearly demonstrate that the Phase-Lock Loop can be operated in the Type Two and Type Three configuration. A constant phase error was necessary to follow the ramp in Type Two, and the parabolic in Type Three, but the range of frequency change was significant. The curve in Appendix C and D show that the frequency can be changed up to $1.5\,\omega_o$ with satisfactory results. In terms of a physical system, using a frequency on the order of 10 kcps, this is a marked improvement over the basic Type One system used by Lt. Wendland.

Recommendations

The computer simulation of the Phase-Lock Loop agrees favorably with the Servo Analysis. The next logical step for further investigation of the PLL would be to integrate a physical component into the computer simulation.....e.g. a physical transistorized Phase Detector could be patched into the Analog Computer simulation to analyze the effect of the higher harmonics generated by the phase detector. This analysis could be followed by the building and testing of a completely physical Phase-Lock Loop. This would require a detailed Phase Detector and VCO circuitry analysis, in order to determine the effects of the physical units on the operation of the loop. The variation of the low pass filter to discover the most accessible physical realization would prove to be very interesting. Because of the low power levels used in the PLL, the physical model would most likely tend to be transistorized to reduce the size and weight.

The comparison between the physical and simulation loops would add much to the knowledge of the analysis of non linear systems.

Bibliography

1. Angelo, E.J. Jr. Electronic Circuits. New York: McGraw-Hill Book Co., 1958.

2. D'Azzo, John J. and C.H. Houpis. Feedback Control System Analysis and Synthesis. New York: McGraw-Hill Book Co., 1960.

3. Enloe, L.H. " Decreasing the Threshold in FM by Frequency Feedback." Proceedings of the IRE, 50:18-30 (January 1962).

4. Jaffe, R., and E. Rechtin. " Design and Performance of Phase-Locked Circuits Capable of Near Optimum Performance over a Wide Range of Input Signal and Noise Level." IRE Transactions on Information Theory, 17:66-76 (March 1955).

5. Johnson, C.L. Analog Computer Techniques. New York: McGraw-Hill Book Co., 1956.

6. Kasischke, F.W. and R.T. Harnett. Preparation of Problems for Electronic Associates Computer. Internal Memo 60-18. Dayton, Ohio: Systems Dynamic Analysis Division. (November 1960).

7. McAleer, H.T. " A New Look at the Phase-Locked Oscillator." Proceedings of the IRE, 47:1137-1143 (June 1959).

8. Ordung, P.F. et al. " Closed Loop Automatic Phase Control." AIEE Transactions, 73:375-381 (September 1954).

9. Preston, G.W. " Basic Theory of Locked Oscillators in Tracking FM Signals." IRE Transactions on Space Electronics and Telemetry, 5:30-32 (March 1959).

10. Preston, G.W. and J.C. Tellier. " The Lock-In Performance of an AFC Circuit." Proceedings of the IRE, 41:249-251 (February 1953).

11. Resolution by Means of Controlled Sin, Cos, Circuits. Report by University of Michigan. (available at the Systems Dynamic Analysis Division, Bldg. 57, WPAFB, Ohio).

12. Rey, T.J. " Automatic Phase Control: Theory and Design." Proceedings of the IRE, 48:1760-1772 (October 1960).

13. Rue, A.K., and P.A. Lux. " Transient Analysis of a Phase-Locked Loop Discriminator." IRE Transactions on Space Electronics and Telemetry, 7:105-112 (December 1961).

14. Sferrazza, P.,et al. " Phase-Locked Loops for Electronically

Scanned Antenna Arrays." IRE Transactions on Space Electronics and Telemetry, 7:95-100 (December 1961).

15. Truxal, J.G. Control System Synthesis. New York: McGraw-Hill Book Co., 1955.

16. Weaver, C.S. " A New Approach to Linear Design and Analysis of Phase-Locked Loops." IRE Transactions on Space Electronics and Telemetry, 5:166-178 (December 1959).

17. Weaver, C.S. " Increasing the Dynamic Tracking Range of a Phase-Locked Loop." Proceedings of the IRE, 47:952-958 (May 1960).

18. Weaver, C.S. " Thresholds and Tracking Ranges in Phase-Locked Loops." IRE Transactions on Space Electronics and Telemetry, 7:60-70 (September 1961).

19. Wendland, G.E. The Analysis of an Automatic-Phase-Control Amplifier System for Use with a Nuclear Magnetic Resonance Gyroscope. Thesis (unpublished). Dayton, Ohio: Air Force Institute of Technology, 1962.

APPENDIX A

Complete Analog Computer Circuit Diagram for Simulation of Phase-Lock Loop

CE/EE/62-20

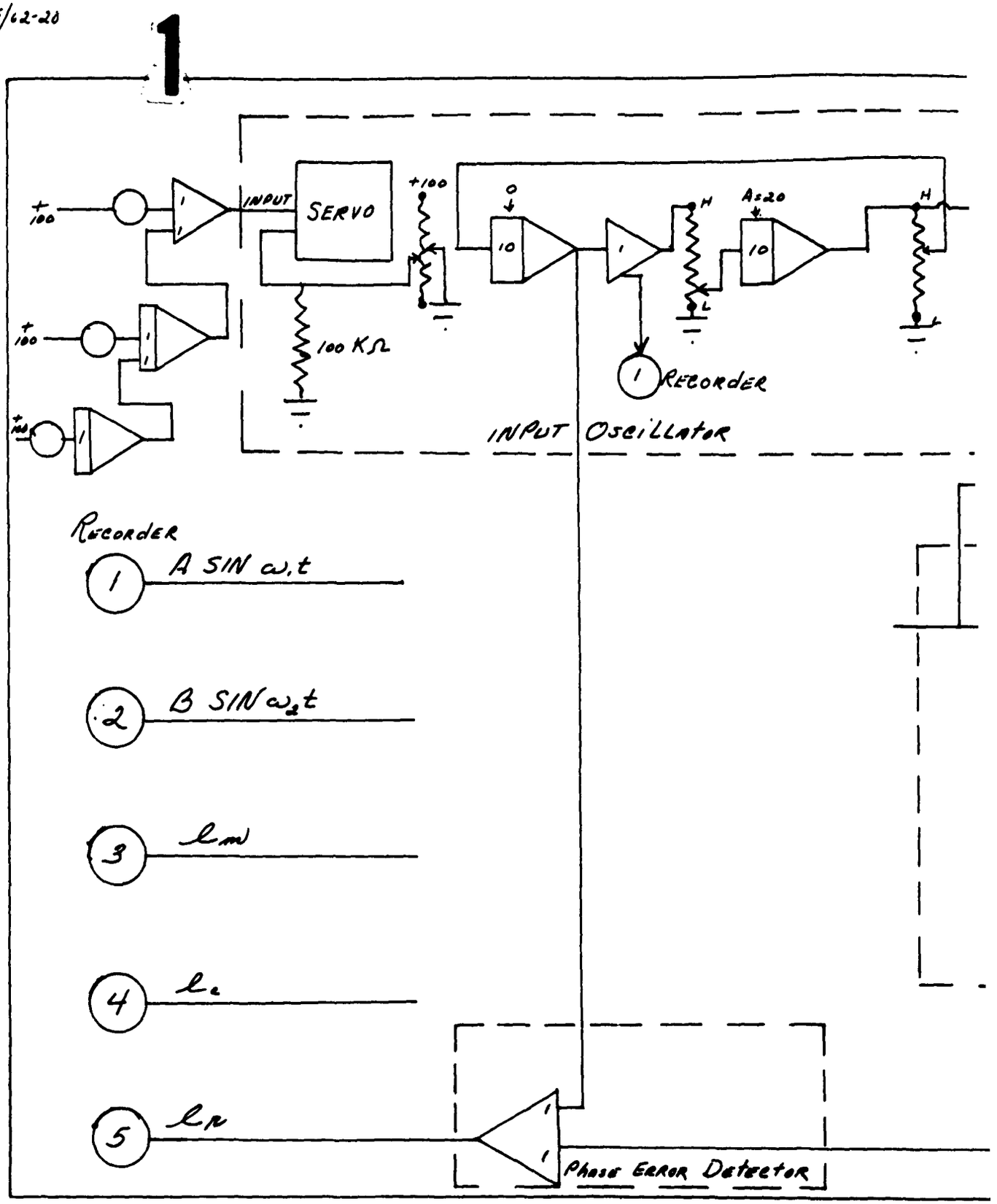
1
+100
+100
+100
INPUT
SERVO
100 KΩ
+100
0
10
1
H
L
A=20
10
H
1
RECORDER
INPUT OSCILLATOR
RECORDER
1
A SIN ω,t
2
B SIN ω₂t
3
ℓm
4
ℓc
5
ℓR
Phase Error Detector

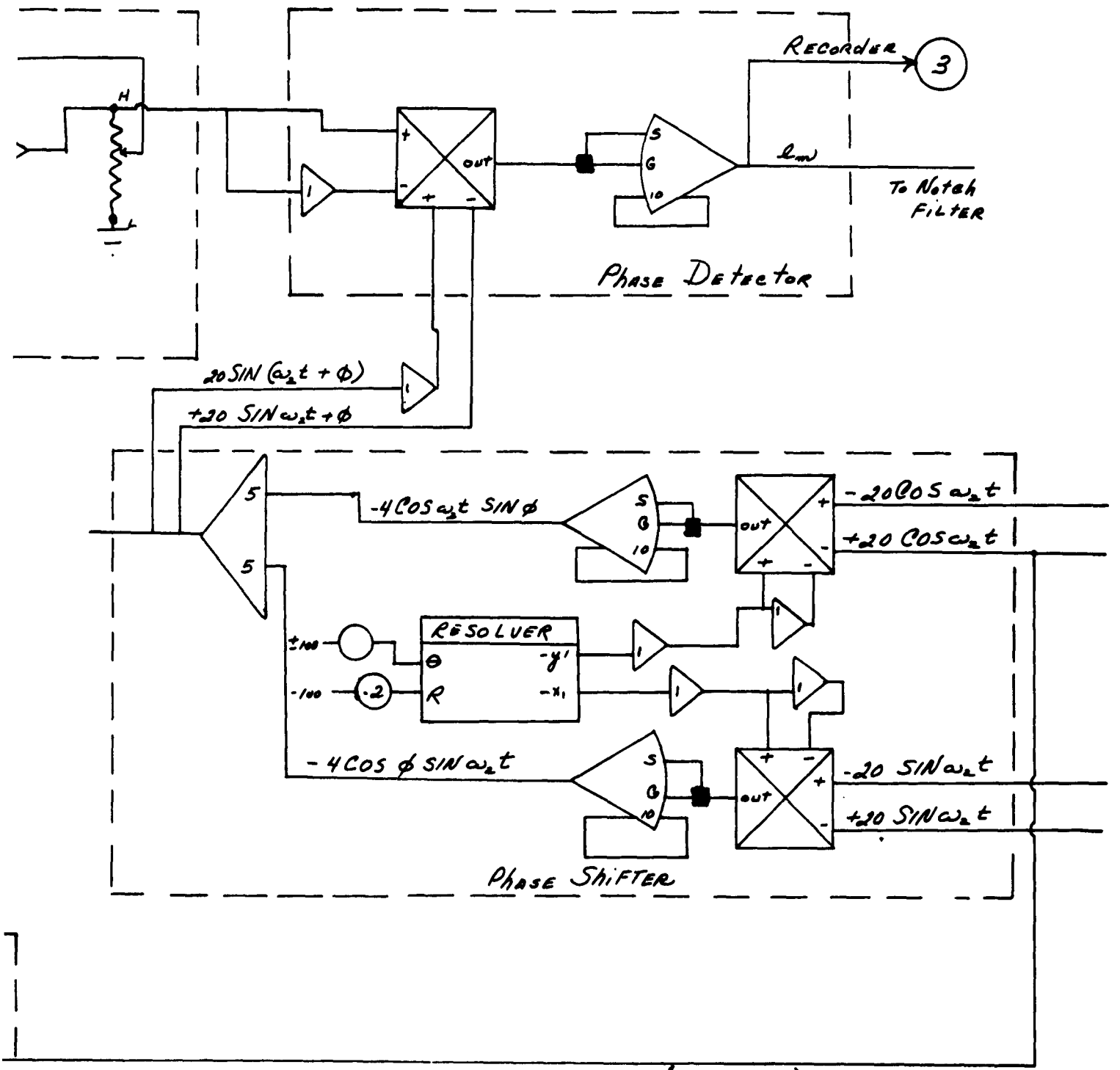

Appendix Figure A-1 (Page 1 of 2)

CE/EE/62-20

1

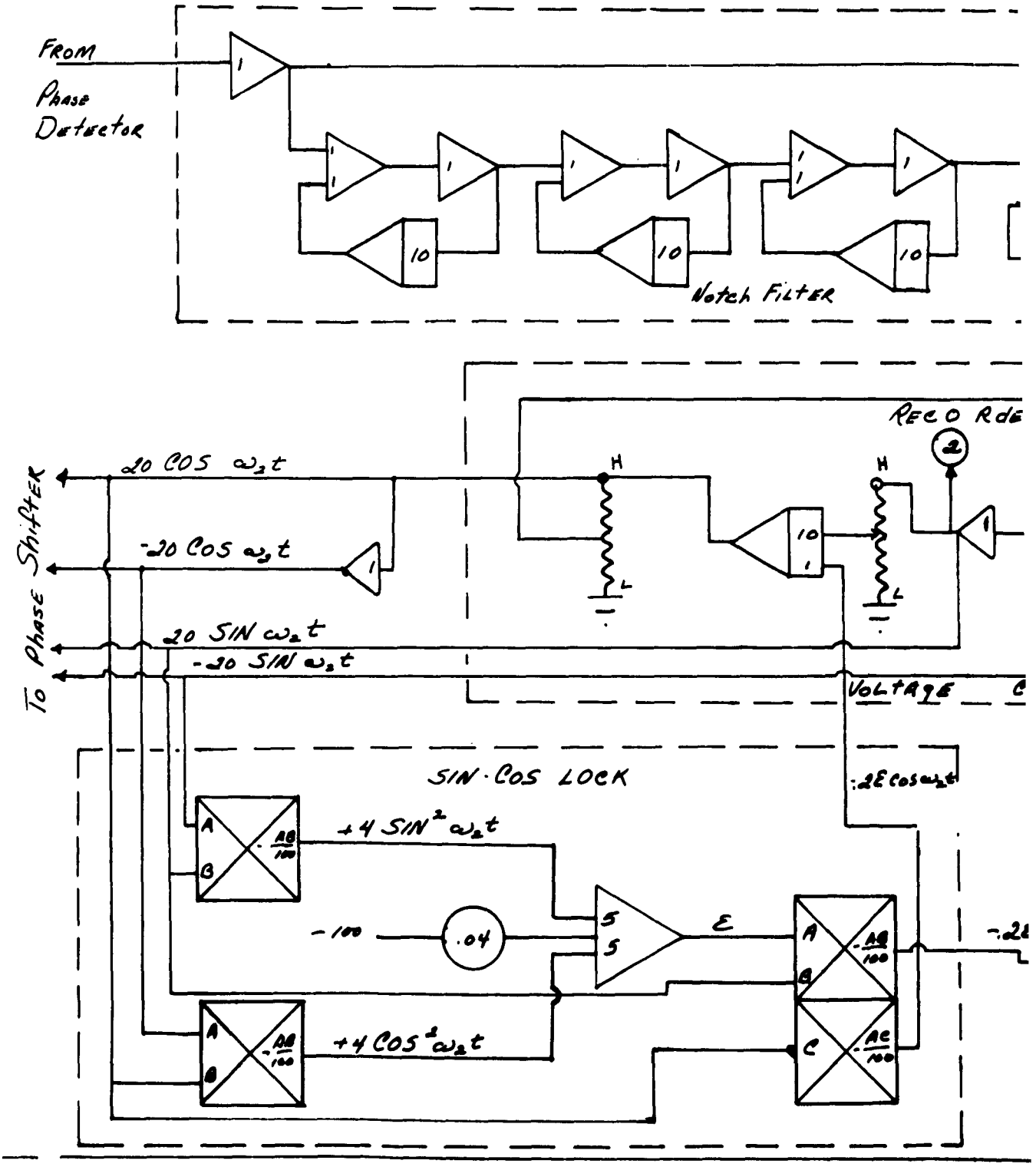
FROM
Phase
Detector
Notch Filter
RECO RdE
2
H
L
10
1
20 COS ω₂t
-20 COS ω₂t
20 SIN ω₂t
-20 SIN ω₂t
TO Phase Shifter
VOLTAGE
SIN · COS LOCK
.2E cos ω₂t
A
B
C
.AB/100
.AC/100
+4 SIN² ω₂t
+4 COS² ω₂t
-100
.04
5
E
-.2E

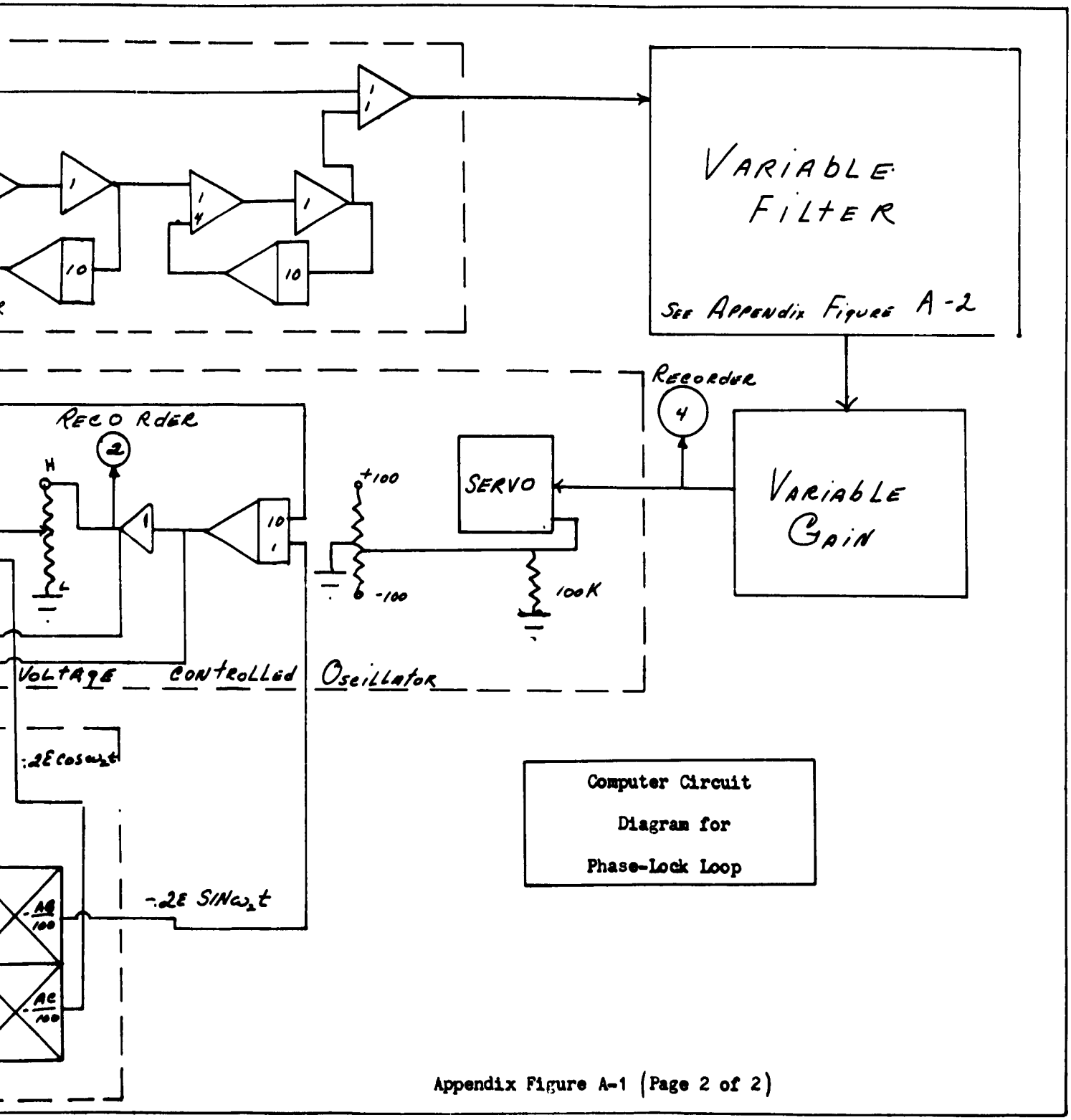

Computer Circuit Diagram for Phase-Lock Loop

Appendix Figure A-1 (Page 2 of 2)

Type II Filter

$$F(s) = \frac{.3(s+.6)(s+.1)}{s(s+1)(s+.5)}$$

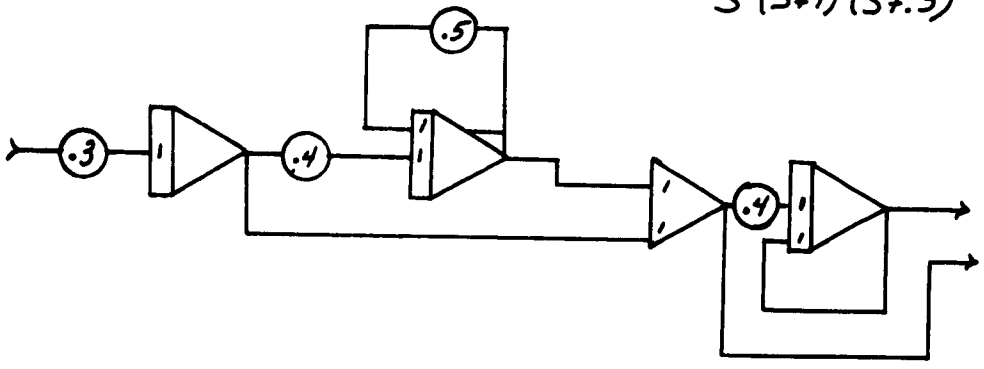

Type III Filter

$$F(s) = \frac{.3(s^2+5s+2.5)(s+.1)}{s^2(s^2+8s+20)}$$

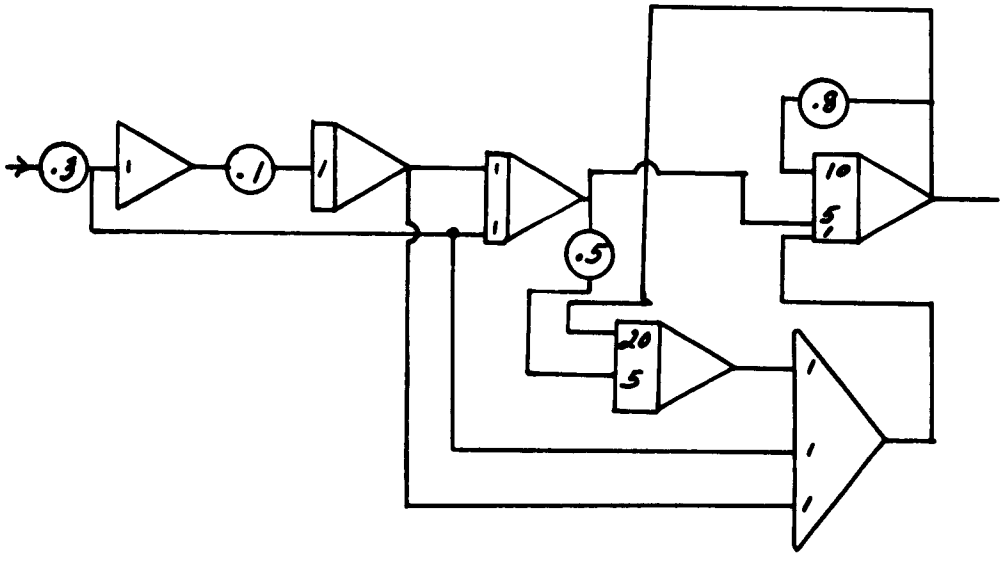

Appendix Figure A-2

APPENDIX B

Computation of Root Loci

I. PROGRAM ABSTRACT

Title: Computation of Root Loci

Subject Classification: 9.4

Authors: Harvey M. Paskin and Charles W. Richard, Jr.
Air Force Institute of Technology

Direct Inquires to: Capt. Charles W. Richard, Jr.
Mathematics Department, AF Institute of Technology
Wright-Patterson AF Base, Ohio
CL3-7111 - Ext. 29115

Purpose/Description: Given the poles and zeros of a rational transfer function G(s), this FORTRAN program calculates the roots of the characteristic equation for a feedback system

$$1 + K\,G(s) = 0$$

The locus of one root is calculated at equal increments in the complex s-plane for monotone variations of the parameter K.

Mathematical Method: Starting at a point on the locus, the next point is calculated, using a modified Newton's method to satisfy the angle condition

$$\text{Arg } G(s) = (2k + 1)\pi \quad k = 0, \pm 1, \pm 2, \cdots$$

Restrictions: The number of poles plus the number of zeros of G(s) must not exceed 25. Points on the locus are calculated only for non-negative values of the parameter K.

Equipment Specifications: IBM 1620 with 20,000 digits of memory. 1622 card reader-punch.

Storage Requirements: Entire 20K memory.

Additional Remarks: 1. This FORTRAN program was compiled using the AFIT Improved Fortran, 1.1.010. Standard AFIT Fortran subroutines are used including absolute value, except that the Print subroutine is modified to carriage return before printing.

Add. Remarks: 2. The object deck has been compressed, using an AFIT compressor. The object deck is sequenced from $\bar{0}01$ through $\bar{2}79$ in columns 78 through 80. The Fortran source deck is sequenced from $\bar{0}01$ through $\bar{1}87$ in columns 78 through 80.

3. Compared with other methods of computing zeros of polynomials, it is believed that this program achieves decreased running time at the expense of decreased accuracy. Accuracy of the results is a function of the number and distribution of the poles and zeros of G(s) and the location of the particular root being computed. For a variety of sample problems the average time to calculate one point on the locus was 15 seconds, exclusive of printing, at a worst known accuracy of 4 decimal digits.

II. DESCRIPTION OF PROGRAM

The transfer function for a feedback system may be written

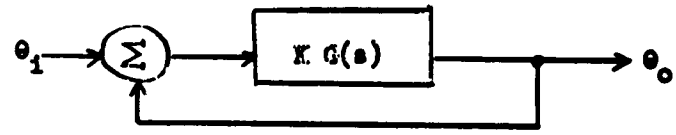

$$\frac{\theta_o(s)}{\theta_i(s)} = \frac{KG(s)}{1 + KG(s)} = \frac{KP(s)}{Q(s) + KP(s)}$$

where the "gain" K is a real number and G(s) is restricted to be a rational function of s in the factored form

$$G(s) = \frac{P(s)}{Q(s)} = \frac{(s - z_1)(s - z_2) \cdots (s - z_m)}{(s - p_1)(s - p_2) \cdots (s - p_n)} \quad n \geq m$$

This program calculates the zeros of the denominator Q(s) + KP(s) for non-negative values of the parameter K. Starting at a known root of Q(s) + KP(s) = 0, a locus of roots, s_L, is calculated at fixed increments, $|\Delta R|$, in the complex plane.

$$s_L = x_L + iy_L$$
$$\Delta R = \pm \left| s_{L+1} - s_L \right|$$

ΔR is considered positive for increasing values of the parameter K and negative for decreasing values of the parameter K. The value of K at each point on the locus is computed and output with the real and imaginary part of the point.

III. METHOD OF COMPUTATION

At a root, s_L, of $Q(s) + KP(s) = 0$

$$G(s_L) = \frac{P(s_L)}{Q(s_L)} = -\frac{1}{K}$$

therefore: $\arg G(s_L) = \pi$ or an odd multiple of π

and $$\left|G(s_L)\right| = \frac{1}{|K|}$$

Defining $\psi_i = \arg (s_L - z_i) \quad i = 1, 2, \cdots m$

$$\varphi_i = \arg (s_L - p_i) \quad i = 1, 2, \cdots n$$

then

$$\arg G(s_L) = \sum_{i=1}^{m} \psi_i - \sum_{i=1}^{n} \varphi_i = (2k + 1)\pi \quad k = 0, \pm 1, \pm 2, \cdots$$

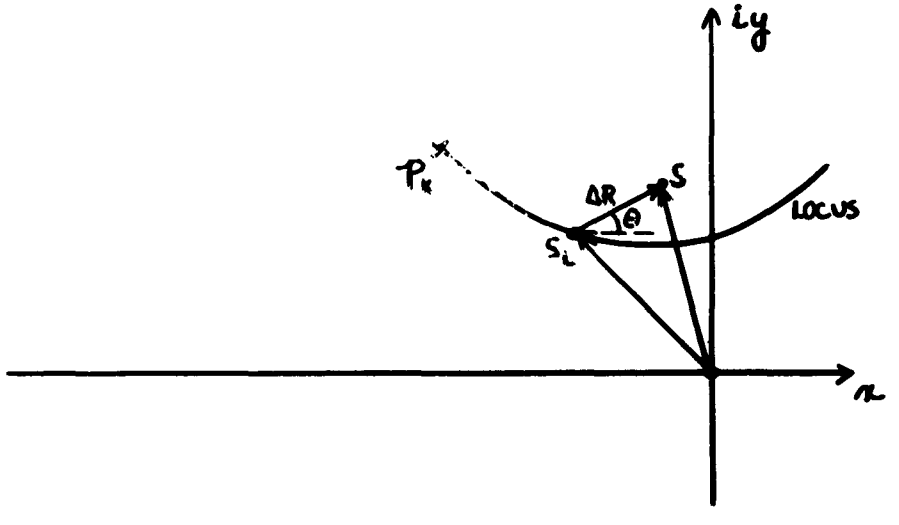

s-plane

Starting at the point s_L on the root locus a new test point s is determined for a given ΔR and initial angle θ.

$$s = s_L + \Delta R (\cos \theta + i \sin \theta)$$

A modified Newton's method is used to determine a θ_N to satisfy

$$\arg G(s) - (2k + 1)\pi = 0$$

This new point $s_{L+1} = s_L + \Delta R (\cos \theta_N + i \sin \theta_N)$ is approximately on the locus.

If the modified Newton's method fails an alternate procedure, essentially a binary search for θ, is used for convergence to θ_N.

After convergence to the new point s_{L+1} on the locus the associated value of the gain K is calculated, using

$$|K| = \frac{1}{|G(s_{L+1})|} = \frac{|Q(s_{L+1})|}{|P(s_{L+1})|} = \frac{\prod_{i=1}^{n} |s_{L+1} - P_i|}{\prod_{i=1}^{m} |s_{L+1} + z_i|}$$

For a more complete description of the mathematical method, see reference 2.

IV. INPUT FORMAT

A. A problem, or series of problems, may be input from cards or typewriter, depending on sense Switch 1.

Sense Switch 1
- ON: from typewriter
- OFF: from cards

All data is input without an input format specified. Therefore, data input either from typewriter or cards may be in any form, with or without a decimal point, or in floating form. There is one restriction for card input. If input cards have extraneous information punched following the data (such as sequence numbers) then a record mark must separate the data from the extraneous information.

Separate numbers must be separated by one or more commas or blanks if there is more than one piece of data in the same input record. There may not be any blanks within a number. If the input is from the typewriter RELEASE, START should be pressed where R/s is indicated below. If the input is from cards each new value of "n", item (1) below, must appear as the first piece of data on a separate card. As many of the numbers following item (1) as will fit may be punched on the same card.

The form and order of the input data are as follows:

(1)	n (R/s)	for n > 0, n = the no. of poles of G(s)
(2)	Re p_1, Im p_1 (R/s) Re p_2, Im p_2 (R/s) ⋮ Re p_n, Im p_n (R/s)	the real and imaginary part of each pole, p_i, of G(s).
(3)	m (R/s)	m = the number of zeros of G(s)
(4)	Re z_1, Im z_1 (R/s) Re z_2, Im z_2 (R/s) ⋮ Re z_m, Im z_m (R/s)	the real and imaginary part of each zero, z_i, of G(s).
(5)	Re s_o, Im s_o (R/s)	the real and imaginary part of the starting point s_o on the locus. This point may be any one of the poles p_k of G(s).
(6)	ΔR, N (R/s)	Increment $\lvert\Delta R\rvert = \lvert s_{L+1} - s_L \rvert$ If ΔR is positive, points on the locus will be calculated for increasing values of K. ΔR is negative for decreasing values of K. $\lvert N \rvert$ = the number of points on the locus to be output. If N < 0 see 6.a.
(6.a)	θ_o (R/s)	Initial search angle in degrees. If in(6) N > 0, this record is <u>not</u> input. Then $\theta_o = 0$ if a new s_o has been input, otherwise $\theta_o = \theta_N$ of the previous point.

IV. B. Alternate form of input data for subsequent runs.

In subsequent runs for the same transfer function G(s), the poles and zeros of G(s) need not be input again. The first record, n, is used as a switch.

OPTION 1. n = 0 for a new starting point s_o

Input data is of the form

(1)	0	(R/s)
(5)	Re s_o, Im s_o	(R/s)
(6)	ΔR, N	(R/s)

OPTION 2. n = -1; to continue on same locus but with new ΔR.

Input data is of the form

(1)	- 1	(R/s)
(6)	ΔR, N	(R/s)

OPTION 3. Manual intervention for new ΔR on same locus. After one or more points on the locus have been output set Switch 2 and Switch 3 OFF. After calculating the current s_{L+1} the typewriter will print

DELTA R, NO. OF POINTS

1. Reset Switch 2 and/or 3
2. Enter from the typewriter

ΔR, N (R/s)

NOTE: Switches 2 and 3 should be set OFF while the root s_{L+1} is being printed. Otherwise, the last point computed will not be output.

C. Comments on the use of the various input options

1. The optional input of an initial search angle θ_o is most useful in the vicinity of a point where two or more loci cross. Different θ_o's may be used to obtain points on the different loci. A new θ_o may be input, as described in A6.a, with either OPTION 1, 2, or 3 above.

IV. C. 2. OPTION 1 is useful for obtaining several loci associated with the same G(s). A different locus starts (i.e., K = 0) at each of the poles of G(s).

3. OPTION 2 is useful for obtaining more points along a particular section of a locus. Quite often the general shape of a locus is known and more points may be desired in the area of crossing loci, intercepts with the axis, etc.

4. OPTION 3 is useful for changing ΔR, the spacing between points, based upon the immediate printed results. A negative ΔR, in order to "back up" on the locus, is useful if it is noted from the printed output that a particular point of interest has just been passed. Alternating use of positive and negative ΔR with $|\Delta R|$ decreasing also will allow for manual convergence to a root with a specified K.

V. <u>OUTPUT FORMAT</u>

The results may be typed, punched on cards, or both. The format of off-line printing is the same as on-line.

Sense Switch 2: ON Type results

Sense Switch 3: ON Punch results

A. Data for each point, s_L, on the locus is output in three columns.

X	Y	GAIN
Re s_L	Im s_L	K_L

B. The poles and zeros of G(s) are output following their input to identify the results. Preceeding each list of N roots, ΔR is output. θ_o is output following ΔR is a θ_o had been input.

VI. SAMPLE PROBLEM

$$G(s) = \frac{s + 19.6}{s(s + 9 + 4i)(s + 9 - 4i)}$$

Assume the following output is desired:

1. 5 points on the locus starting at the pole s = 0 with an initial angle of 180 degrees and a $\Delta R = 2.0$.

2. 5 points on the locus starting at the pole s = -9 + 4i with an increment $\Delta R = 1.0$ continuing with 4 more points with $\Delta R = 0.5$.

Input Data - 3 cards)

```
3  0. 0.  -9. -4.  -9. 4.  1  -19.6 0.  0. 0.  2. -5  180.
0  -9. 4.  1. 5
-1  .5 4
```

Printed Output

```
VALUE ØF PØLES
  .000000E-99      .000000E-99
-9.000000E+00    -4.000000E+00
-9.000000E+00     4.000000E+00

VALUE ØF ZERØS
-1.960000E+01      .000000E-99

DELTA R            2.0000
INITIAL THETA    180.0   DEG.

        X                Y              GAIN
  .000000E-99      .000000E-99     .000000E-99
-2.000000E+00      .000000E-99    7.386363E+00
-4.000000E+00      .000000E-99    1.051282E+01
-6.000000E+00      .000000E-99    1.102941E+01
-8.000000E+00      .000000E-99    1.172413E+01

DELTA R            1.0000
-9.000000E+00     4.000000E+00     .000000E-99
-8.318490E+00     3.268191E+00    5.554888E+00
-7.678918E+00     2.499460E+00    8.791001E+00
-7.080038E+00     1.698621E+00    1.038586E+01
-6.518831E+00     8.709456E-01    1.095099E+01

DELTA R             .5000
-6.247419E+00     4.510221E-01    1.101978E+01
-5.748261E+00     4.800138E-01    1.104028E+01
-5.505700E+00     9.172369E-01    1.110832E+01
-5.276290E+00     1.361501E+00    1.128243E+01
```

VII. OPERATING INSTRUCTIONS

1. Clear memory, if desired, as follows:

   a. Set all check switches to PROGRAM.

   b. Depress INSTANT STOP and RESET.

   c. Depress INSERT.

   d. Type 16 00010 00000.
   (12 digits, no spaces or punctuation)

   e. Depress RELEASE and START (or the R/S key)

   f. After the MAR lights have cycled through memory at least once, depress INSTANT STOP.

   g. Depress RESET.

2. Load the object deck as follows:

   a. If the computer is not in manual mode, press INSTANT STOP and RESET.

   b. Set the OVERFLOW switch to PROGRAM, all other check switches to STOP.

   c. Clear the card reader by removing any cards in the hopper and pressing READER STOP and NON-PROCESS RUNOUT. Then remove all cards from the stacker.

   d. Put the object deck in the reader hopper.

   e. Depress LOAD.

   f. When the reader stops on the last two cards, depress READER START.

   g. Remove the cards from the read stacker and check for the last card.

3. a. Set the program switches

SWITCH	ON	OFF
1	Input from typewriter	Input from cards
2	Print output	Do not print
3	Punch output	Do not punch
4	For error in typed input only. See 8 below	Normal

   b. Check switches; set the OVERFLOW SWITCH to PROGRAM, all other check switches to STOP.

VII. 4. If data cards are to be read (Switch 1 OFF), place two blank cards after the data deck, place in the read hopper, and depress READER START.

5. If output cards are to be punched (Switch 3 ON), place blank cards in the punch hopper and press PUNCH START.

6. Set paper in the typewriter three lines below start of a new page. Set typewriter margins to allow for at least 46 characters.

7. Press START twice. Execution of the program will begin.

8. If typewriter input is called for, an identification of the data to be entered will be typed, then the typewriter will be energized. Enter the appropriate data and depress the R/S key. If a typing error is made, and it is found before the R/S key is pressed, it may be corrected as follows:

   a. Turn Switch 4 ON.

   b. Depress R/S.

   c. Turn Switch 4 OFF

   d. Retype the entire line

   e. Depress R/S

   Note that Switch 4 must be OFF whenever information is being entered at the typewriter, except when an error is being corrected.

   If the typing error is not discovered until after R/S is pressed, it is too late to correct it.

9. After the specified N points on the locus have been output, the program will always begin again and call for new data.

10. To manually stop the program at any time in order to input new data, depress INSTANT STOP, RESET, INSERT, RELEASE, START. Repeat steps 3 through 7.

11. If the results were punched, the output data deck may be removed at the end of computation as follows:

   a. Lift the blank cards from the punch hopper.

   b. Depress NON-PROCESS RUNOUT for a few seconds.

```
C       CØMPUTATIØN ØF RØØT LØCI
        DIMENSIØN A(25),B(25)
        TØL=10E-07
174     IF (SENSE SWITCH 2) 74,171
171     IF (SENSE SWITCH 3) 74,172
172     PRINT 173
173     FØRMAT (/17HSET SWITCH 2 ØR 3,/)
        PAUSE
        GØ TØ 174
 74     IF(SENSE SWITCH 1)13,9
 13     PRINT 8
  8     FØRMAT (//12HNØ. ØF PØLES)
        ACCEPT ,K
        IF (K) 121,7,5
  5     KØLES = K
        PRINT 10
 10     FØRMAT (/14HVALUE ØF PØ
        DØ 12 J=1,KØLES
 12     ACCEPT, A(J), B(J)
        PRINT 1
  1     FØRMAT (/12HNØ. ØF ZERØS)
        ACCEPT, ERØS
        M = KØLES+JERØS
        N=KØLES+1
        IF (JERØS) 7,7,3
  3     PRINT 4
  4     FØRMAT (/14HVALUE ØF ZERØS)
        DØ 6 I=N,M
  6     ACCEPT, A(I),B(I)
  7     PRINT 14
 14     FØRMAT (/5HPØINT)
        ACCEPT, XL,YL
        THETA=0.0
121     PRINT 16
 16     FØRMAT(/22HDELTA R, NØ. ØF PØINTS)
        ACCEPT,DELR,L
        IF(L)120,156,156
120     PRINT 19
 19     FØRMAT (/13HINITIAL THETA)
        ACCEPT, ANGLE
        THETA=ANGLE*.0174533
        GØ TØ 156
  9     READ, K
        IF (K) 153,33,18
 18     KØLES=K
        DØ 20 J=1,KØLES
 20     READ, A(J), B(J)
        READ, JERØS
        M=KØLES+JERØS
        N=KØLES+1
        IF (JERØS) 33,33,21
 21     DØ 24 I=N,M
```

```
 24   READ, A(I), B(I)                                                  2
 33   READ, XL, YL
      THETA=0.0
 153  READ,DELR,L
      IF(L)123,124,124
123   READ , ANGLE
      THETA=ANGLE*.0174533
 124  IF(SENSE SWITCH 2)127,156
 127  IF(K)131,131,90
 90   PRINT 10
      DØ 92 J=1,KØLES
 92   PRINT 17, A(J), B(J)
      PRINT 4
      DØ 93 I=N,M
 93   PRINT 17, A(I), B(I)
 131  PRINT 130,DELR
 130  FØRMAT(/7HDELTA R,F16.4)
      IF(L)154,156,156
 154  PRINT 151,ANGLE
 151  FØRMAT(13HINITIAL THETA,F7.1,7H   DEG.)
 156  IF(SENSE SWITCH 3)125,150
 150  IF(SENSE SWITCH 2)152,79
 79   PRINT 173
      PAUSE
      GØ TØ 156
 125  IF(K)132,132,94
 22   FØRMAT (/6X, 1HX, 15X, 1HY, 13X, 4HGAIN)
 17   FØRMAT (E13.6, 3X, E13.6)
 94   PUNCH 10
      Dø 96 J=1,KØLES
 96   PUNCH 17, A(J), B(J)
      PUNCH 4
      DØ 97 I=N,M
 97   PUNCH 17, A(I), B(I)
 132  PUNCH 130,DELR
      IF(L)352,152,152
 352  PUNCH 151,ANGLE
 152  IF(K)252,95,195
 195  PRINT 22
      IF(SENSE SWITCH 3)295,95
 295  PUNCH 22
 95   X=XL
      Y=YL
      GANE=0.0
      DEL=1.0
      GØ TØ 56
 252  IF(DELR*DEL)332,121,230
 332  IF(L)230,333,333
 333  THETA=THETA+3.1415927
 230  K=1
      D=ABS(DELR)
```

```
      DEL=DELR/D
 23   X=D*CØS(THETA)+XL
      Y=D*SIN(THETA)+YL
      BETA=0.0
      DØ 29 I=1,M
      P=0.0
      IF (X-A(I)) 25,26,27
 25   P=3.14159265
 27   PSI=ATAN((Y-B(I))/(X-A(I)))
 32   IF (Y-B(I)) 28,30,30
 28   P=0.0-P
 30   BETA=BETA-PSI-P
      IF (I-KØLES) 29,31,29
 26   PSI=0.0
      P=1.57079633
      GØ TØ 32
 31   BETA=0.0-BETA
 29   CØNTINUE
      EPSIL=ABS(BETA)
 44   EPSIL=EPSIL-6.2831853
      IF (EPSIL) 42,56,44
 42   EPSIL=EPSIL+3.14159265
      IF (BETA) 45,46,46
 45   EPSIL=0.0-EPSIL
 46   GØ TØ (51,530,99),K
 51   DELTH=EPSIL
      K=2
      GØ TØ 52
530   IF (ABS(EPSIL-EPSAL)-1.0E-07) 98,53,53
 53   DELTH=EPSIL*ABS((THETA-THATA)/(EPSIL-EPSAL))
 52   IF (TØL-ABS(DELTH)) 54,56,56
 54   THATA=THETA
      EPSAL=EPSIL
      IF (0.78539816-ABS(DELTH)) 80,55,55
 55   THETA=THETA-(DEL*DELTH)
      GØ TØ 23
 80   IF (EPSIL) 81,56,82
 81   THETA=THETA+0.78539816
      GØ TØ 23
 82   THETA=THETA-0.78539816
      GØ TØ 23
 98   K=3
      Z=2.0
 99   IF (EPSIL*DELTH) 100,56,102
100   Z=0.5
101   DELTH=(-0.5)*DELTH
      GØ TØ 103
102   DELTH=Z*DELTH
103   IF(TØL-ABS(DELTH))55,56,56
 56   UP=1.0
      DØ 58 I=1,M
```

```
      WSLZ=SQRT'(X-A(I))*'X-A(I))+'Y-B(I))*'Y-B(I)))
      UP=UP*WSLZ
      IF '(I-KØLES) 58,59,58
 59   IF 'UP) 60,61,60
 60   UP=1.0/UP
 58   CØNTINUE
      PGANE=GANE
      IF 'UP) 63,62,63
 63   GAAN=1.0/UP
 163  IF'DEL*'GAAN-PGANE))65,66,66
 65   THETA=THETA+1.8
      GØ TØ 230
 61   GANE=0.0
      GØ TØ 64
 62   GANE=1.0E50
      GØ TØ 64
 66   GANE=GAAN
 64   XL=X
      YL=Y
 73   IF 'SENSE SWITCH 3) 70, 133
 70   PUNCH 67, XL, YL, GANE
 133  IF (SENSE SWITCH 2) 71, 75
 71   PRINT 67, XL, YL, GANE
 67   FØRMAT (E13.6, 3X, E13.6, 3X, E13.6)
 75   IF 'SENSE SWITCH 3) 72,175
 175  IF (SENSE SWITCH 2) 72,76
 76   K=-1
      GØ TØ 121
 72   IF'L) 77,78,78
 77   L=-L
 78   L=L-1
      IF'L)174,174,230
      END
```

APPENDIX C

Dynamic Response for Type Two Phase-Lock Loop

APPENDIX C

This Appendix contains the step and ramp responses of the Type Two Phase-Lock Loop. The following values apply to these curves.

$A = 20$

$B = 20$

$K_1 = 2$

$K_2 = .3$

$K_3 = 5$

$K_4 = (289)\ (.05)\ G$

$\phi = 0$

$$F(s) = \frac{K\ (s + .1)\ (s + .6)}{s\ (s + 1)\ (s + .5)}$$

$G = 10$ to $G = 160$

Step = .05 radians/sec

Ramp = .05 radians/sec^2

The various curves shown on the following pages are from top to bottom.

Curve	Signal	Amplitude Scale v/cm
1	A SIN $\omega_1 t$	20
2	B SIN $\omega_2 t$	20
3	ℓ_m	5
4	ℓ_c	as marked
5	ℓ_r	as marked

The time scale of these curves are 5 sec/cm.

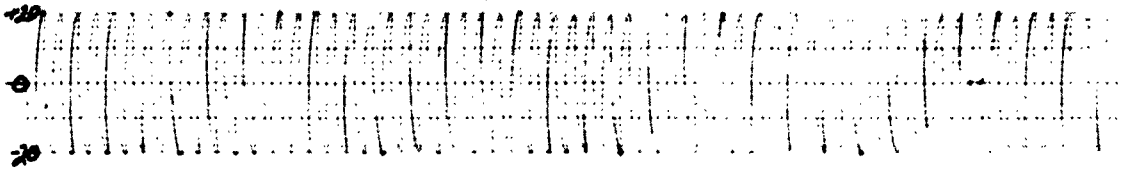

A SIN $\omega_1 t$

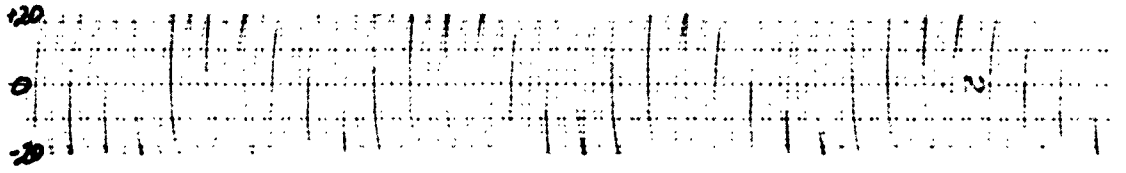

B SIN $\omega_2 t$

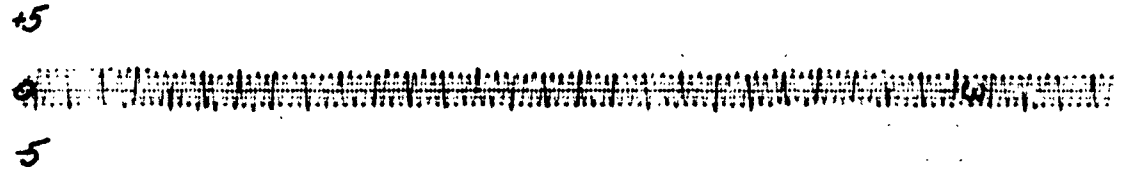

e_m

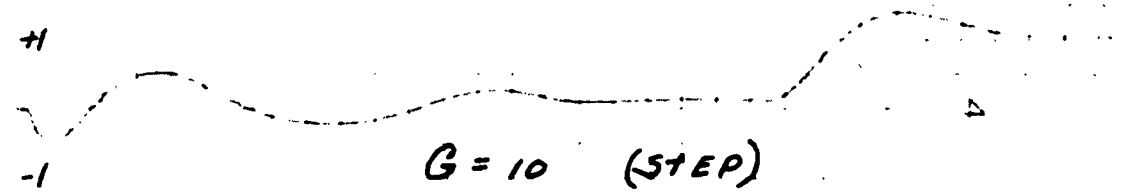

e_c

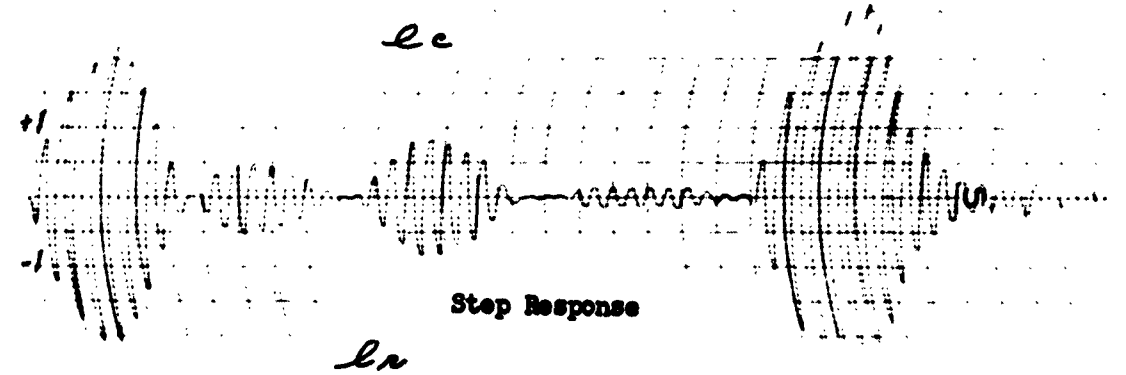

Step Response

e_r

Appendix Figure C-1

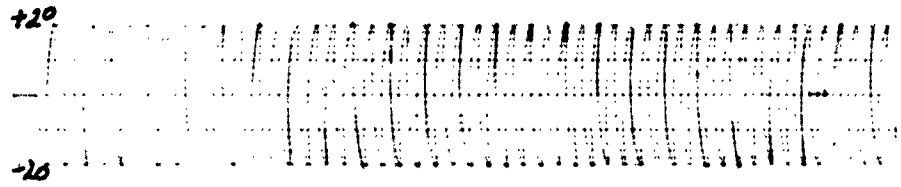

A SIN $\omega_1 t$

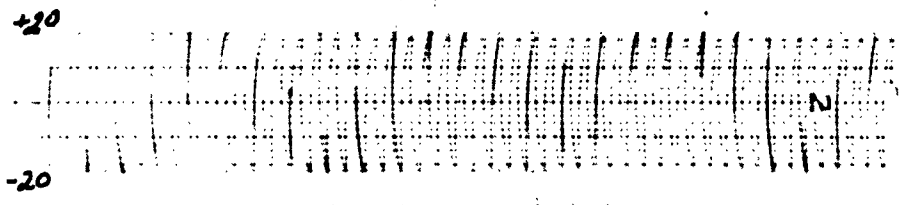

B SIN $\omega_2 t$

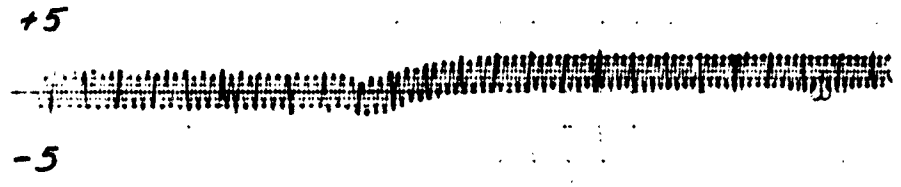

e_m

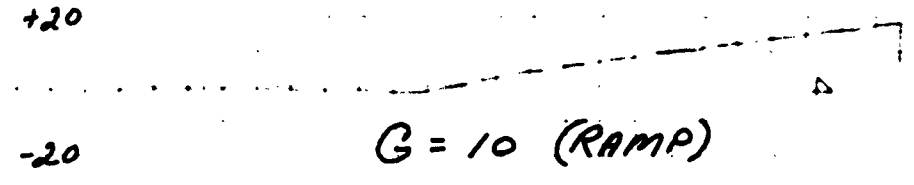

G = 10 (RAMP)

e_c

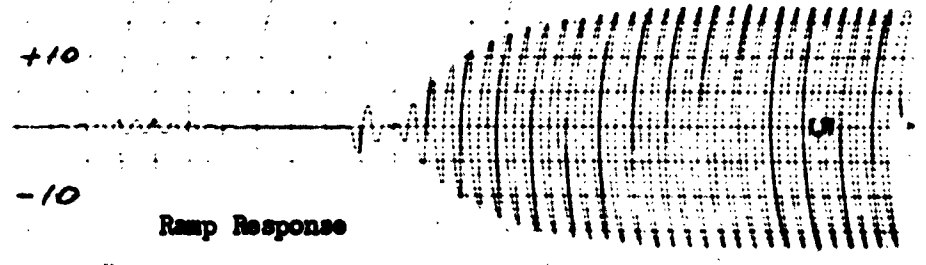

Ramp Response

e_a

Appendix Figure C-2

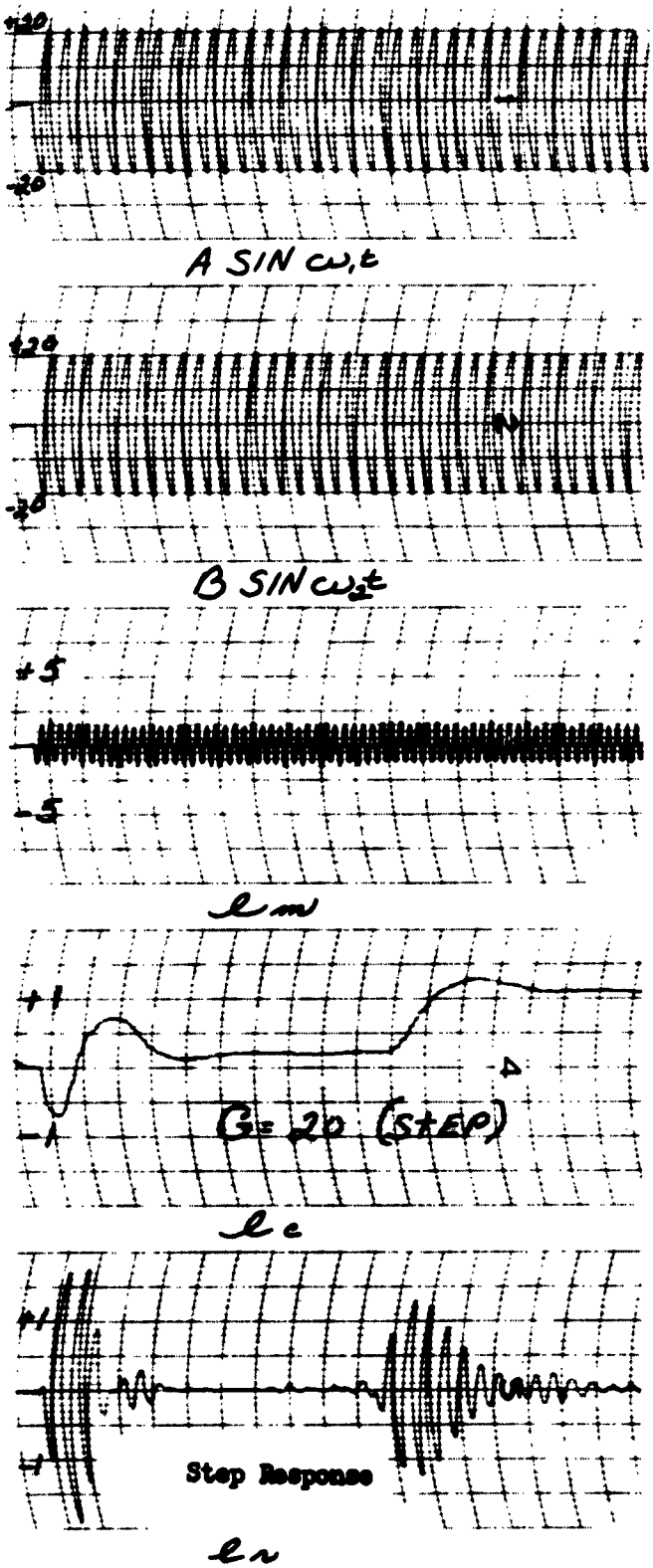

Appendix Figure C-3

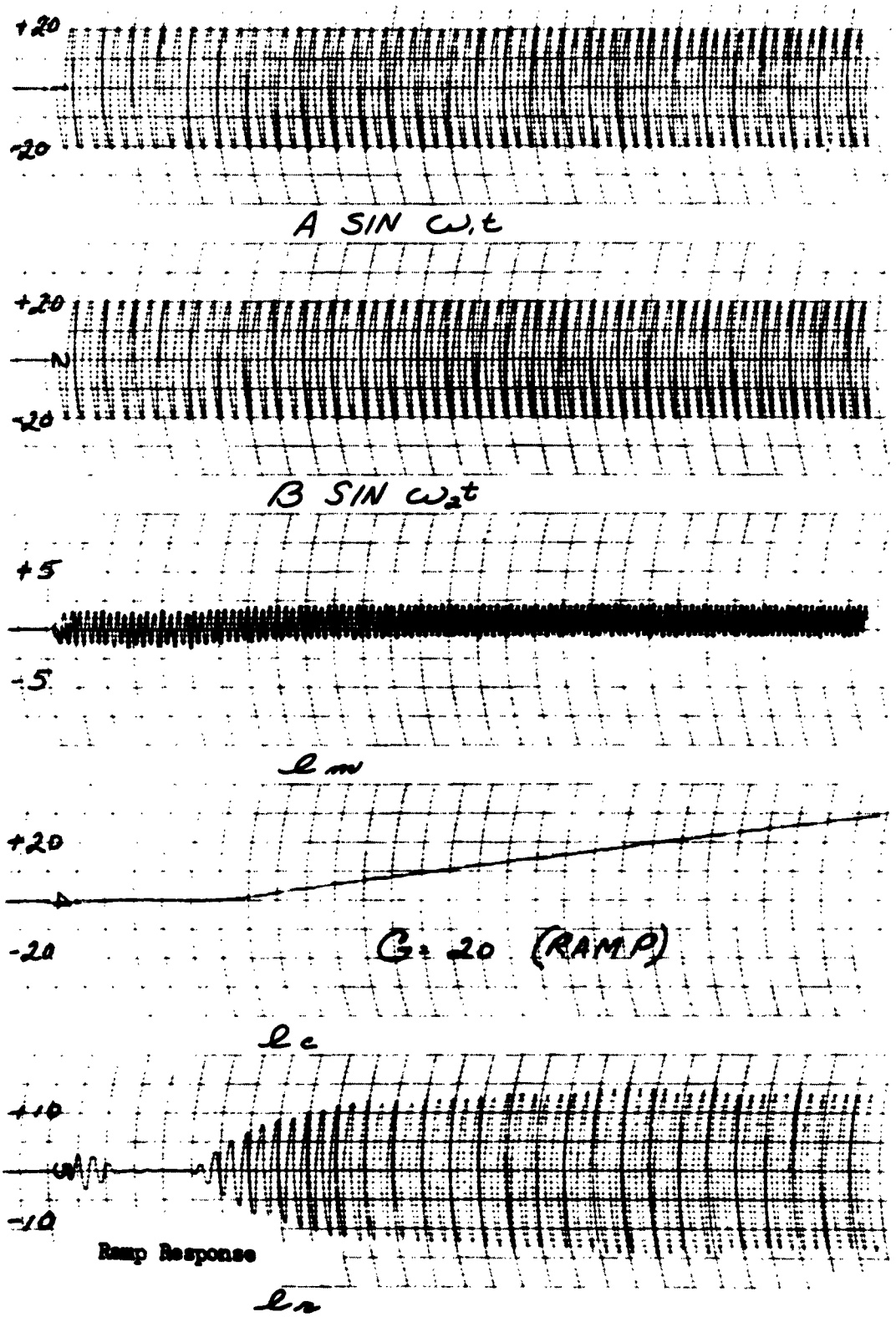

Appendix Figure C-4

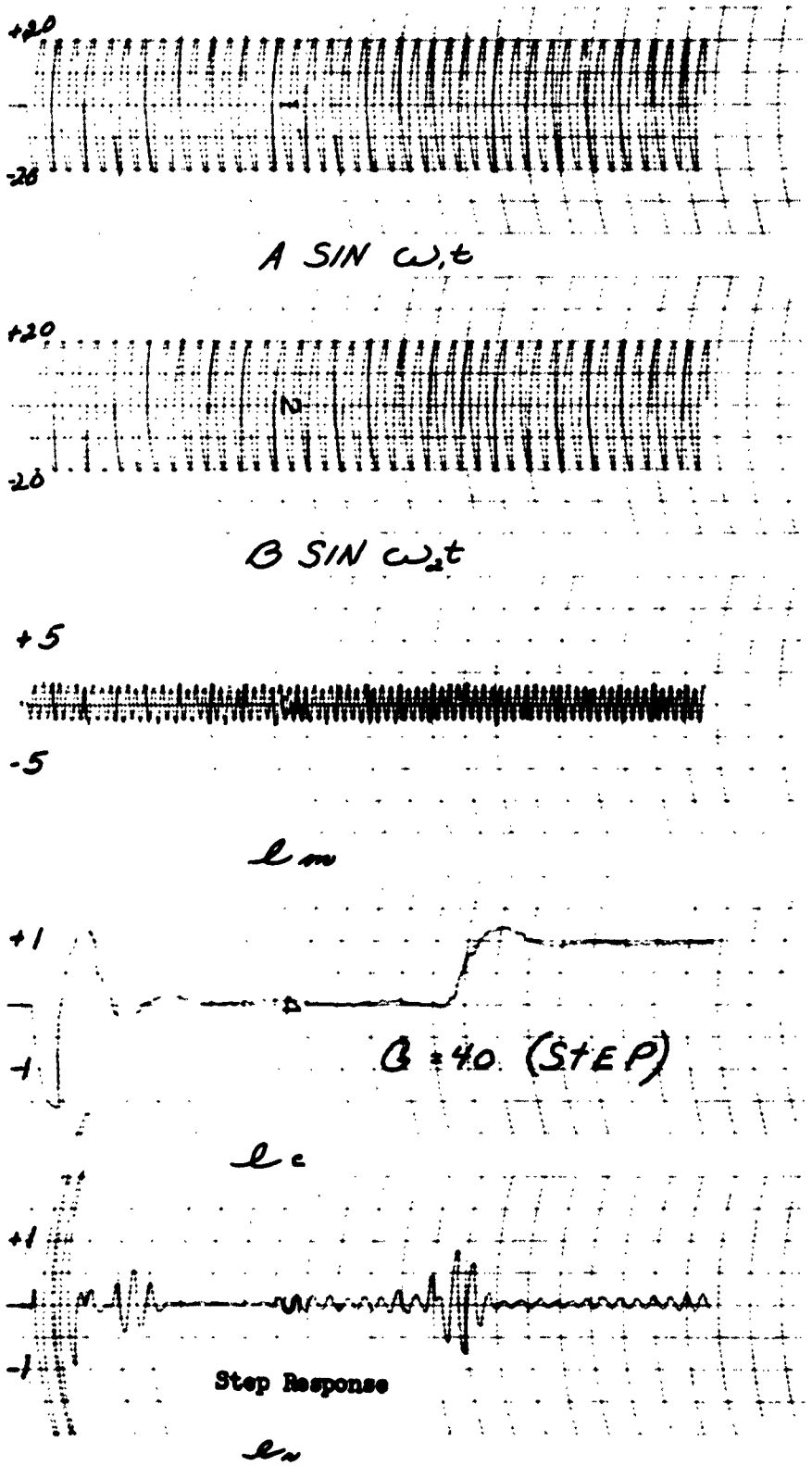

Appendix Figure C-5

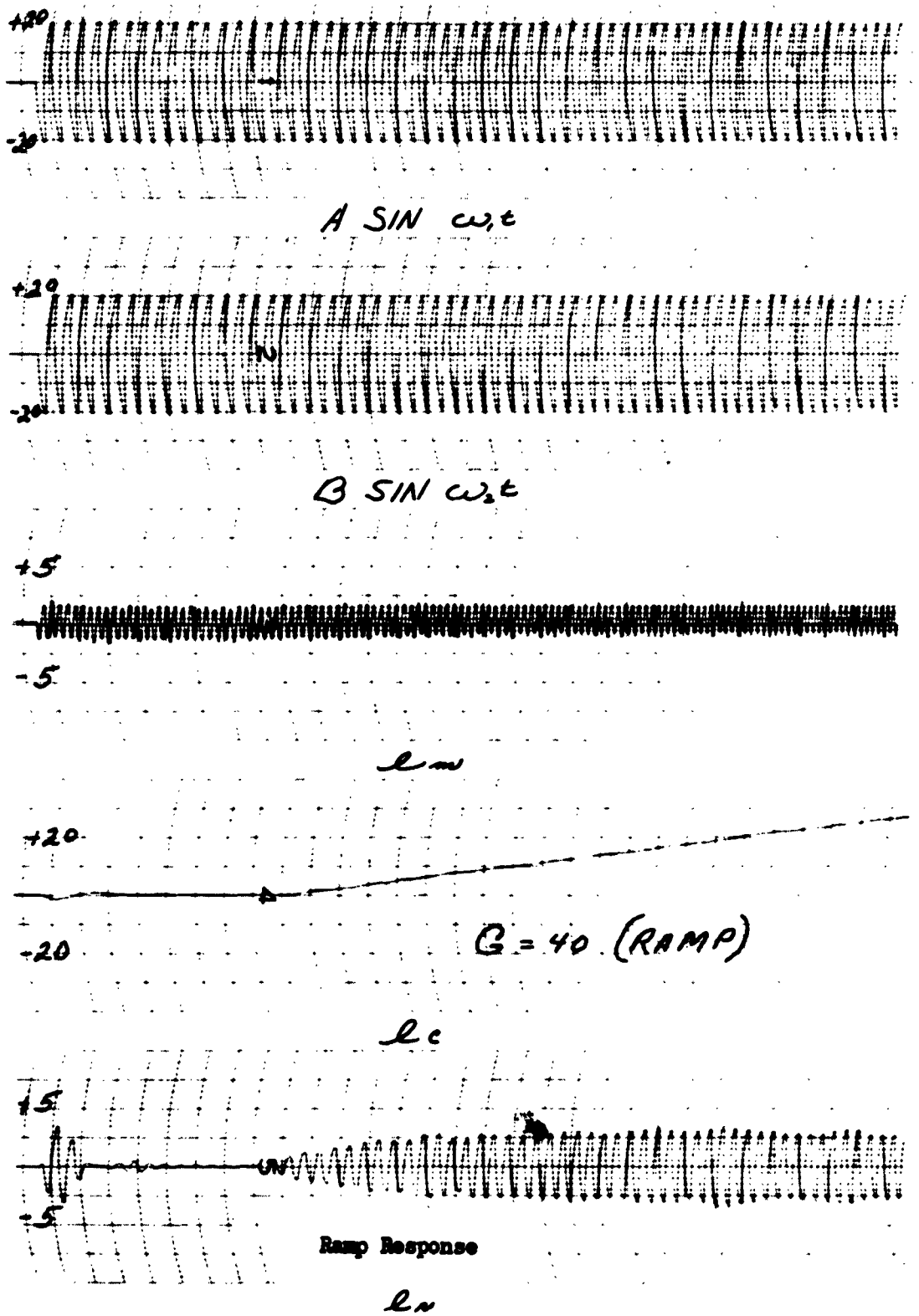

Ramp Response

Appendix Figure C-6

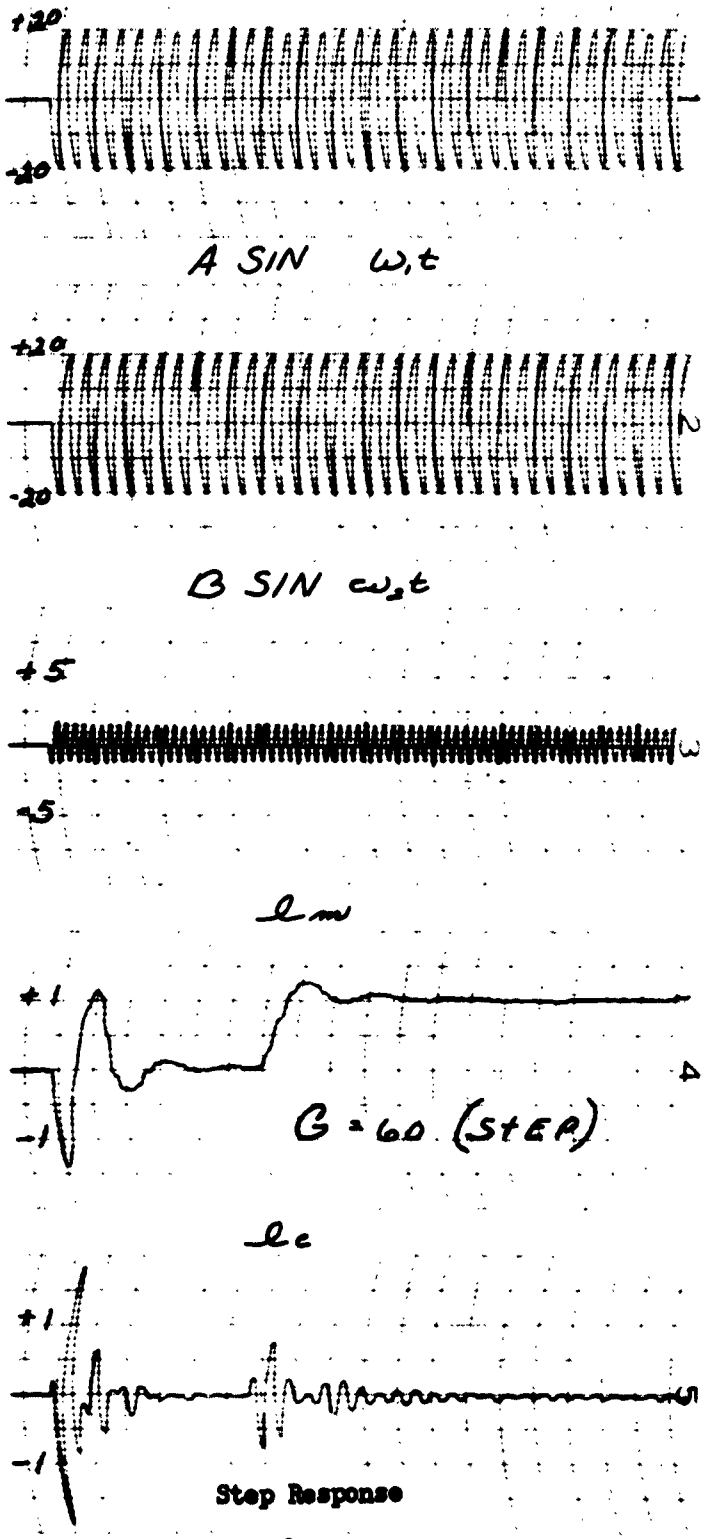

Appendix Figure C-7

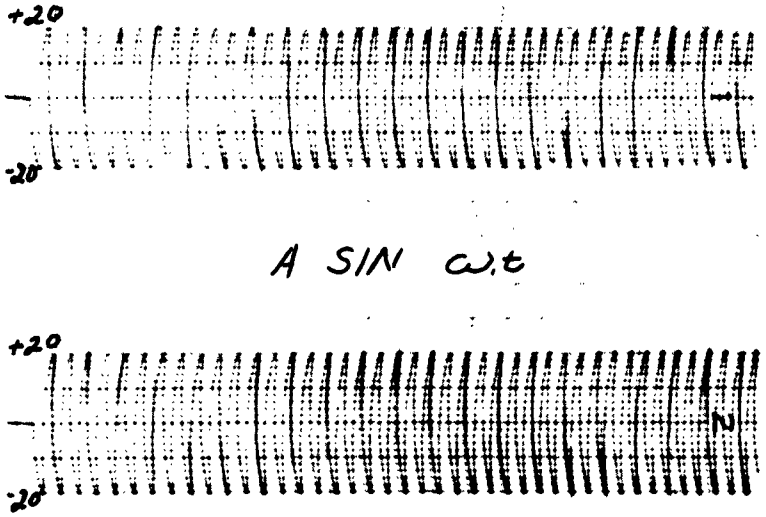

Appendix Figure C-8

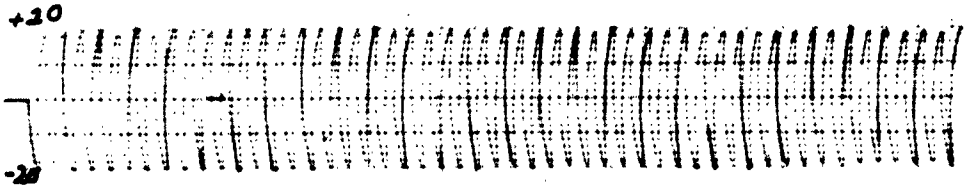

A SIN $\omega_1 t$

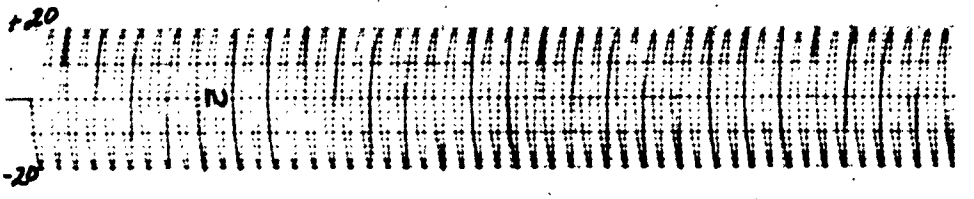

B SIN $\omega_2 t$

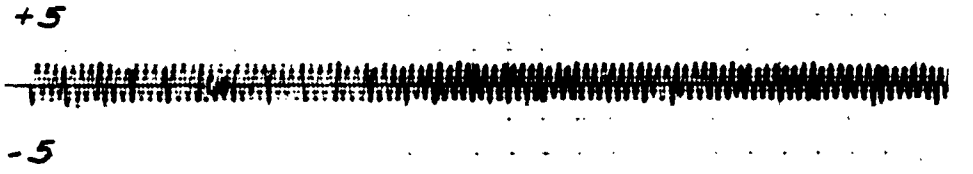

e_m

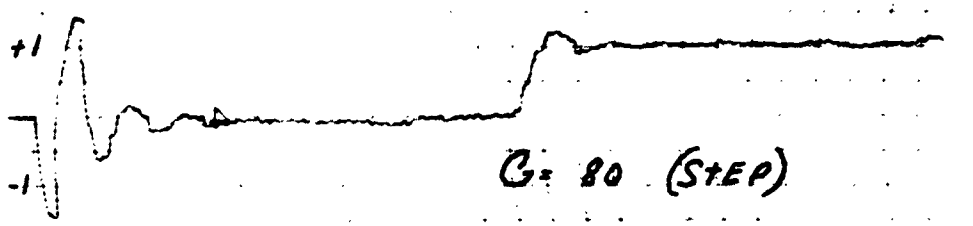

e_c

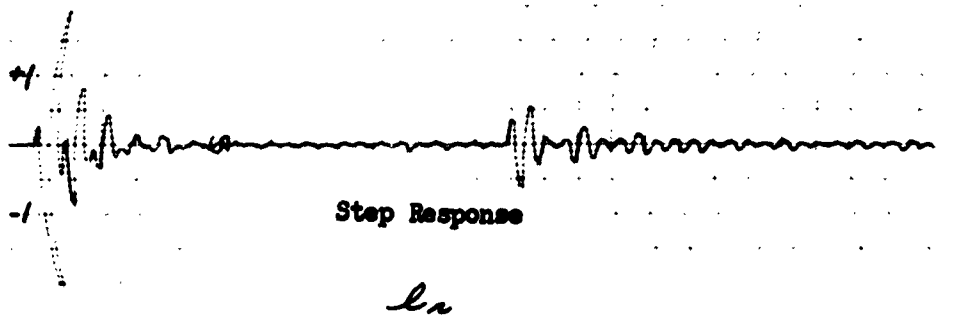

Step Response

e_r

Appendix Figure C-9

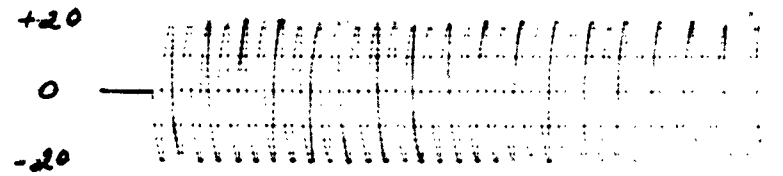

$A \sin \omega_1 t$

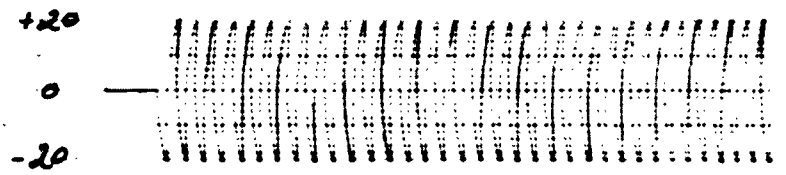

$B \sin \omega_2 t$

e_m

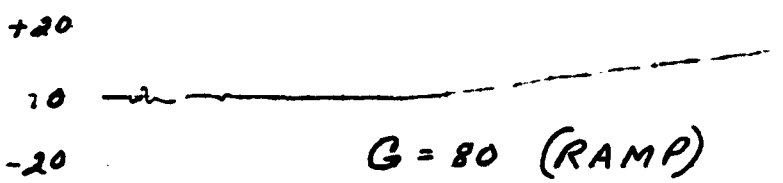

e_c

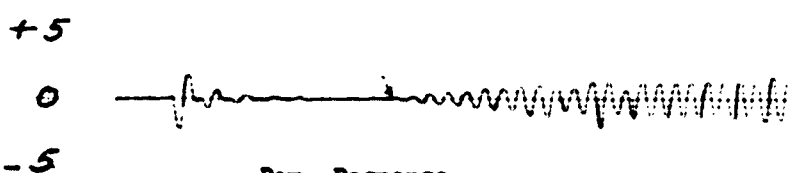

Ramp Response

e_n

Appendix Figure C-10

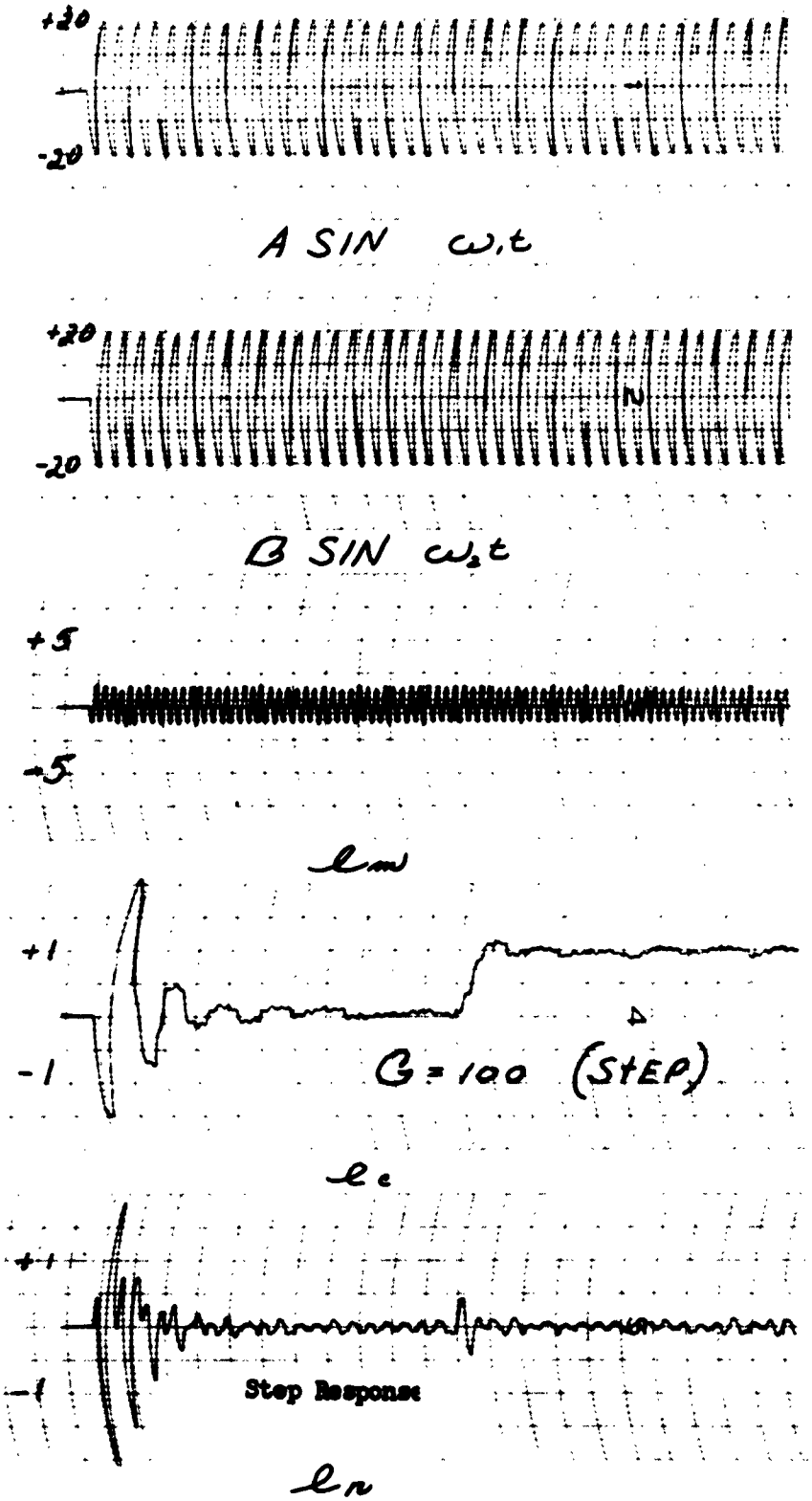

Appendix Figure C-11

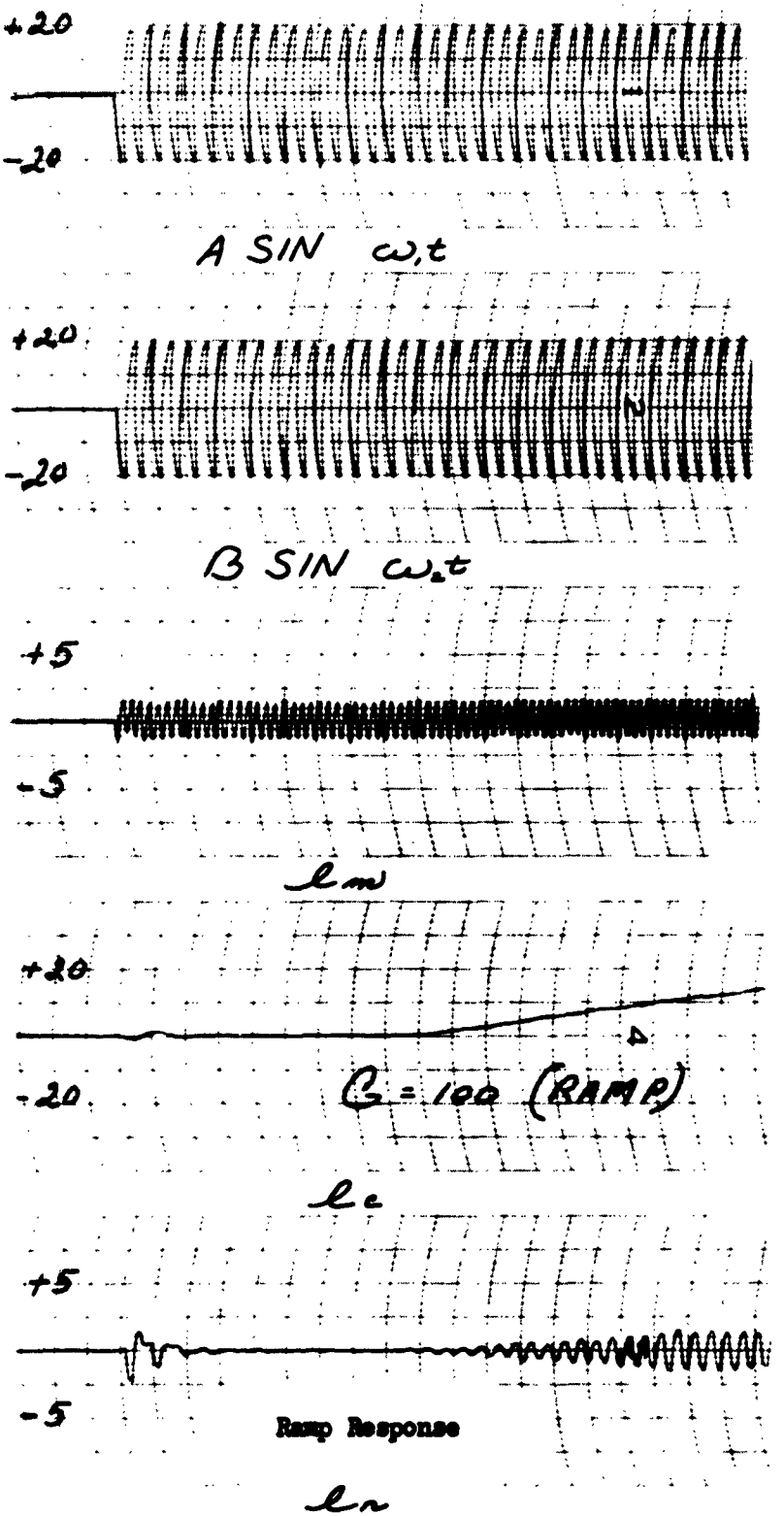

Ramp Response

Appendix Figure C-12

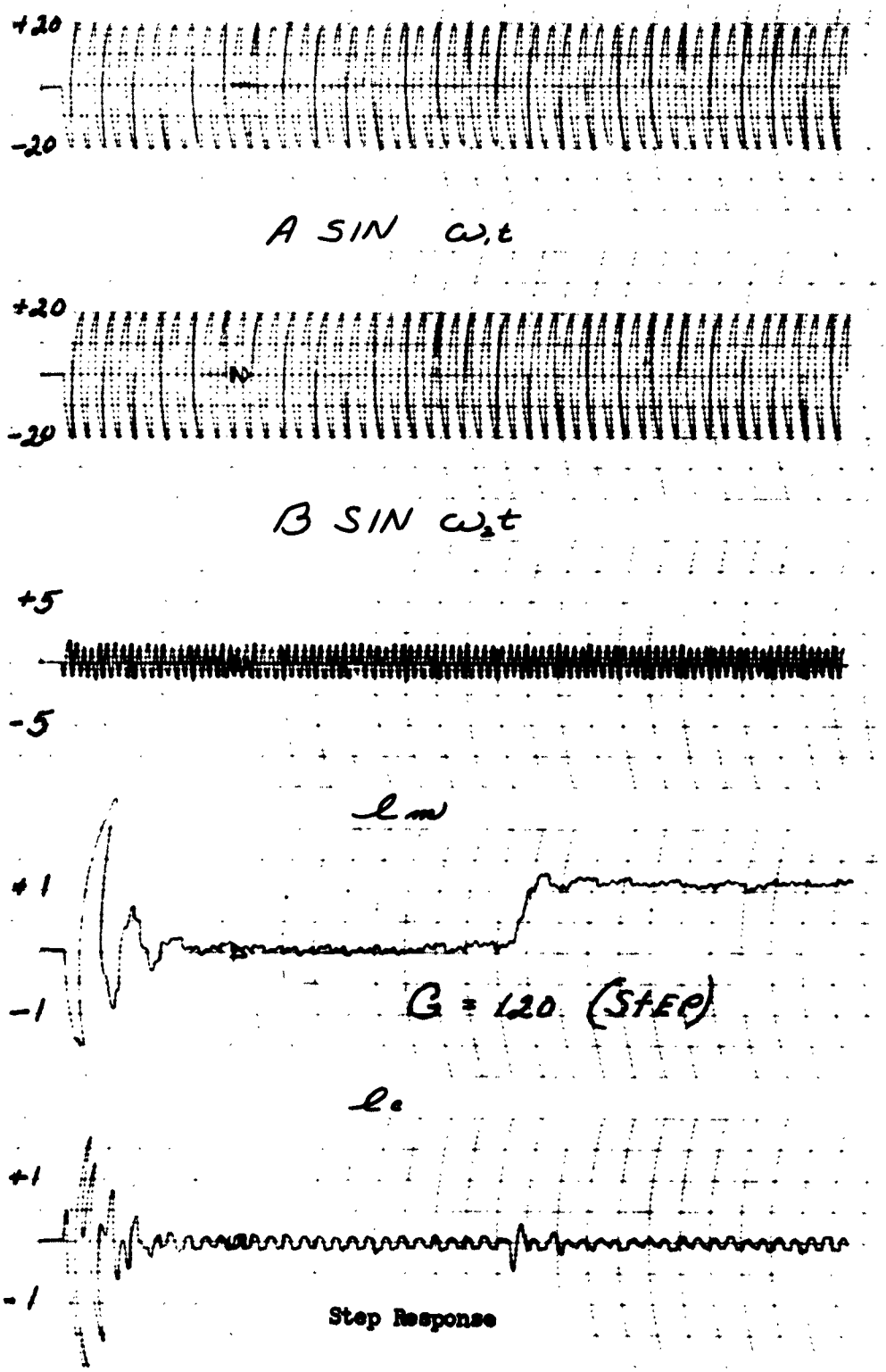

Appendix Figure C-13

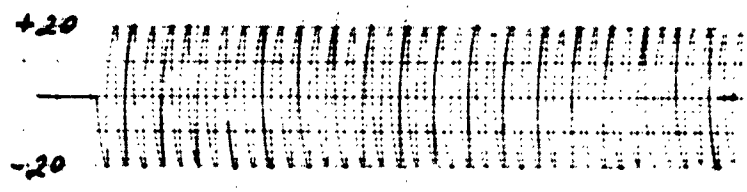

A SIN $\omega_1 t$

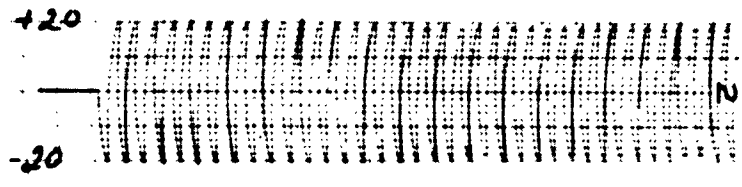

B SIN $\omega_2 t$

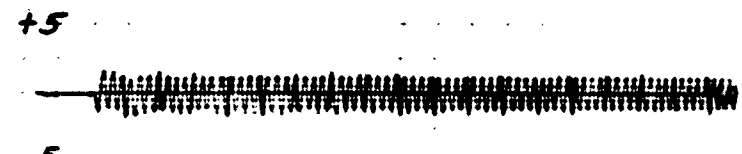

e_m

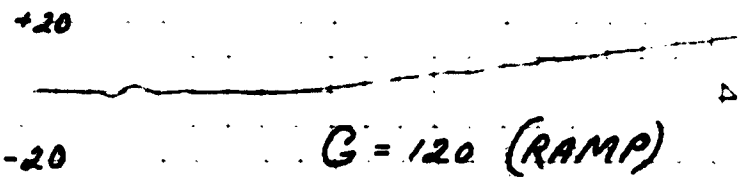

e_c

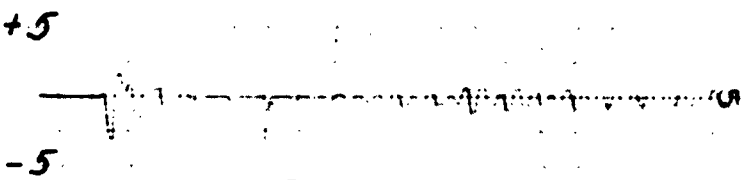

Ramp Response

e_n

Appendix Figure C-14

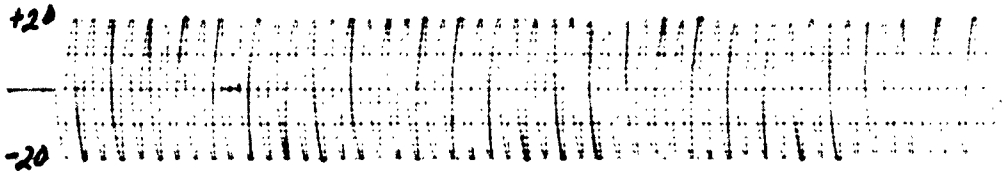

A SIN $\omega_1 t$

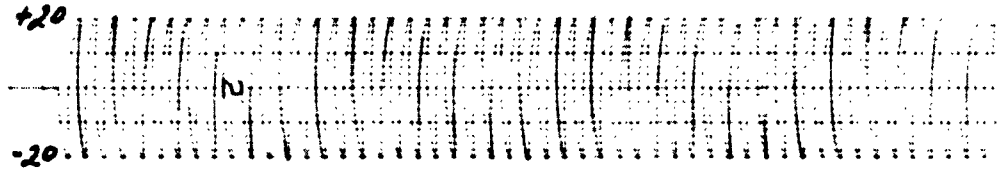

B SIN $\omega_2 t$

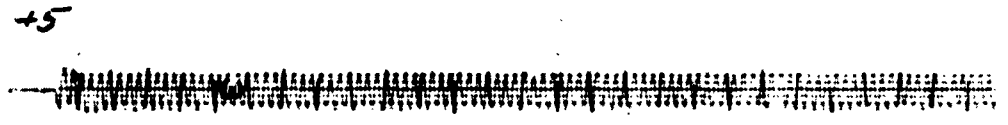

ℓ_m

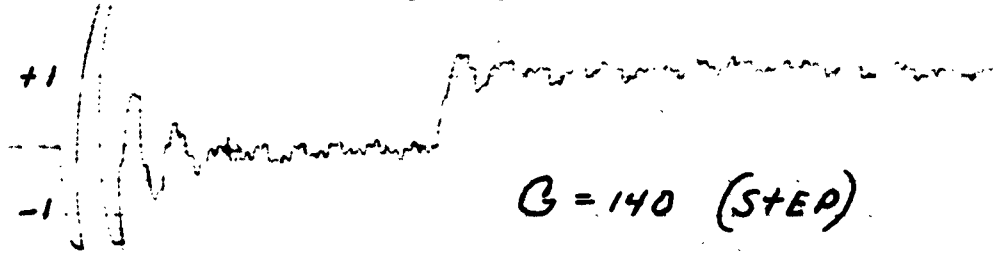

ℓ_c

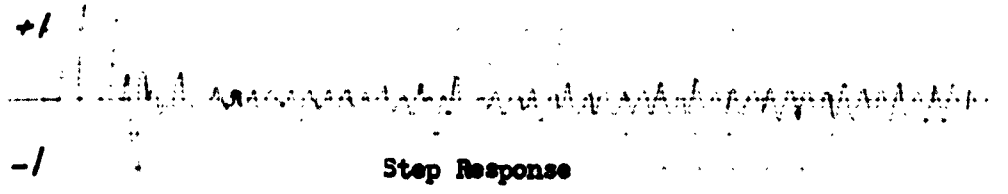

Step Response

ℓ_n

Appendix Figure C-15

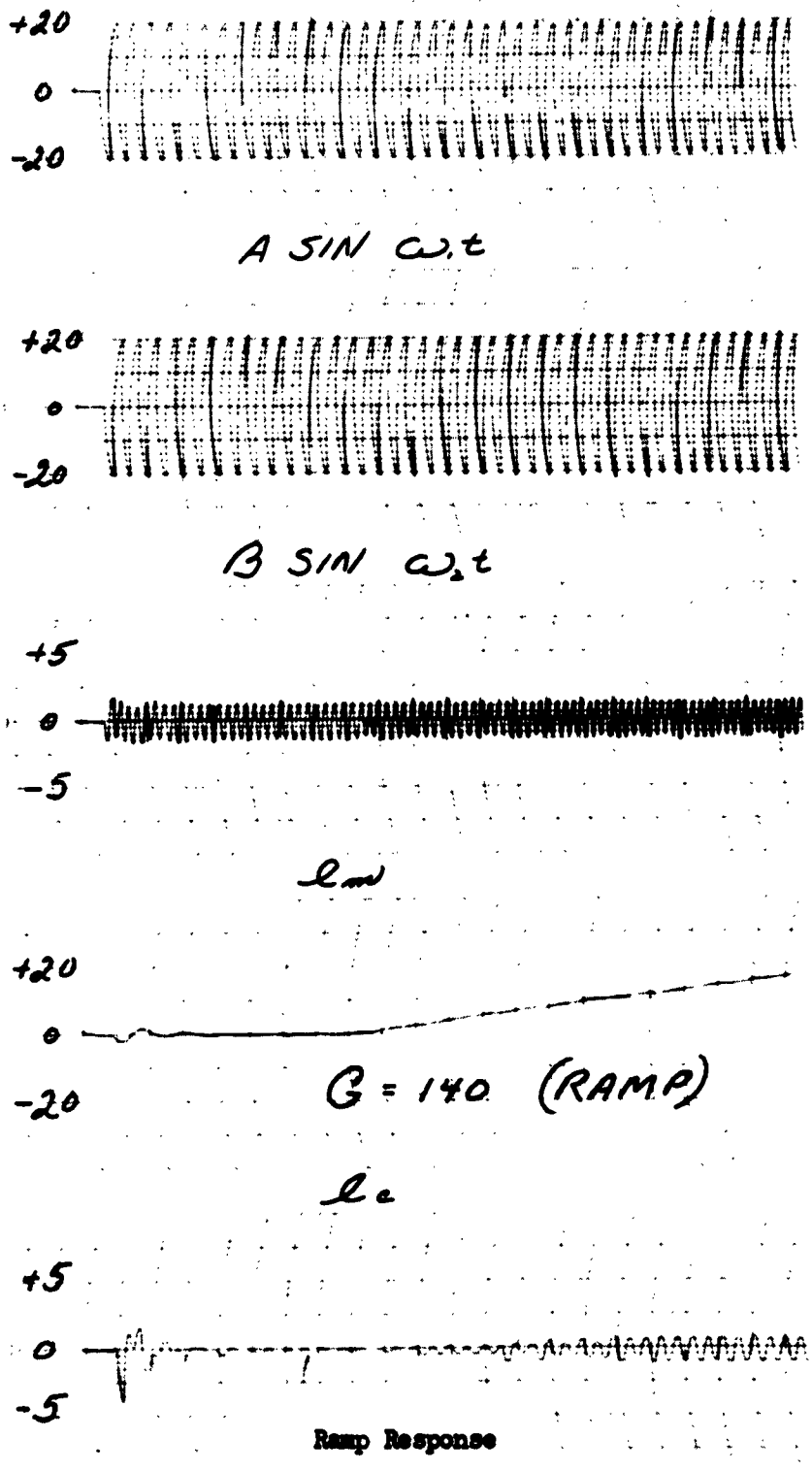

Ramp Response

Appendix Figure C-16

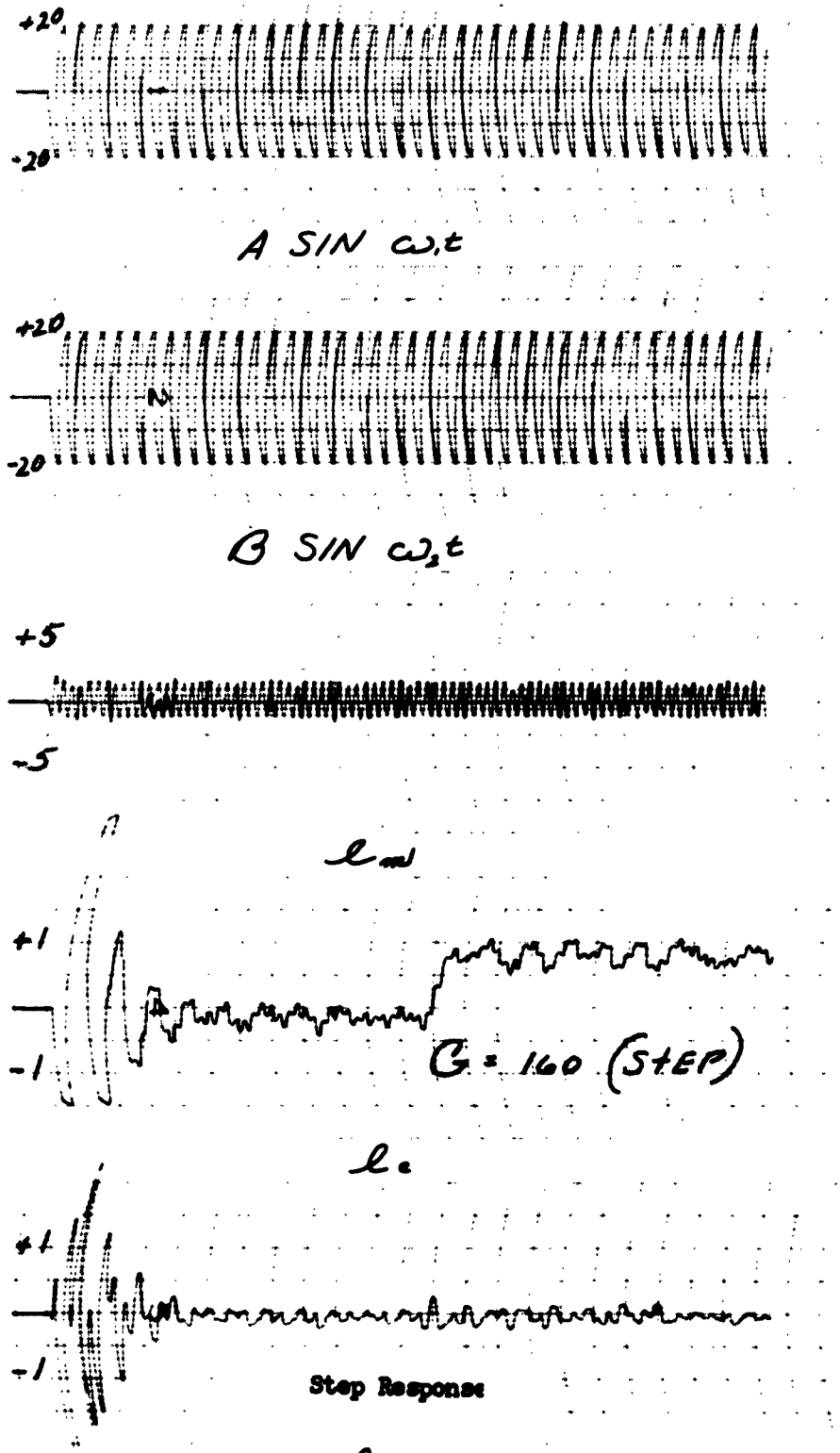

Appendix Figure C-17

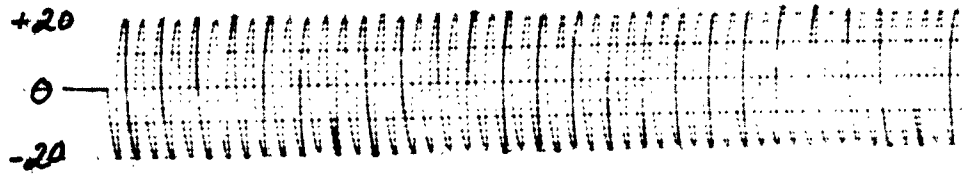

$A \sin \omega_1 t$

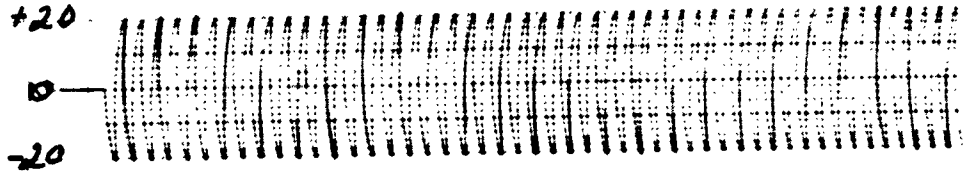

$B \sin \omega_2 t$

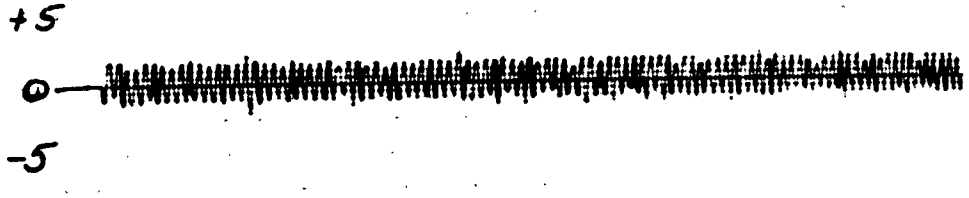

ℓ_m

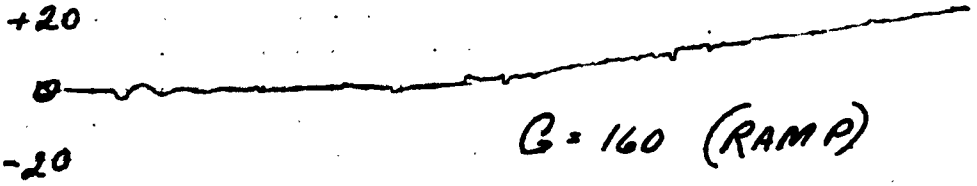

ℓ_c

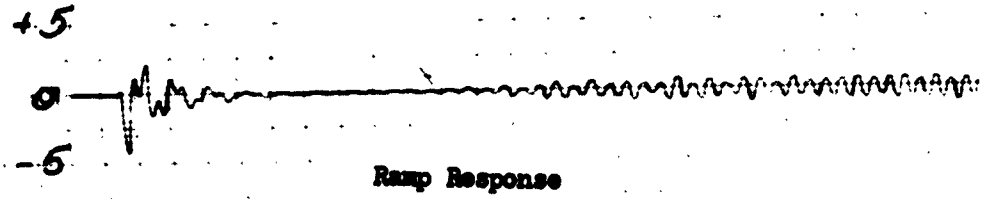

Ramp Response

ℓ_N

Appendix Figure C-18

APPENDIX D

Dynamic Response for Type Three Phase-Lock Loop

APPENDIX D

This Appendix contains step, ramp, and parabolic response curves for the Type Three Phase-Lock Loop. The following values apply to these curves.

$A = 20$

$B = 20$

$K_1 = 2$

$K_2 = .3$

$K_3 = 5$

$K_4 = (289)\ (.05)\ G$

$\phi = 0$

$$F(s) = \frac{K_2\ (s + .1)\ (s^2 + 5s + 2.5)}{s^2\ (s^2 + 8s + 20)}$$

$G = 60$ to $G = 300$

Step = .05 radians/sec

Ramp = .0065 radians/sec^2

Parabolic = .0065 radians/sec^3

The various curves shown on the following pages are from top to bottom.

Curve	Signal	Amplitude Scale volt/cm
1	A SIN $\omega_1 t$	20
2	B SIN $\omega_2 t$	20
3	ℓ_m	2.0
4	ℓ_e	as marked
5	ℓ_n	as marked

The time scale of these curves are 5 sec/cm.

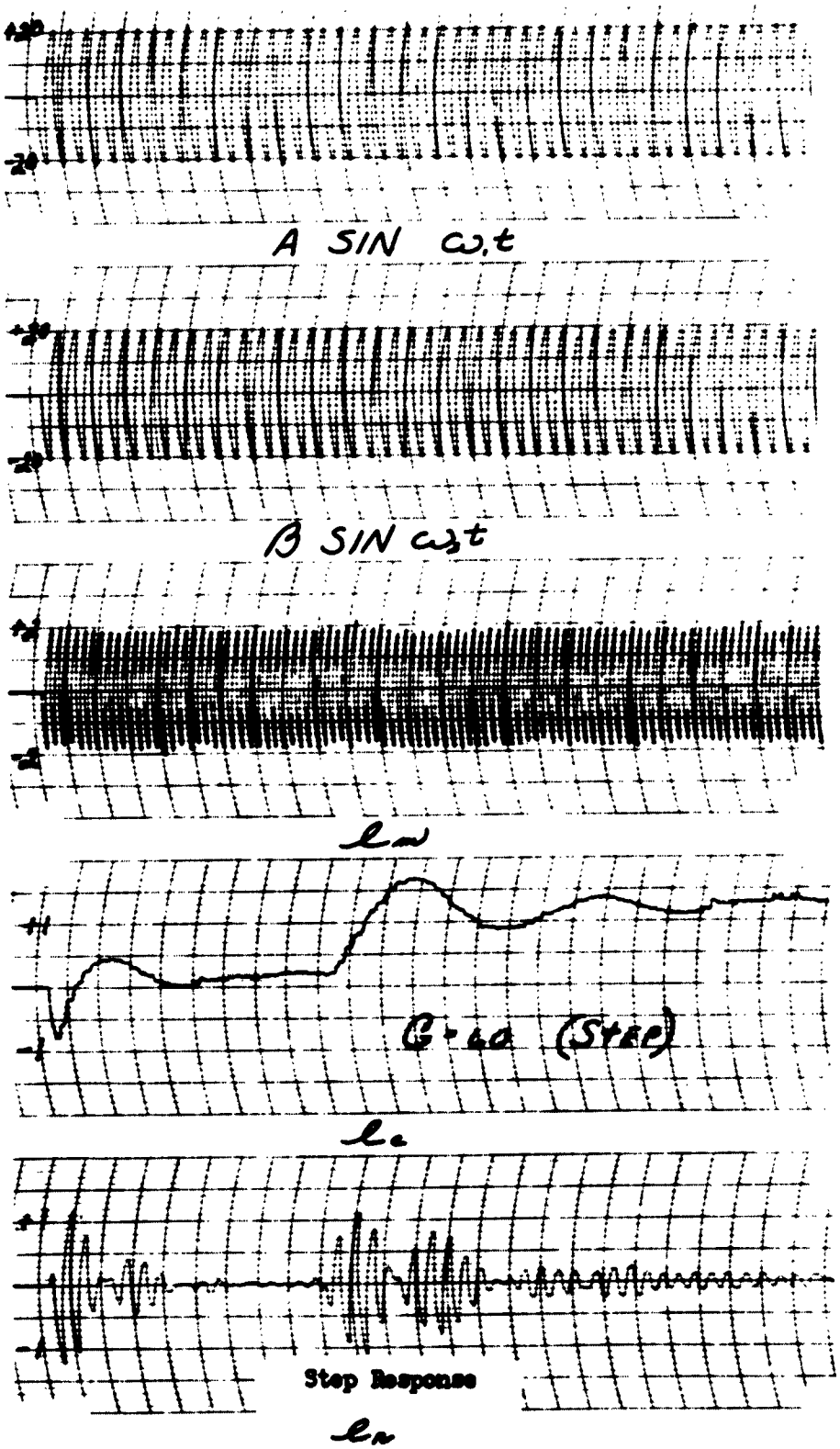

Step Response

Appendix Figure D-1

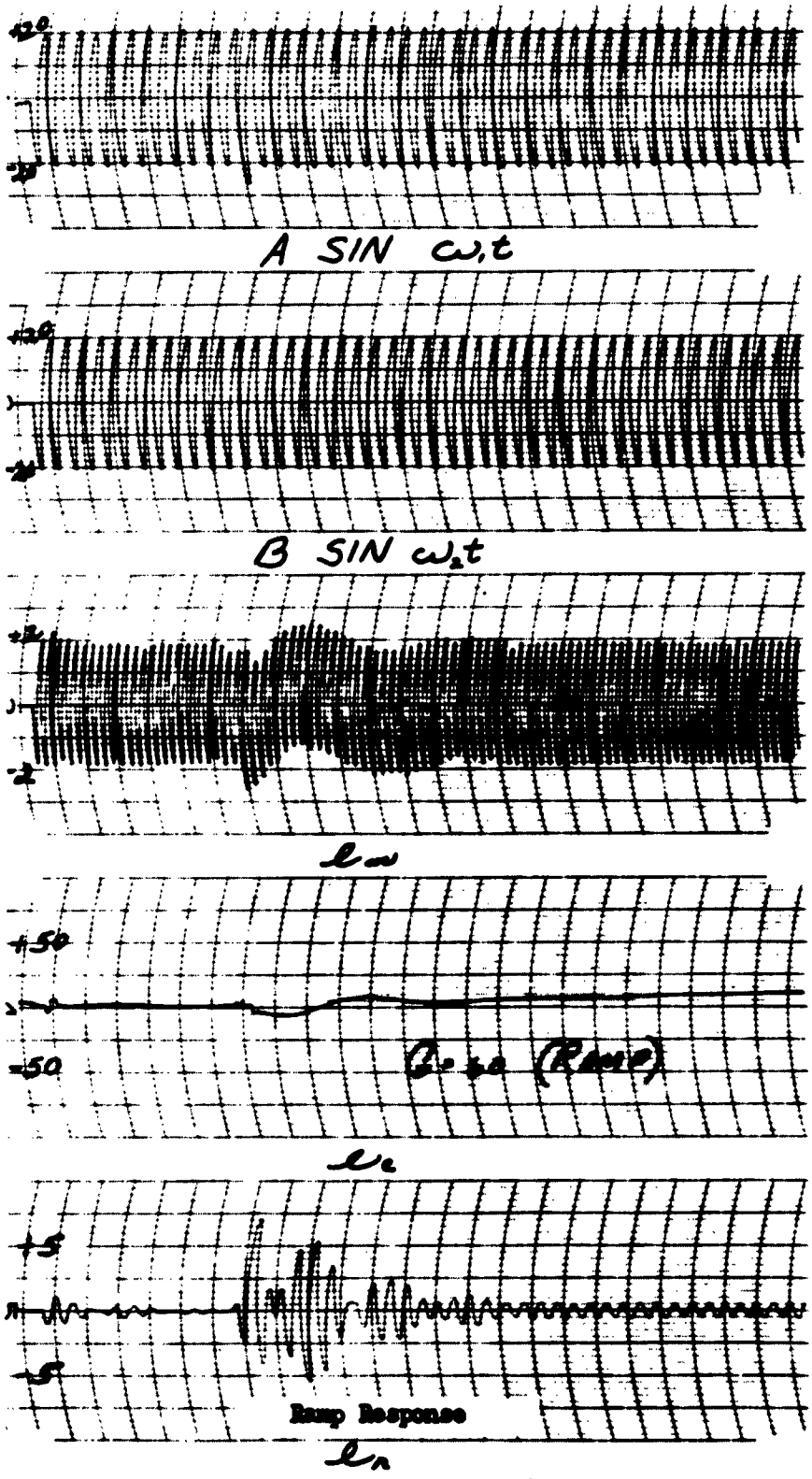

Appendix Figure D-2

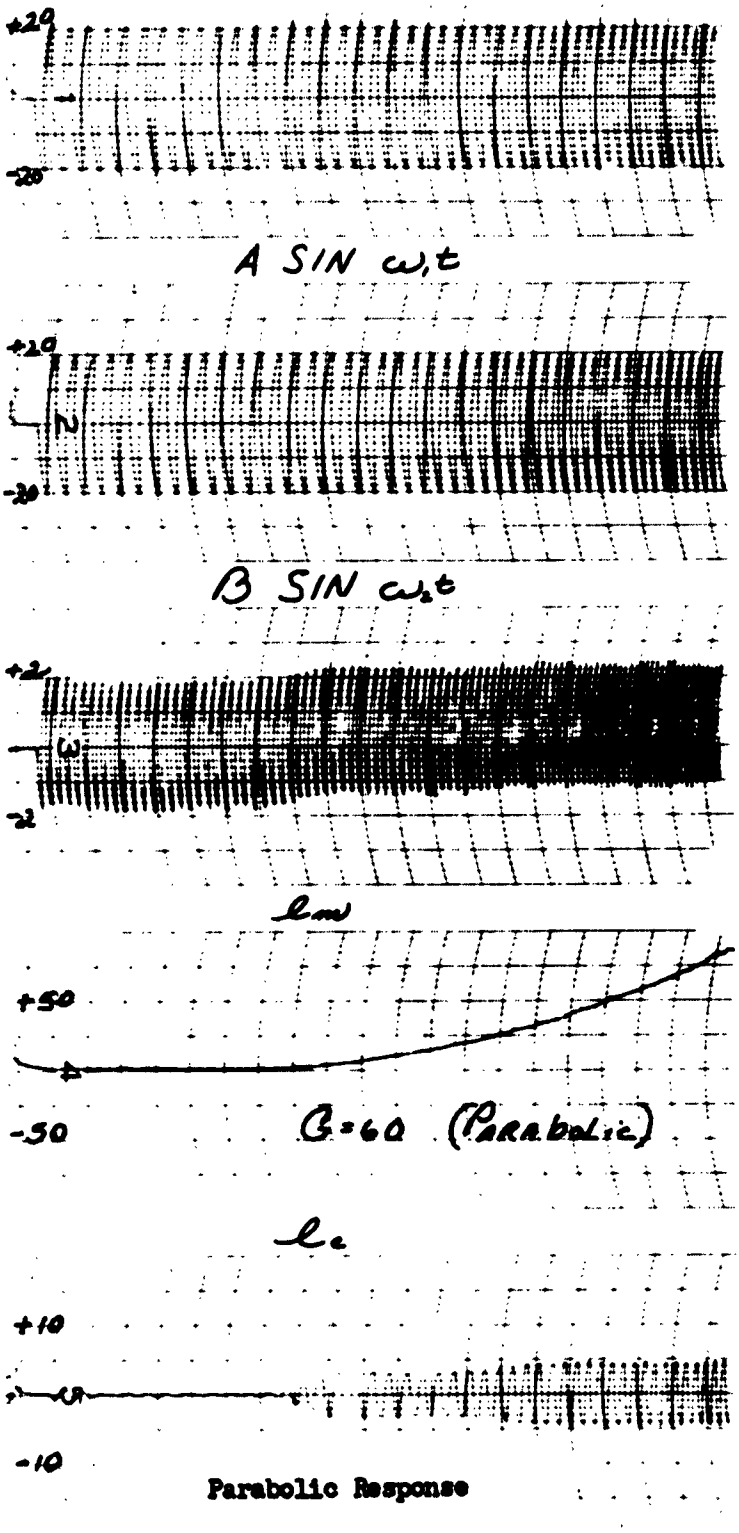

Parabolic Response

ℓ_n

Appendix Figure D-3

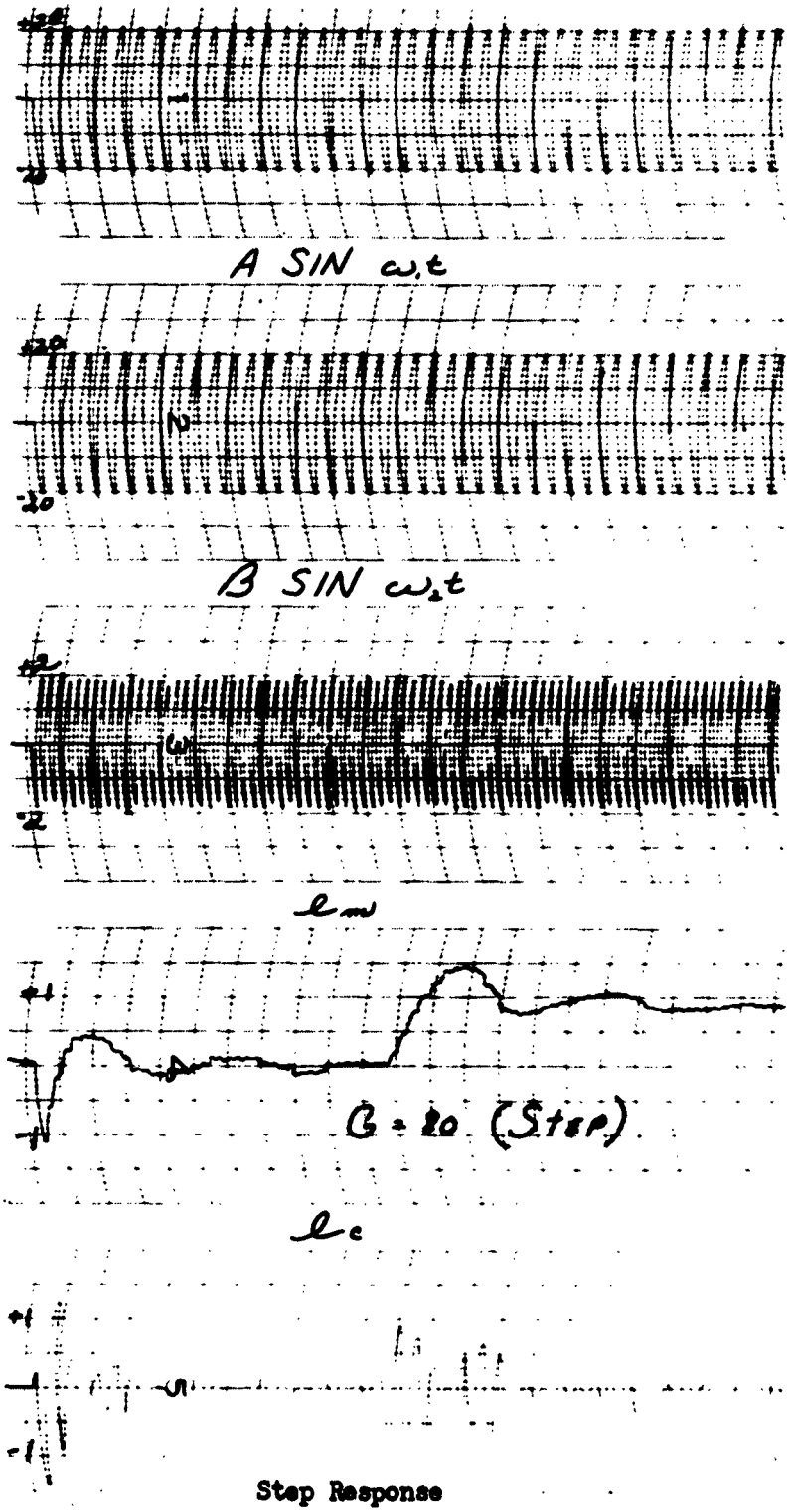

Step Response

Appendix Figure D-4

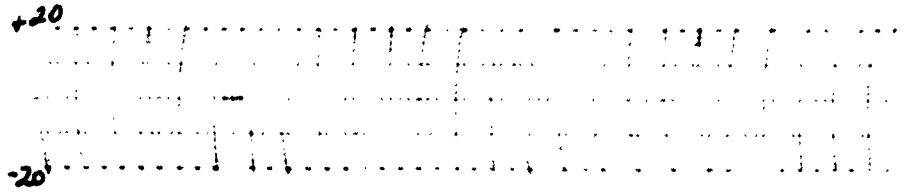

A SIN $\omega_1 t$

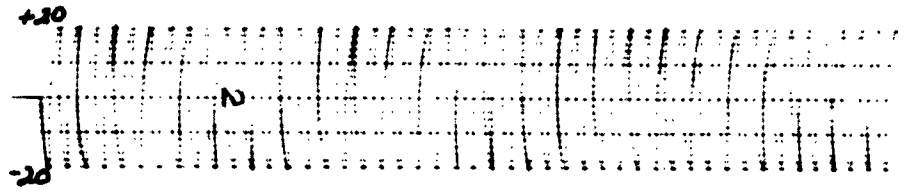

B SIN $\omega_2 t$

ℓ_m

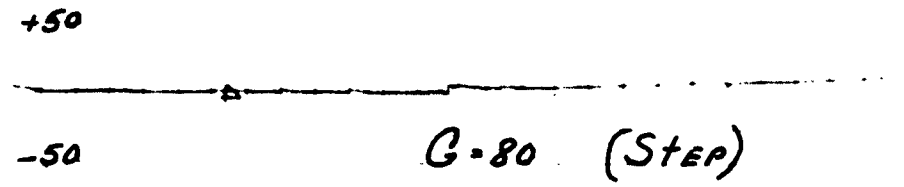

G = 80 (Step)

ℓ_c

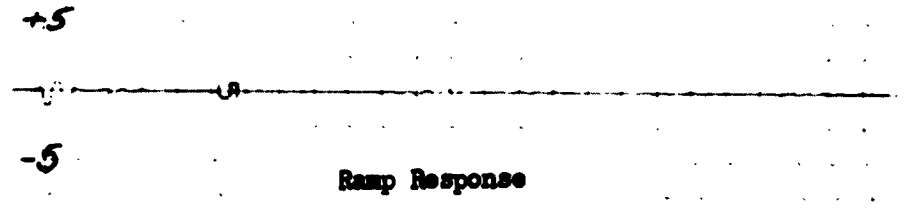

Ramp Response

ℓ_n

Appendix Figure D-5

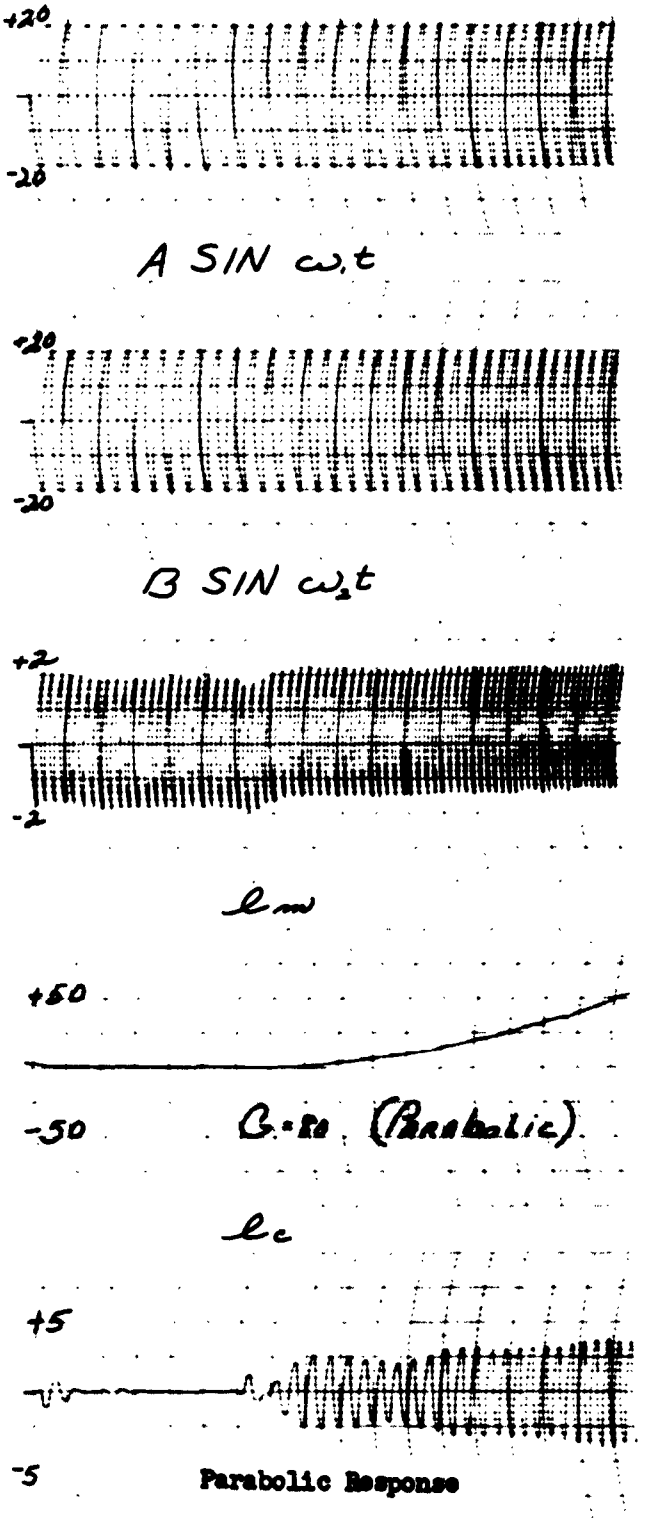

Parabolic Response

Appendix Figure D-6

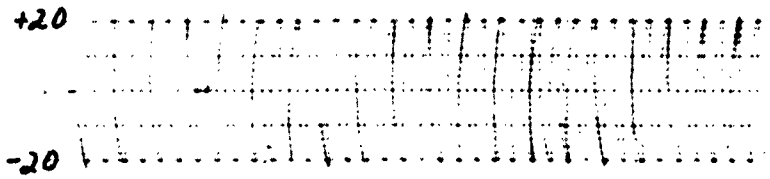

A SIN $\omega_1 t$

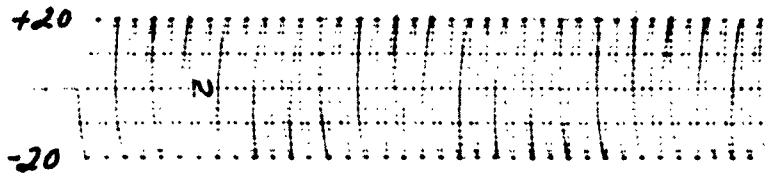

B SIN $\omega_2 t$

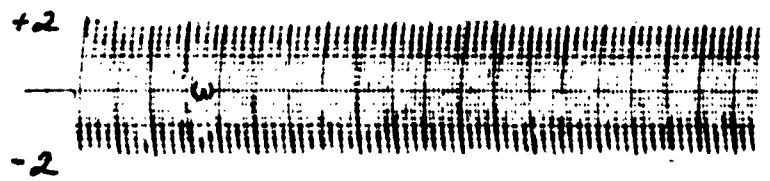

e_m

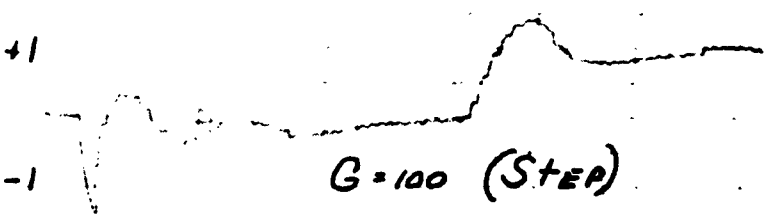

e_c

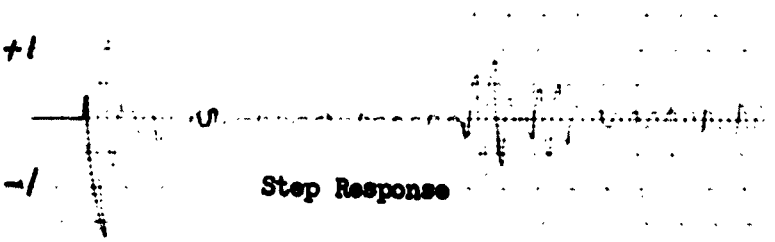

e_n

Appendix Figure D-7

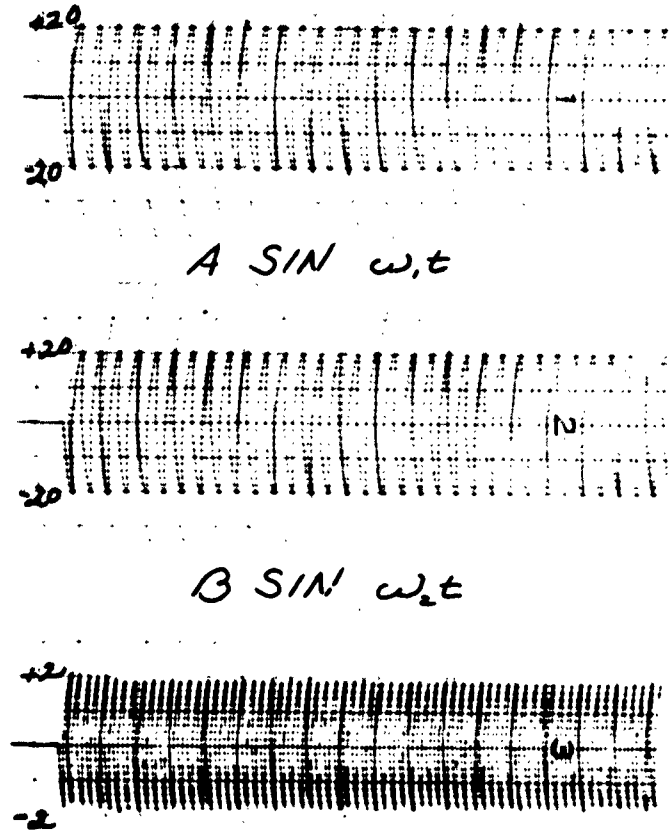

Appendix Figure D-8

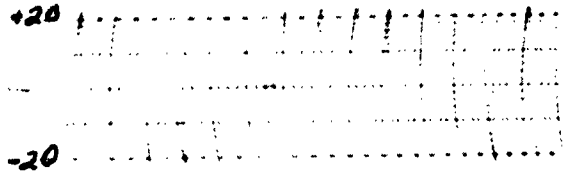

A SIN $\omega_1 t$

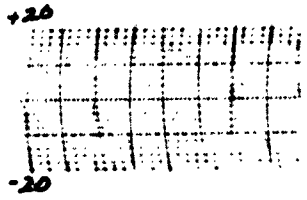

A SIN $\omega_1 t$

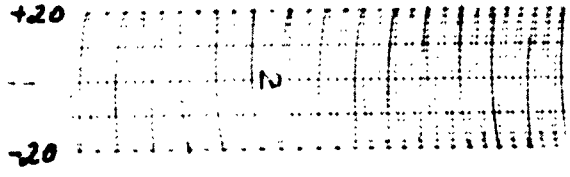

B SIN $\omega_2 t$

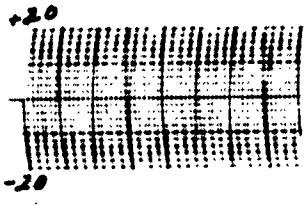

B SIN $\omega_2 t$

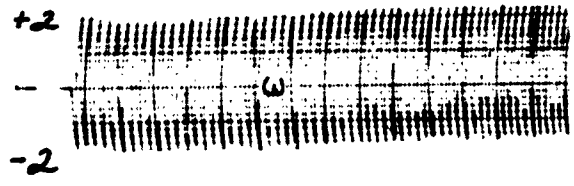

ℓ_m

ℓ_m

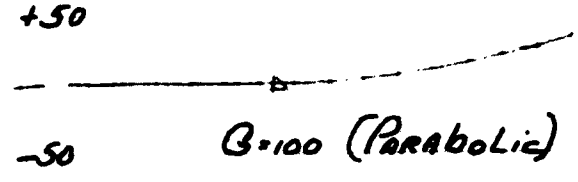

G=100 (Parabolic)

ℓ_c

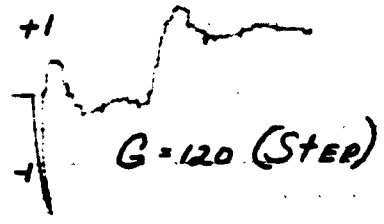

G=120 (Step)

ℓ_c

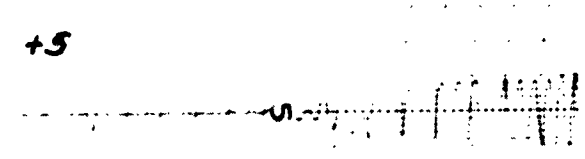

Parabolic Response

ℓ_n

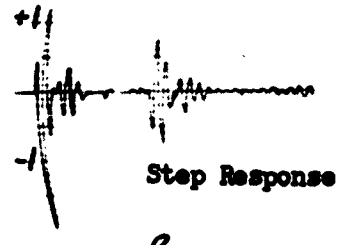

Step Response

ℓ_n

Appendix Figure D-9

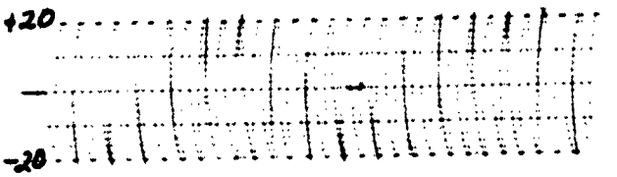

A SIN $\omega_1 t$

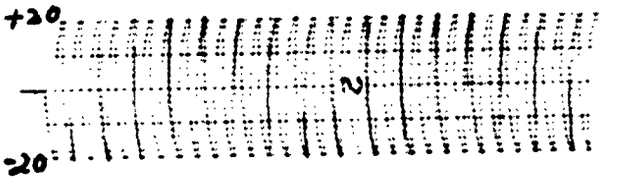

B SIN $\omega_2 t$

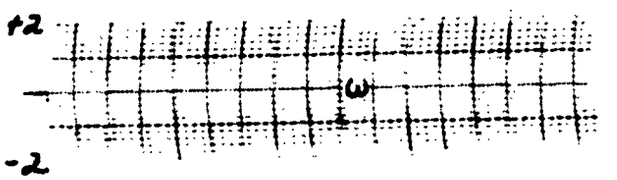

e_{mi}

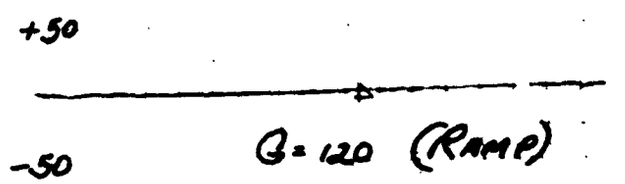

e_c

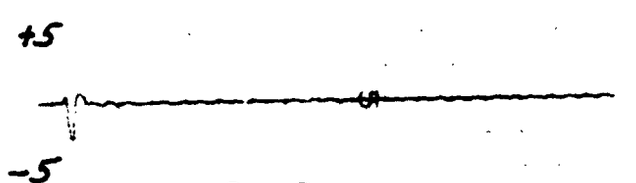

Ramp Response

e_r

Appendix Figure D-10

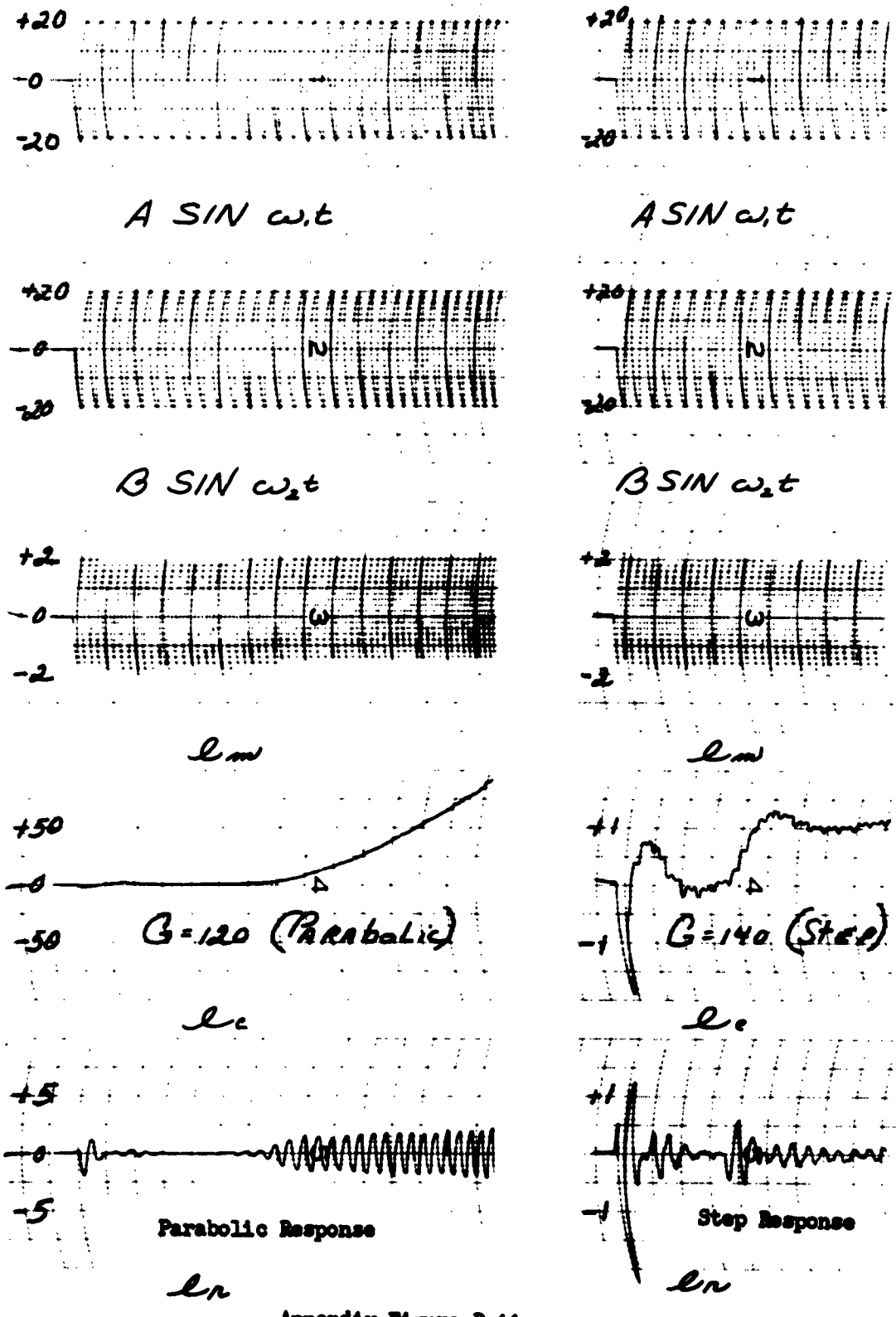

Appendix Figure D-11

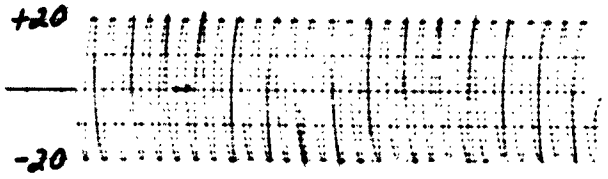

$A \sin \omega_1 t$

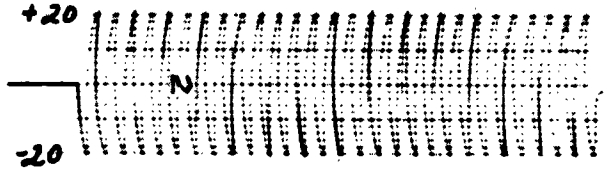

$B \sin \omega_2 t$

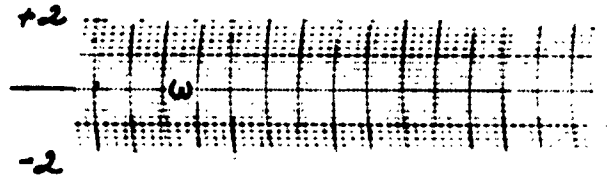

e_m

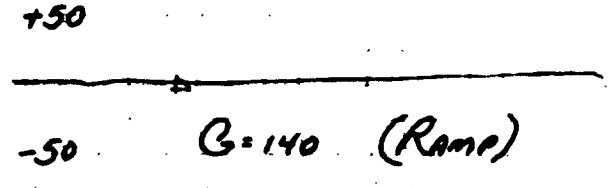

e_c

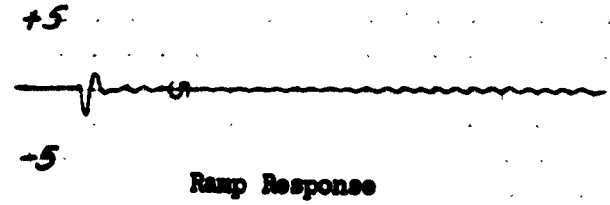

Ramp Response

e_n

Appendix Figure D-12

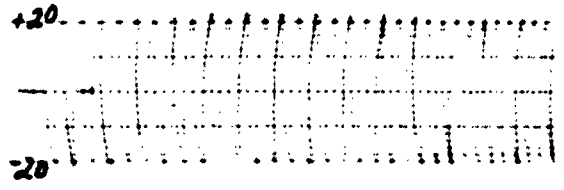

$A \sin \omega_1 t$

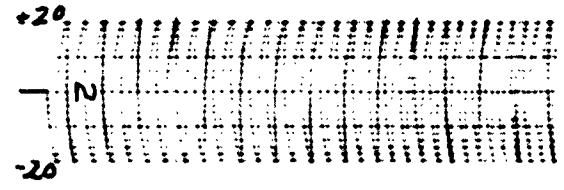

$B \sin \omega_2 t$

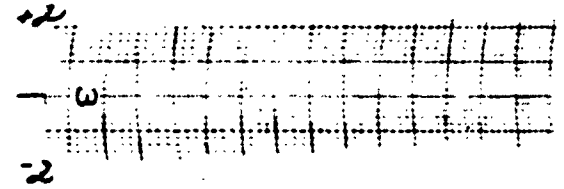

e_{in}

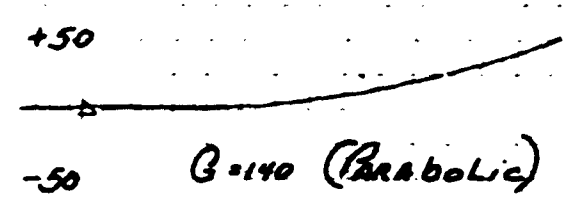

e_c

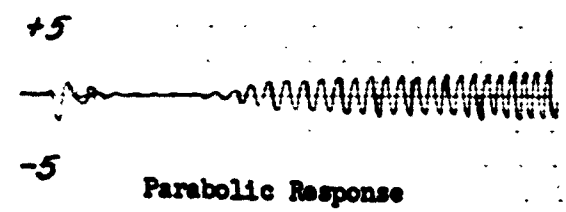

Parabolic Response

e_n

Appendix Figure D-13

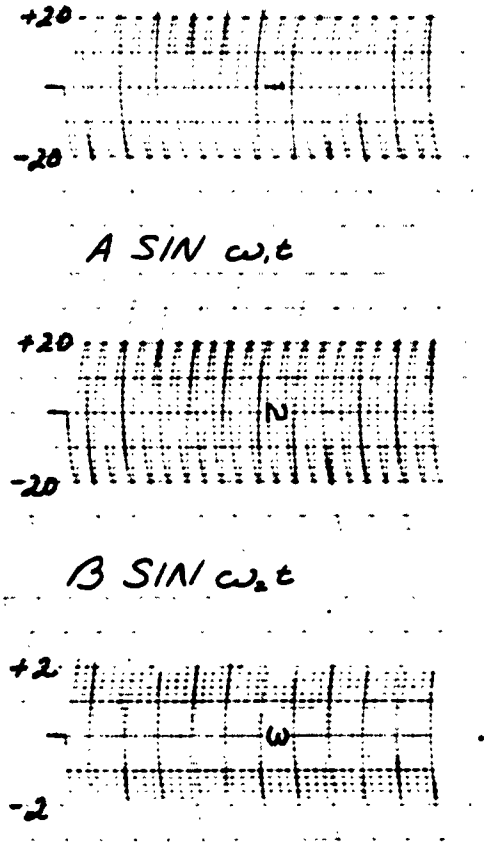

Appendix Figure D-14

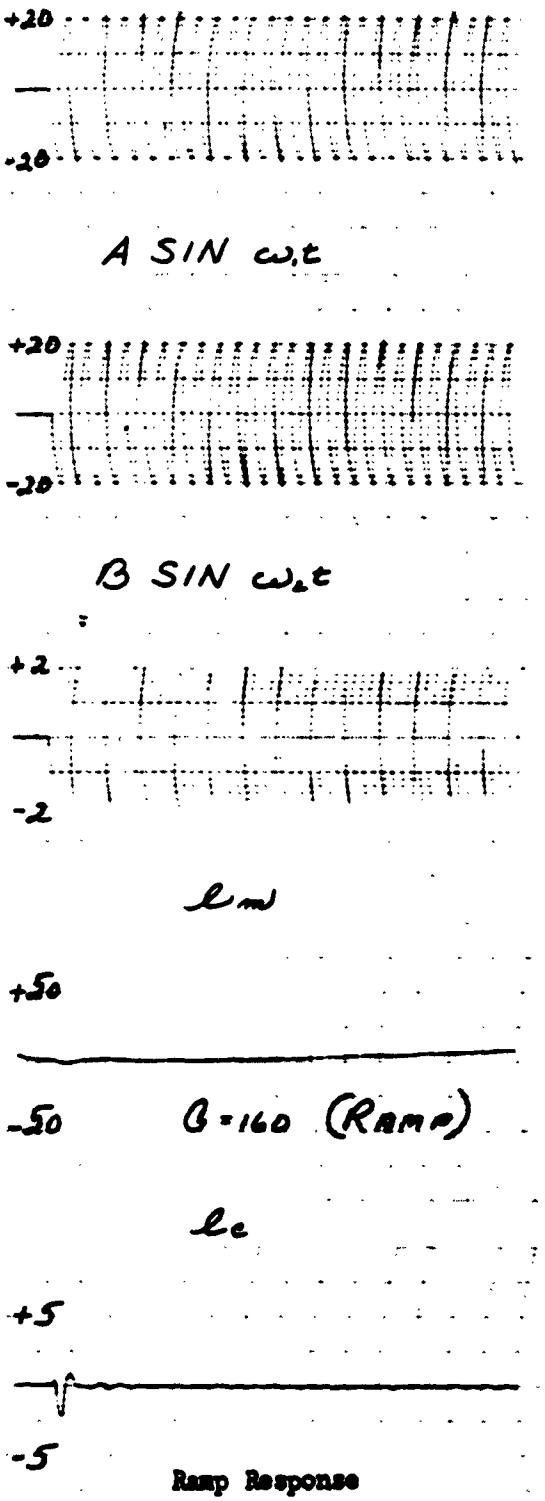

Ramp Response

Appendix Figure D-15

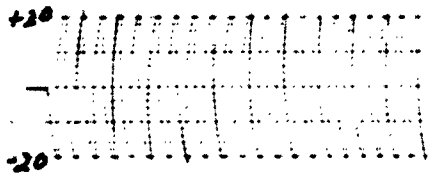

A SIN $\omega_1 t$

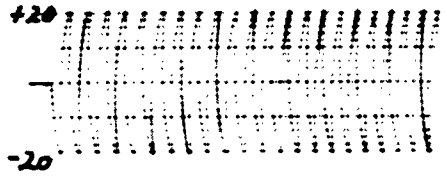

B SIN $\omega_2 t$

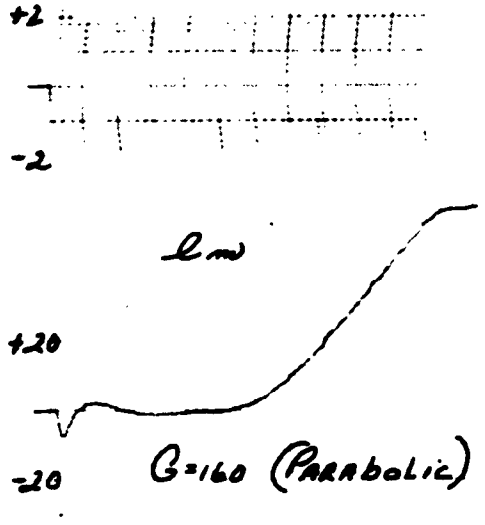

Appendix Figure D-16

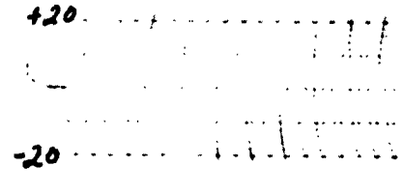

A SIN $\omega_1 t$

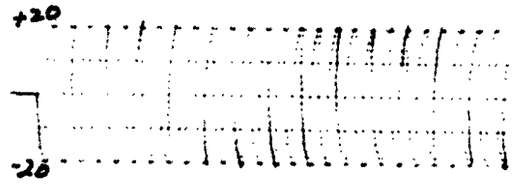

A SIN $\omega_1 t$

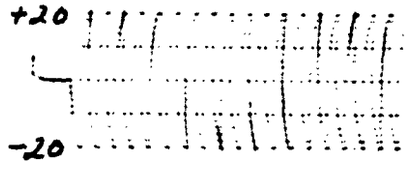

B SIN $\omega_2 t$

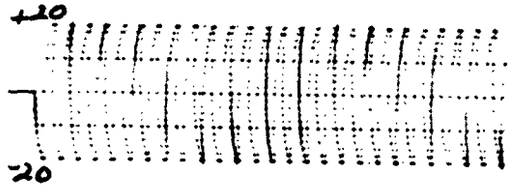

B SIN $\omega_2 t$

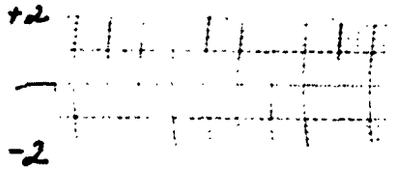

ℓ_m

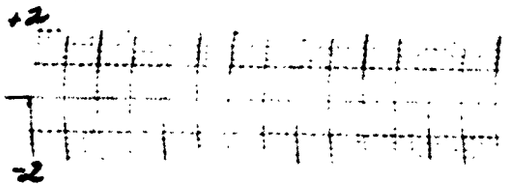

ℓ_m

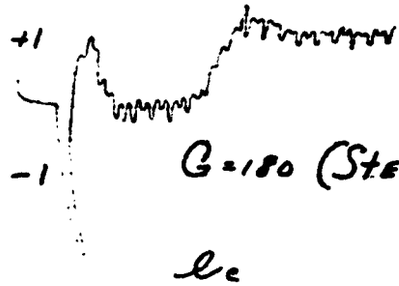

G=180 (Step)

ℓ_c

G=180 (Ramp)

ℓ_c

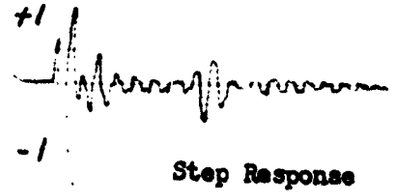

Step Response

ℓ_r

Ramp Response

ℓ_r

Appendix Figure D-17

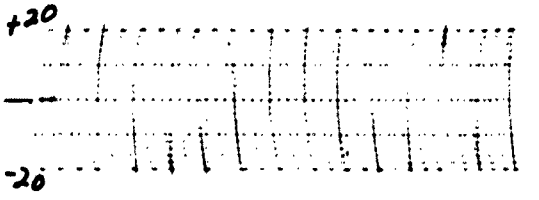

A SIN $\omega_1 t$

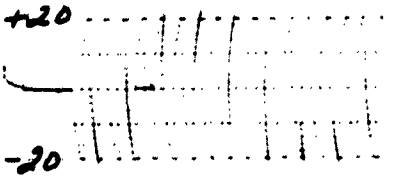

A SIN $\omega_1 t$

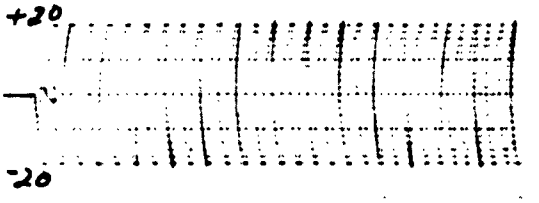

B SIN $\omega_2 t$

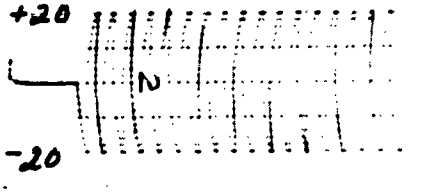

B SIN $\omega_2 t$

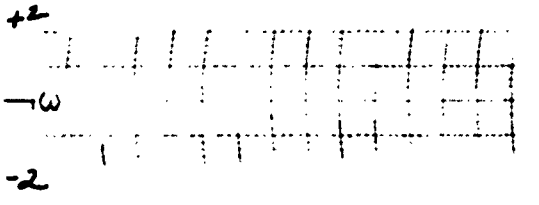

ℓ_{mw}

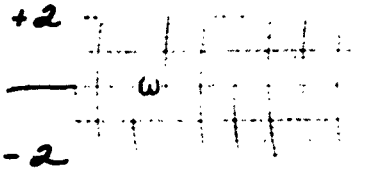

ℓ_{mw}

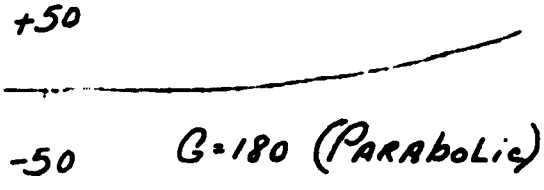

G=180 (Parabolic)

ℓ_c

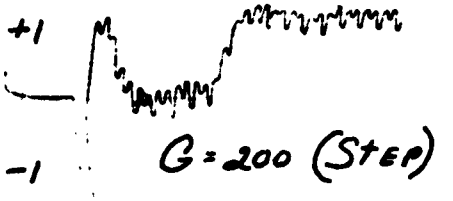

G=200 (Step)

ℓ_c

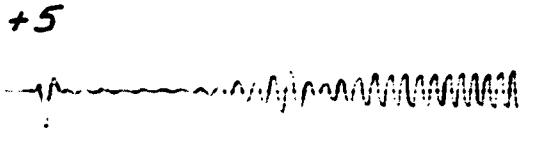

Parabolic Response

ℓ_r

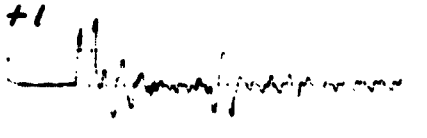

Step Response

ℓ_r

Appendix Figure D-18

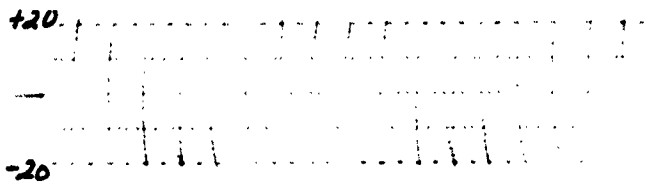

$A \sin \omega_1 t$

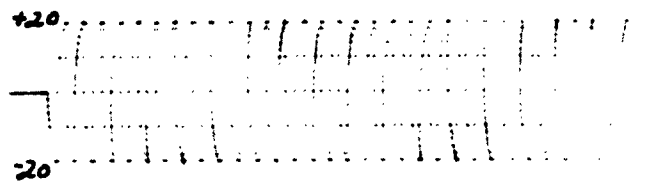

$B \sin \omega_2 t$

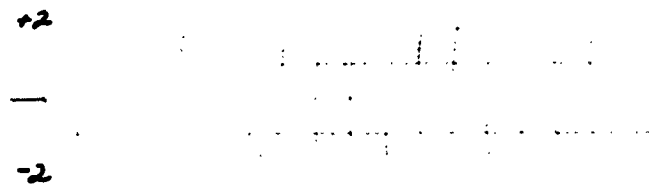

e_m

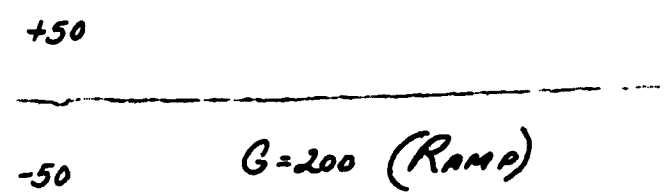

e_c

Ramp Response

e_r

Appendix Figure D-19

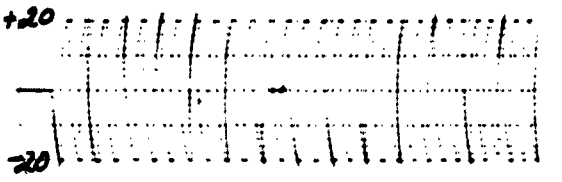

A SIN $\omega_1 t$

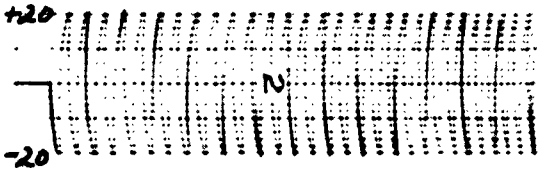

B SIN $\omega_2 t$

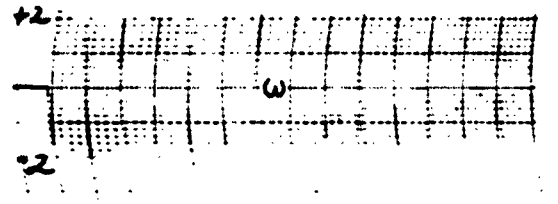

$\ell_{m\omega}$

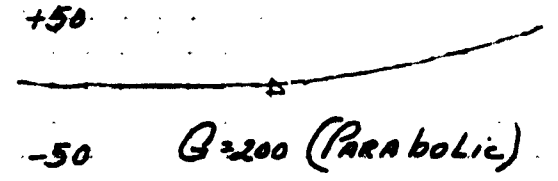

Q=200 (Parabolic)

ℓ_c

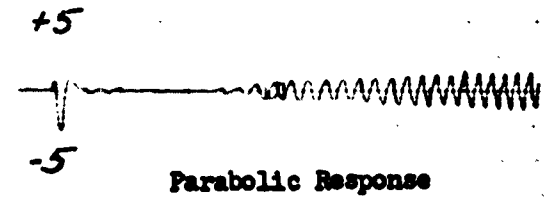

Parabolic Response

ℓ_n

Appendix Figure D-20

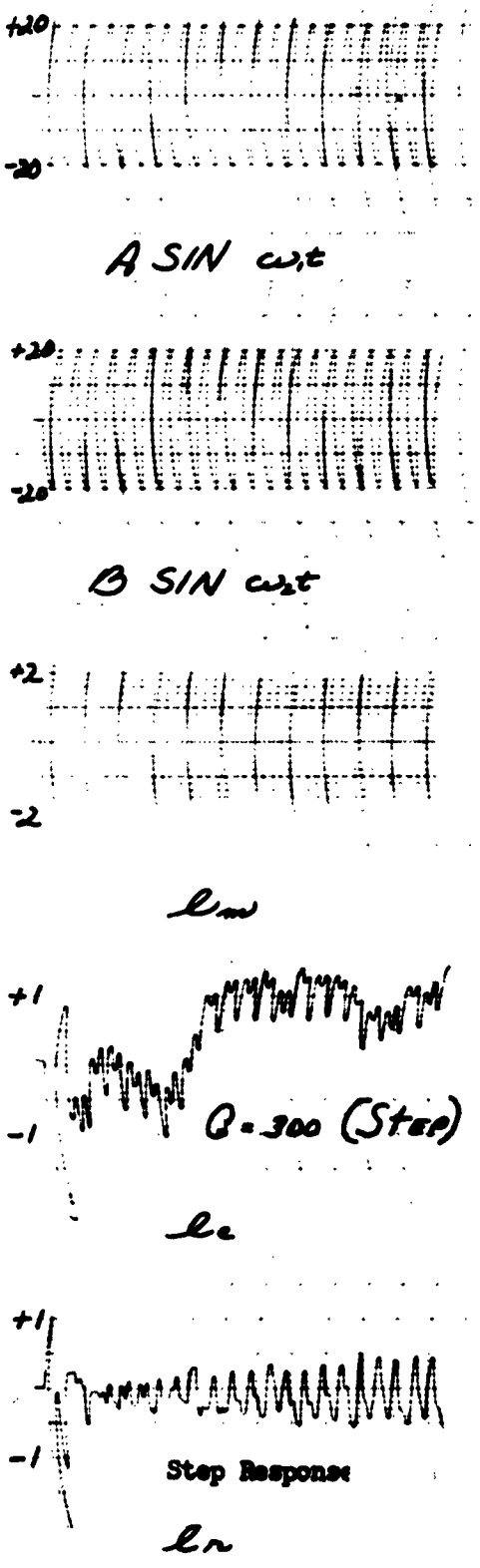

Appendix Figure D-21

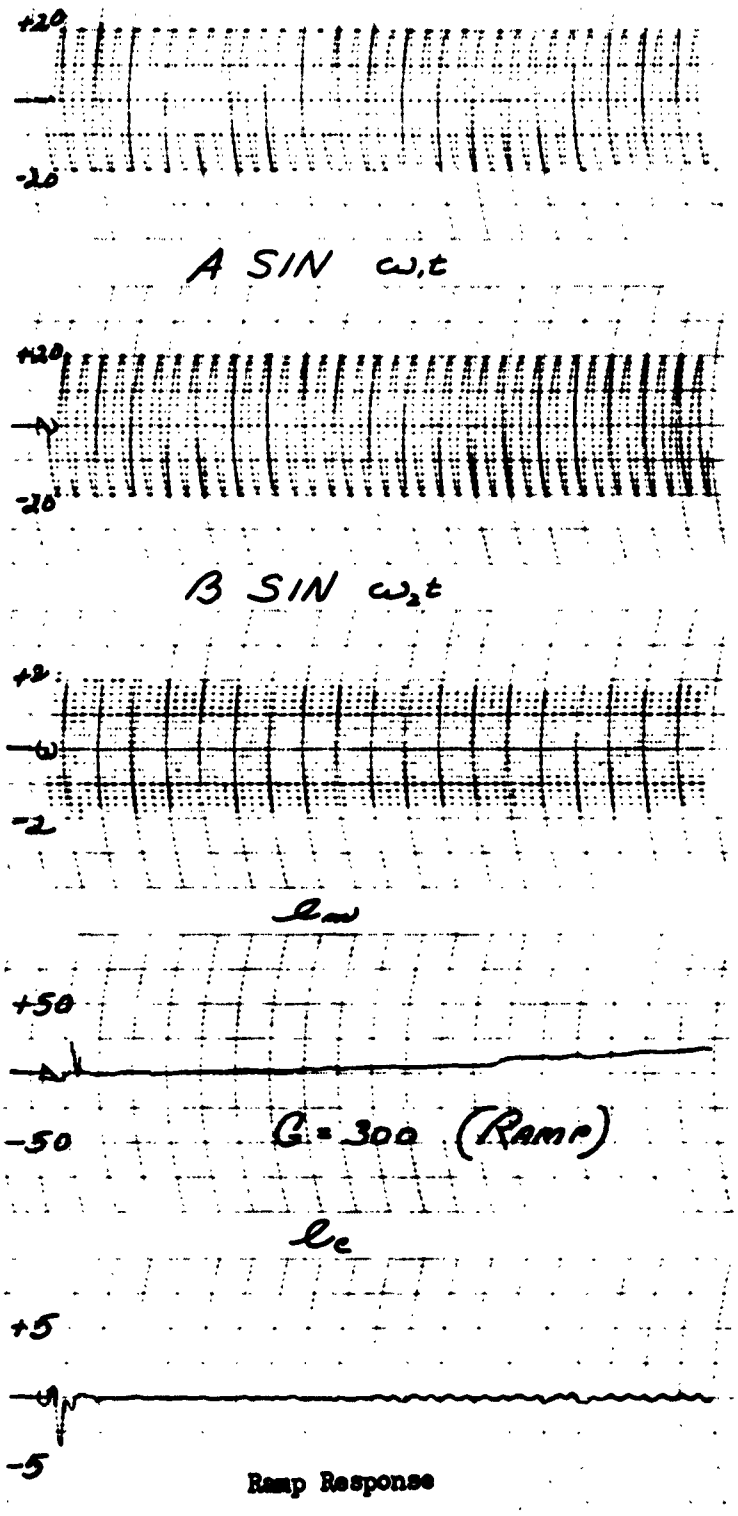

Ramp Response

e_r

Appendix Figure D-22

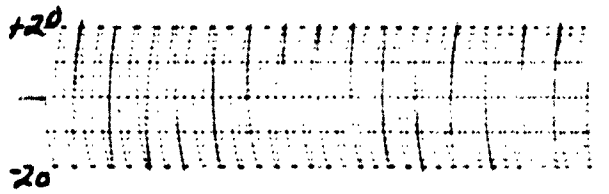

A SIN $\omega_1 t$

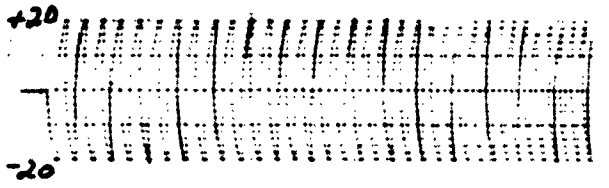

B SIN $\omega_2 t$

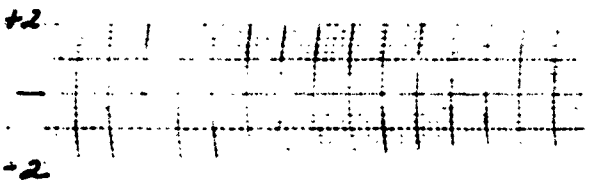

ℓ_m

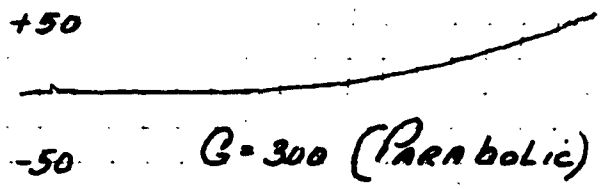

G = 300 (Parabolic)

ℓ_c

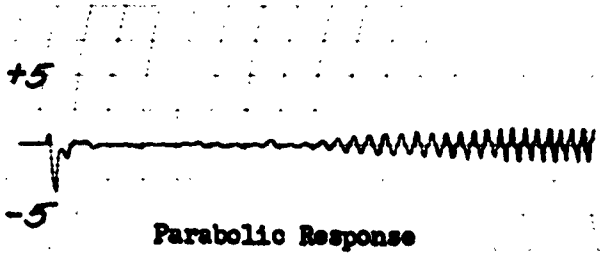

Parabolic Response

ℓ_r

Appendix Figure D-23